International Journal of Non-Linear Mechanics 126 (2020) 103554

Contents lists available at ScienceDirect

International Journal of Non-Linear Mechanics

journal homepage: www.elsevier.com/locate/nlm

Nonlinear vibration analysis of a servo controlled precision motion stage with friction isolator

Sunit Kumar Gupta, Jiamin Wang, Oumar R. Barry *

Department of Mechanical Engineering, Virginia Tech, Blacksburg, VA 24061, USA

ARTICLE INFO

Keywords:
Precision motion stage
LuGre model
Method of multiple scales
Subcritical and supercritical bifurcation
Friction isolator
Floquet theory

ABSTRACT

Precision motion stages are used in advanced manufacturing, metrological applications, and semiconductor industries for high precision positioning with high speed. However, friction-induced vibration undermines the performance of a servo-controlled motion stage. Recently, it was found that passive isolation in the form of friction isolator is very effective to mitigate the undesirable effects of friction in precision motion stages. This work presents, for the first time, a detailed nonlinear analysis of the dynamics of motion stage with a friction isolator. We consider a lumped parameter model of the precision motion stage with PID and a friction isolator modeled as two degrees of freedom system. Linear analysis of the system in the space of integral gain and reference velocity reveals that the inclusion of friction isolator increases the local stability region of steady states. We further observe the sensitivity of the stability of steady states towards the internal resonance between the motion stage and friction isolator. The influence of friction isolator on the nonlinear response of the system is examined analytically using the method of multiple scales and harmonic balance. We observe that the inclusion of friction isolator does not change the nature of Hopf bifurcation for higher values of reference velocity, and it remains subcritical bifurcation with or without friction isolator. However, for lower values of reference velocity, the inclusion of friction isolator leads to change in bifurcation from supercritical to subcritical for the given values of parameters. This observation further implies that the inclusion of friction isolator increases the local stability of steady states, whereas the global stability of steady states depends on the interaction between friction isolator and operating parameters. Furthermore, a detailed numerical bifurcation analysis of the system reveals the existence of period-2, period-4, quasi-periodic, and chaotic solutions. Also, the stability of period-1 solutions near Hopf point is determined by Floquet theory, which further reveals the existence of period-doubling bifurcation.

1. Introduction

High-speed and high-precision motion stages (at macro and nano-level) are widely used for inspections and assembly processes in machining, additive manufacturing, and semiconductor manufacturing industries [1–4]. Depending on the type of supporting interface between the motion stage and rigid structure, these high-precision motion stages can be broadly classified into four different categories: (1) flexural-based, (2) magnetic-based, (3) fluidic-based, and (4) mechanical-bearing based [1,5–7]. However, the use of mechanical bearing-based motion stages (MBMS) has been found more popular as compared to other motion stages due to their large motion range, high off-axis stiffness, cost-effectiveness, and easy installation [7]. In most applications, the motion of MBMS is controlled by either one or a combination of proportional (P), integral (I), and derivative (D) terms [8–10]. The increasing demands for high-performance control systems (i.e., high operating velocity and acceleration) lead to self-excited limit cycles due to the friction between contact surfaces. These vibrations, further, cause errors in positioning precision, long settling times, and stick–slip phenomena [8,11–16]. Therefore, it would be significantly beneficial for industries to develop effective methodologies and understand the dynamics of MBMS to mitigate or control these self-excited vibrations in the system.

Different compensation methods are used to control or mitigate friction-induced vibrations. The main idea behind these methods is to provide an equal and opposite force, through a control system, to cancel out friction. These methods include (1) high-gain feedback [13], (2) model-based feedforward and feedback controllers [8,15,17,18], and (3) advanced controllers (adaptive controller, model predictive controller) [19–22]. Even though high-gain feedback methods could be very effective in suppressing friction-induced vibrations, they make the resulting systems to be very sensitive to instability, sensor noise, chattering, and limit cycles. Whereas, model-based controllers often suffer from robustness and stability problems due to the rapid and nonlinear changes of pre-motion friction, thus limiting their practicality [13].

* Corresponding author.
E-mail address: obarry@vt.edu (O.R. Barry).

https://doi.org/10.1016/j.ijnonlinmec.2020.103554
Received 7 April 2020; Received in revised form 14 June 2020; Accepted 16 July 2020
Available online 21 July 2020
0020-7462/

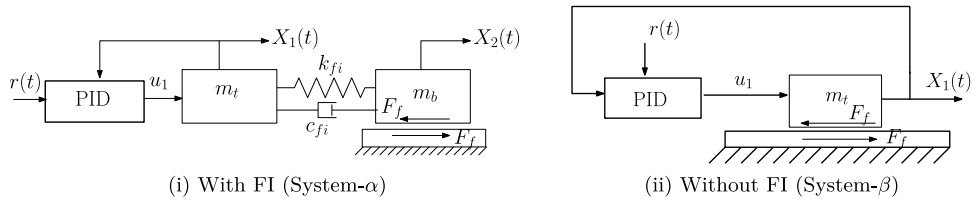

(i) With FI (System-α) (ii) Without FI (System-β)

Fig. 1. Schematic of precision motion stage (i) with FI (System-α) and (ii) without FI (System-β).

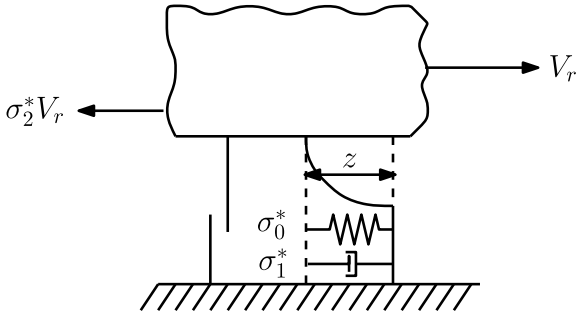

Fig. 2. Schematic of the friction dynamics between the contact surfaces.

For the case of advanced controllers, the algorithm complexity (determined by the structural model) leads to unsatisfactory performance at high-frequency controls due to hardware limitations [23,24].

Recently an efficient and more robust method has been developed to mitigate the effect of friction by connecting the mechanical bearing to the motion stage using a joint that is very compliant in the motion direction and hence, isolating the motion stage from the nonlinearities associated with friction. This method is known as a compliant joint method, and the device is known as friction isolator (FI) [17,18]. It has been experimentally demonstrated that a motion stage with FI achieves a significantly reduced settling time compared to the conventional stage without FI [18]. A detailed parametric analysis on the stability of the steady states under the effect of dynamical friction model, i.e., the LuGre model [25] reveals that a proper choice of FI properties allows to use high values of control gain (PID), which further help in controlling/suppressing self-excited friction-induced vibrations [26].

We emphasize that the use of FI to control friction-induced instabilities is new in the literature, and existing work only provides information [26,27] about the local stability properties of steady states. A detailed nonlinear analysis of a PID controlled motion stage with FI has not been performed, and therefore, this work is believed to be the first study to examine this problem. In this work, we model FI as a lumped parameter model with a linear spring–mass–damper system. Further, we perform the linear and nonlinear analysis of the combined system analytically under the effect of the LuGre friction model [25]. We observed that the inclusion of FI increases the local stability of the steady states of the system in the space of control parameters, more specifically in the space of integral feedback gain-reference velocity, and allows the use of higher value of integral feedback gain for a given value of reference velocity. However, the global stability of the steady states, i.e., the nature of Hopf bifurcation depends on the complex interaction between FI and integral control, and can change from supercritical to subcritical or remains subcritical depending on the value of reference velocity. The rest of the paper is organized as follows. In Section 2, we present the complete mathematical model of MBMS. It also includes a brief description of the LuGre model, along with the nondimensionalization of governing equations of motion. Linear stability analysis and accordingly, the analytical forms of the Hopf points are presented in Section 3. In Section 4, a detailed analytical nonlinear analysis of the system is presented using the method of multiple scales and harmonic balance. Results from linear and nonlinear analysis along with a numerical bifurcation analysis are presented in Section 5. In Section 6, some conclusions are drawn from the findings of the analysis.

2. Mathematical formulation

In this section, we formulate a lumped parameter model to study the dynamics of a PID controlled precision motion stage with and without friction isolator (FI). We model the PID controlled motion stage as two degrees of freedom system with FI and single degree of freedom system without FI as shown in Fig. 1(i) and (ii), respectively. For the sake of convenience, the motion stage with and without FI are referred to as System-α and System$-\beta$, respectively. In Fig. 1, u_1 is the feedback control force from PID, $r(t)$ is the reference/setpoint signal, m_t and m_b are the masses of the motion stage and FI, respectively. Also, the effect of FI on the dynamics of the precision motion stage is realized through a spring–damper system with the stiffness k_{fi} and the damping coefficient c_{fi}. Note that, in the case of System-α, FI is in direct contact with the supporting rigid surface, and hence, the frictional force, F_f, acts between FI and the supporting surface. However, in the absence of FI, i.e., in the case of System-β, the precision motion stage is in direct contact with the rigid surface, and therefore, the friction force acts between the motion stage and the supporting surface. Therefore, if $X_1(t)$ and $X_2(t)$ are the motion of precision motion stage and FI, respectively, then the governing equations of motion for System-α and System-β can be written as

System-α:

$$m_t\ddot{X}_1 + k_{fi}\left(X_1 - X_2\right) + c_{fi}\left(\dot{X}_1 - \dot{X}_2\right) = u_1\,, \tag{1a}$$

$$m_b\ddot{X}_2 + k_{fi}\left(X_2 - X_1\right) + c_{fi}\left(\dot{X}_2 - \dot{X}_1\right) = -F_f\,, \tag{1b}$$

System-β:

$$m_t\ddot{X}_1 = u_1 - F_f\,. \tag{2}$$

In the above governing equations of motions, the controller force from PID, u_1, is defined as

$$u_1 = -k_p^* e - k_d^*\dot{e} - k_i^*\int e\,\mathrm{d}t\,, \tag{3}$$

where k_p^*, k_d^*, and k_i^* represent the proportional, differential and integral gains, respectively, and e represents the tracking error. This tracking error can be expressed in terms of the motion of the stage (X_1) and the reference signal (r) as $e = X_1 - r$.

On substituting the expression for control force, u_1, in Eqs. (1), (2), and rewriting resulting equations in terms of tracking error (e) we get the modified equations for

System-α:

$$m_t\ddot{e} + k_d^*\dot{e} + k_p^* e + k_i^*\int e\mathrm{d}t + k_{fi}\left(e - e_b\right) + c_{fi}\left(\dot{e} - \dot{e}_b\right) = -m_t\ddot{r}\,, \tag{4a}$$

$$m_b\ddot{e}_b + k_{fi}\left(e_b - e\right) + c_{fi}\left(\dot{e}_b - \dot{e}\right) = -F_f - m_b\ddot{r}\,, \tag{4b}$$

and System-β:

$$m_t\ddot{e} + k_d^*\dot{e} + k_p^* e + k_i^*\int e\mathrm{d}t = -F_f - m\ddot{r}\,. \tag{5}$$

In the above governing equations of motions for System-α, we define $e_b = X_2 - r$. Next, we model the dynamical friction between the contact surfaces using the LuGre friction model [25]. The LuGre model

is one of the most widely used forms of a dynamic friction model as it includes viscous friction, pre-motion friction (pre-sliding/pre-rolling), and hysteresis effects together [25,28]. In this model, the asperities in the contact surfaces are considered as elastic spring-like bristles with damping, and the microscopic degrees of freedom associated with the bristle deflections are used to define the friction force (as shown in Fig. 2). Therefore, the total friction force in the LuGre friction model is considered to be a summation of the average force associated with the deflection of the bristles and a viscous term proportional to the relative velocity between the surfaces in contact. If z represents the average bristle deflection (internal state variable), then the friction force in the LuGre model is given by

$$F_f = \sigma_0^* z + \sigma_1^* \dot{z} + \sigma_2^* V_r \,, \tag{6}$$

where σ_0^* and σ_1^* are the contact stiffness and the micro-damping of the bristle, respectively, σ_2^* is the macroscopic viscous friction between the contact surfaces and V_r is the relative velocity between moving surfaces. It can be observed from Eq. (6), that unlike other friction models, the LuGre friction model does not only depend on the relative velocity but also on the evolution of the internal state variable z. Therefore, instead of providing a unique value of the friction force for a given relative velocity during acceleration and deceleration, the LuGre model can give different values of friction force in these two phases depending on the evolution of the internal state variable.

The evolution of the average bristle deflection, i.e., z, with time is governed by the following differential equation:

$$\dot{z} = V_r - \frac{\sigma_0^* |V_r|}{g(V_r)} z = V_r \left(1 - \frac{\sigma_0^* \,\mathrm{sgn}(V_r)}{g(V_r)} z \right), \tag{7}$$

where sgn(.) is the Signum function, and $g(V_r)$ is a positive valued function, i.e., $g(V_r) > 0$ which further describes the Stribeck effect in the system. We emphasize that for the case of System-α, FI is in direct contact with the supporting rigid surface, therefore, the relative velocity for System-α, $V_{r\alpha}$, is defined as $\dot{X}_2 = \dot{e}_b + \dot{r}$. However, in contrary to System-α, for the case of System-β, the motion stage is in direct contact with the surface, which further implies the relative velocity for System-β as $V_{r\beta} = \dot{X}_1 = \dot{e} + \dot{r}$.

To capture dropping characteristic, Wit et al. [25] suggested the use of Gaussian function model for $g(V_r)$ in the form of :

$$g(V_r) = f_C^* + (f_S^* - f_C^*) e^{-(V_r/V_s)^2} \,, \tag{8}$$

where f_C^* is the Coulomb friction, f_S^* is the static friction, and V_s is the Stribeck velocity threshold. However, the limitations of this model have been observed in the analytical analysis of a system with the LuGre model [29,30]. To overcome this shortcoming, the positive valued function $g(V_r)$ was modified and represented by an exponential function [30]

$$g(V_r) = f_C^* + (f_S^* - f_C^*) e^{-\tilde{a}|V_r|} \,, \tag{9}$$

where $\tilde{a}$ is the slope parameter. Note that Eq. (7) along with Eqs. (4) and (5) define the dynamics of System-α and -β, respectively. Having defined the equations of motion, now we introduce the following nondimensional scales and parameters to nondimensionalize the system, which further ease the analytical treatment of the system:

$$\begin{aligned}
&x = \frac{e}{X_0},\ x_b = \frac{e_b}{X_0},\ \tilde{z} = \frac{z}{X_0},\ X_0 = \frac{g}{\omega_p^2},\ \omega_p = \sqrt{\frac{k_p^*}{m_t}},\ \tau = \omega_p t,\\
&\zeta = \frac{k_d^*}{2 m_t \omega_p},\ k_i = \frac{k_i^*}{m_t \omega_p^3},\ v_{r\alpha} = \frac{V_{r\alpha}}{X_0 \omega_p},\\
&v_{r\beta} = \frac{V_{r\beta}}{X_0 \omega_p},\ \sigma_0 = \frac{\sigma_0^*}{m_t \omega_p^2},\ \sigma_1 = \frac{\sigma_1^*}{m_t \omega_p},\ \sigma_2 = \frac{\sigma_2^*}{m_t \omega_p},\\
&f_c = \frac{f_c^*}{m_t X_0 \omega_p^2},\ f_s = \frac{f_s^*}{m_t X_0 \omega_p^2},\ a = \tilde{a} \omega_p X_0,\\
&\kappa = \frac{c_{fi}}{2 m_t \omega_p},\ k_r = \frac{k_{fi}}{k_p}, m_r = \frac{m_t}{m_b}.
\end{aligned} \tag{10}$$

Using the above-mentioned nondimensional scales and parameters and assuming constant reference velocity signal ($\ddot{r} = 0$), the governing equations of motion can be nondimensionalized and written as for System-α:

$$\ddot{x} + 2\zeta \dot{x} + x + k_i \int x \mathrm{d}\tau + k_r \left(x - x_b \right) + 2\kappa \left(\dot{x} - \dot{x}_b \right) = 0 \,, \tag{11a}$$

$$\begin{aligned}
&\ddot{x}_b + k_r m_r \left(x_b - x \right) + 2\kappa m_r \left(\dot{x}_b - \dot{x} \right)\\
&\quad = -m_r \left(\sigma_0 \tilde{z} + \sigma_1 v_{r\alpha} \left(1 - \frac{\sigma_0 \mathrm{sgn}(v_{r\alpha})}{g(v_{r\alpha})} \tilde{z} \right) + \sigma_2 v_{r\alpha} \right),
\end{aligned} \tag{11b}$$

$$\dot{\tilde{z}} = v_{r\alpha} \left(1 - \frac{\sigma_0 \mathrm{sgn}(v_{r\alpha})}{g(v_{r\alpha})} \tilde{z} \right), \tag{11c}$$

and for System-β:

$$\ddot{x} + 2\zeta \dot{x} + x + k_i \int x \mathrm{d}\tau = -\left(\sigma_0 \tilde{z} + \sigma_1 v_{r\beta} \left(1 - \frac{\sigma_0 \mathrm{sgn}(v_{r\beta})}{g(v_{r\beta})} \tilde{z} \right) + \sigma_2 v_{r\beta} \right), \tag{12a}$$

$$\dot{\tilde{z}} = v_{r\beta} \left(1 - \frac{\sigma_0 \mathrm{sgn}(v_{r\beta})}{g(v_{r\beta})} \tilde{z} \right). \tag{12b}$$

In the above governing equations of motion, overhead dot $(\dot{\cdot})$ represents the derivative with respect to the nondimensional time τ. Further, for the sake of simplicity in the analytical treatment of the governing equations, we rewrite Eqs. (11) and (12) compactly in the state–space form as for
System-α:

$$\dot{x}_{1\alpha} = x_{2\alpha} \,, \tag{13a}$$

$$\dot{x}_{2\alpha} = -2\zeta x_{2\alpha} - x_{1\alpha} - k_i x_{3\alpha} - k_r \left(x_{1\alpha} - x_{4\alpha} \right) - 2\kappa \left(x_{2\alpha} - x_{5\alpha} \right) , \tag{13b}$$

$$\dot{x}_{3\alpha} = x_{1\alpha} \,, \tag{13c}$$

$$\dot{x}_{4\alpha} = x_{5\alpha} \,, \tag{13d}$$

$$\begin{aligned}
\dot{x}_{5\alpha} = &-2\kappa m_r \left(x_{5\alpha} - x_{2\alpha} \right) - k_r m_r \left(x_{4\alpha} - x_{1\alpha} \right)\\
&- m_r \left(\sigma_0 x_{6\alpha} + \sigma_1 v_{r\alpha} \left(1 - \frac{\sigma_0 x_{6\alpha}}{g\left(v_{r\alpha}\right)} \mathrm{sgn}(v_{r\alpha}) \right) + \sigma_2 v_{r\alpha} \right),
\end{aligned} \tag{13e}$$

$$\dot{x}_{6\alpha} = v_{r\alpha} \left(1 - \frac{\sigma_0 x_{6\alpha}}{g\left(v_{r\alpha}\right)} \mathrm{sgn}(v_{r\alpha}) \right), \tag{13f}$$

and for System-β

$$\dot{x}_{1\beta} = x_{2\beta} \,, \tag{14a}$$

$$\begin{aligned}
\dot{x}_{2\beta} = &-2\zeta x_{2\beta} - x_{1\beta} - k_i x_{3\beta}\\
&- \left(\sigma_0 x_{4\beta} + \sigma_1 v_{r\beta} \left(1 - \frac{\sigma_0 x_{4\beta}}{g\left(v_{r\beta}\right)} \mathrm{sgn}(v_{r\beta}) \right) + \sigma_2 v_{r\beta} \right),
\end{aligned} \tag{14b}$$

$$\dot{x}_{3\beta} = x_{1\beta} \,, \tag{14c}$$

$$\dot{x}_{4\beta} = v_{r\beta} \left(1 - \frac{\sigma_0 x_{4\beta}}{g\left(v_{r\beta}\right)} \mathrm{sgn}(v_{r\beta}) \right). \tag{14d}$$

For System-α, $[x_{1\alpha}, x_{2\alpha}, x_{3\alpha}, x_{4\alpha}, x_{5\alpha}, x_{6\alpha}] = [x(\tau), \dot{x}(\tau), \int x \mathrm{d}\tau, x_b(\tau), \dot{x}_b(\tau), \tilde{z}(\tau)]$, whereas for System-$\beta$, $[x_{1\beta}, x_{2\beta}, x_{3\beta}, x_{4\beta}] = [x(\tau), \dot{x}(\tau), \int x \mathrm{d}\tau, \tilde{z}(\tau)]$. Further, if v_{rv} represents the nondimensional constant reference velocity signal, then the nondimensional relative velocity for the case of System-α is $v_{r\alpha} = \dot{x}_b + v_{rv} = x_{5\alpha} + v_{rv}$, however, for the System-β, $v_{r\beta}$ is determined by $v_{r\beta} = \dot{x} + v_{rv} = x_{2\beta} + v_{rv}$. For the analytical treatment of System-α and System-β, we expand $\frac{1}{g(v_r)}$ in a Taylor series for small amplitude motion and keep terms till third order. This step leads to:

for System-α

$$\frac{1}{g(v_{rv}+x_5)} = g_0 + g_1 x_5 + g_2 x_5^2 + g_3 x_5^3 , \tag{15}$$

and for System-β

$$\frac{1}{g(v_{rv}+x_2)} = g_0 + g_1 x_2 + g_2 x_2^2 + g_3 x_2^3 , \tag{16}$$

where $g_i's$ are given by

$$g_0 = \frac{1}{g(v_{rv})} = \frac{1}{g},\ g_1 = -\frac{1}{g^2}\frac{\partial g}{\partial v_{rv}},\ g_2 = \frac{1}{g^3}\left[\left(\frac{\partial g}{\partial v_{rv}}\right)^2 - \frac{g}{2}\frac{\partial^2 g}{\partial v_{rv}^2}\right],$$
$$g_3 = -\frac{1}{g^4}\left[\left(\frac{\partial g}{\partial v_{rv}}\right)^3 - g\frac{\partial g}{\partial v_{rv}}\frac{\partial^2 g}{\partial v_{rv}^2} + \frac{g^2}{6}\frac{\partial^3 g}{\partial v_{rv}^3}\right]. \tag{17}$$

On substituting Eqs. (15) and (16) in Eqs. (13) and (14), respectively, and simplifying equations for pure slipping motion, i.e., $v_{rn} > 0$, for $n = \alpha,\ \beta$ (which further implies $\mathrm{sgn}(v_{rn}) = 1$ for $n = \alpha,\ \beta$), we get the governing equations for System-α

$$\dot{x}_{1\alpha} = x_{2\alpha} , \tag{18a}$$
$$\dot{x}_{2\alpha} = -2\zeta x_{2\alpha} - x_{1\alpha} - k_i x_{3\alpha} - k_r\left(x_{1\alpha} - x_{4\alpha}\right) - 2\kappa\left(x_{2\alpha} - x_{5\alpha}\right) , \tag{18b}$$
$$\dot{x}_{3\alpha} = x_{1\alpha} , \tag{18c}$$
$$\dot{x}_{4\alpha} = x_{5\alpha} , \tag{18d}$$

$$\begin{aligned}\dot{x}_{5\alpha} = {} & m_r\sigma_1\sigma_0 x_{6\alpha} g_3 x_{5\alpha}^4 + \left(m_r\sigma_1 v_{rv}\sigma_0 x_{6\alpha} g_3 + m_r\sigma_1\sigma_0 x_{6\alpha} g_2\right) x_{5\alpha}^3 \\ & + \left(m_r\sigma_1 v_{rv}\sigma_0 x_{6\alpha} g_2 + m_r\sigma_1\sigma_0 x_{6\alpha} g_1\right) x_{5\alpha}^2 \\ & - \left(m_r\sigma_1 + 2\kappa m_r - m_r\sigma_1\sigma_0 x_{6\alpha} g_0 + m_r\sigma_2 - m_r\sigma_1 v_{rv}\sigma_0 x_{6\alpha} g_1\right) x_{5\alpha} \\ & - m_r\sigma_0 x_{6\alpha} + 2\kappa m_r x_{2\alpha} - k_r m_r x_{4\alpha} + k_r m_r x_{1\alpha} \\ & - m_r\sigma_2 v_{rv} - m_r\sigma_1 v_{rv} + m_r\sigma_1 v_{rv}\sigma_0 x_{6\alpha} g_0 ,\end{aligned} \tag{18e}$$

$$\begin{aligned}\dot{x}_{6\alpha} = {} & -\sigma_0 x_{6\alpha} g_3 x_{5\alpha}^4 - \left(\sigma_0\, x_{6\alpha} g_2 + v_{rv}\,\sigma_0\, x_{6\alpha} g_3\right) x_{5\alpha}^3 \\ & - \left(v_{rv}\,\sigma_0\, x_{6\alpha} g_2 + \sigma_0\, x_{6\alpha} g_1\right) x_{5\alpha}^2 - \left(-1 + v_{rv}\,\sigma_0\, x_{6\alpha} g_1 + \sigma_0\, x_{6\alpha} g_0\right) x_{5\alpha} \\ & + v_{rv} - v_{rv}\,\sigma_0\, x_{6\alpha} g_0 ,\end{aligned} \tag{18f}$$

and for System-β

$$\dot{x}_{1\beta} = x_{2\beta} , \tag{19a}$$

$$\begin{aligned}\dot{x}_{2\beta} = {} & -x_{1\beta} - k_i x_{3\beta} + \Big(\sigma_1\sigma_0 g_3 x_{2\beta}^4 + \left(\sigma_1\sigma_0 g_0 + \sigma_1 v_{rv}\sigma_0 g_1\right) x_{2\beta} \\ & + \left(\sigma_1 v_{rv}\sigma_0 g_2 + \sigma_1\sigma_0 g_1\right) x_{2\beta}^2 - \sigma_0 + \sigma_1 v_{rv}\sigma_0 g_0 \\ & + \left(\sigma_1\sigma_0 g_2 + \sigma_1 v_{rv}\sigma_0 g_3\right) x_{2\beta}^3\Big) x_{4\beta} - \sigma_1 v_{rv} \\ & - \left(2\zeta + \sigma_2 + \sigma_1\right) x_{2\beta} - \sigma_2 v_{rv} ,\end{aligned} \tag{19b}$$

$$\dot{x}_{3\beta} = x_{1\beta} , \tag{19c}$$

$$\begin{aligned}\dot{x}_{4\beta} = {} & \Big(-\sigma_0 g_3 x_{2\beta}^4 - \left(v_{rv}\sigma_0 g_2 + \sigma_0 g_1\right) x_{2\beta}^2 - \left(v_{rv}\sigma_0 g_1 + \sigma_0 g_0\right) x_{2\beta} \\ & - \left(\sigma_0 g_2 + v_{rv}\sigma_0 g_3\right) x_{2\beta}^3 - v_{rv}\sigma_0 g_0\Big) x_{4\beta} + x_{2\beta} + v_{rv} .\end{aligned} \tag{19d}$$

The steady states of Eqs. (18) and (19) can be obtained by setting the derivatives of states as 0 to obtain for System-α

$$x_{1\alpha s} = 0,\ x_{2\alpha s} = 0,\ x_{3\alpha s} = -\frac{g_0\sigma_2 v_{rv} + 1}{g_0 k_i},\ x_{4\alpha s} = -\frac{g_0\sigma_2 v_{rv} + 1}{g_0 k_r},$$
$$x_{5\alpha s} = 0,\ x_{6\alpha s} = \frac{1}{\sigma_0 g_0} ; \tag{20}$$

and for System-β

$$x_{1\beta s} = 0,\ x_{2\beta s} = 0,\ x_{3\beta s} = -\frac{g_0\sigma_2 v_{rv} + 1}{g_0 k_i},\ x_{4\beta s} = \frac{1}{\sigma_0 g_0} . \tag{21}$$

Now, we introduce a small parameter ϵ ($\epsilon \ll 1$), in the governing equations by shifting the origin of the solution to the equilibrium state as

$$x_{in}(t) = x_{ins} + \epsilon y_{in}(t) , (i = 1, 2, \ldots, 6 \text{ for } n = \alpha,\ i = 1, 2, 3, 4 \text{ for } n = \beta) , \tag{22}$$

where $y_{in}(t)$'s are shifted coordinates. Thus, the governing equations of motion in these shifted coordinates can be written as for System-α

$$\dot{y}_{1\alpha} = y_{2\alpha} , \tag{23a}$$
$$\dot{y}_{2\alpha} = -2\zeta y_{2\alpha} - y_{1\alpha} - k_i y_{3\alpha} - k_r\left(y_{1\alpha} - y_{4\alpha}\right) - 2\kappa\left(y_{2\alpha} - y_{5\alpha}\right) , \tag{23b}$$
$$\dot{y}_{3\alpha} = y_{1\alpha} , \tag{23c}$$
$$\dot{y}_{4\alpha} = y_{5\alpha} , \tag{23d}$$

$$\begin{aligned}\dot{y}_{5\alpha} = {} & 2\kappa m_r y_{2\alpha} - k_r m_r\left(y_{4\alpha} - y_{1\alpha}\right) - m_r h_{1\alpha} y_{5\alpha} - m_r h_{2\alpha} y_{6\alpha} \\ & + \epsilon\left(y_{5\alpha}^2 m_r\sigma_1 h_0 h_{3\alpha} + y_{6\alpha} y_{5\alpha} m_r\sigma_1 h_{4\alpha}\right) \\ & + \epsilon^2\left(y_{5\alpha}^2 y_{6\alpha} m_r\sigma_1\sigma_0 h_{3\alpha} + y_{5\alpha}^3 m_r\sigma_1 h_{5\alpha}\right) + \mathcal{O}(\epsilon^3) ,\end{aligned} \tag{23e}$$

$$\begin{aligned}\dot{x}_{6\alpha} = {} & -v_{rv} g_1 h_0 y_{5\alpha} - v_{rv}\sigma_0 g_0 y_{6\alpha} - \epsilon\left(y_{5\alpha}^2 h_0 h_{3\alpha} + y_{6\alpha} y_{5\alpha}\sigma_0 h_{4\alpha}\right) \\ & - \epsilon^2\left(y_{6\alpha} y_{5\alpha}^2\sigma_0 h_{3\alpha} + y_{5\alpha}^3 h_{5\alpha}\right) + \mathcal{O}(\epsilon^3) ,\end{aligned} \tag{23f}$$

and for System-β

$$\dot{y}_{1\beta} = y_{2\beta} , \tag{24a}$$

$$\begin{aligned}\dot{y}_{2\beta} = {} & -y_{1\beta} - h_{1\beta} y_{2\beta} - 2\zeta y_{2\beta} - k_i y_{3\beta} - h_{2\beta} y_{4\beta} \\ & + \epsilon\left(h_0\sigma_1 h_{3\beta} y_{2\beta}^2 + \sigma_1 h_{4\beta} y_{2\beta} y_{4\beta}\right) \\ & + \epsilon^2\left(\sigma_1 h_{5\beta} y_{2\beta}^3 + \sigma_0\sigma_1 h_{3\beta} y_{4\beta} y_{2\beta}^3\right) + \mathcal{O}(\epsilon^3) ,\end{aligned} \tag{24b}$$

$$\dot{y}_{3\beta} = y_{1\beta} , \tag{24c}$$

$$\begin{aligned}\dot{y}_{4\beta} = {} & -v_{rv} g_1 h_0 y_2 - v_{rv}\sigma_0 g_0 y_{4\beta} - \epsilon\left(h_0 h_{3\beta} y_{2\beta}^2 + h_{4\beta} y_{2\beta} y_{4\beta}\right) \\ & - \epsilon^2\left(h_{5\beta} y_{3\beta}^3 + \sigma_0 h_{3\beta} y_{2\beta}^2 y_{4\beta}\right) + \mathcal{O}(\epsilon^3) ,\end{aligned} \tag{24d}$$

where $h_0 = \frac{1}{g_0}$, $h_{1\alpha} = \sigma_2 - h_0\sigma_1 v_{rv} g_1 + 2\kappa$, $h_{2\alpha} = \sigma_0\left(1 - \sigma_1 v_{rv} g_0\right)$, $h_{3\alpha} = \left(v_{rv} g_2 + g_1\right)$, $h_{4\alpha} = \sigma_0\left(g_0 + v_{rv} g_1\right)$, $h_{5\alpha} = h_0\left(g_2 + v_{rv}\, g_3\right)$, $h_{1\beta} = \sigma_2 - h_0\sigma_1 v_{rv} g_1$, $h_{2\beta} = \sigma_0\left(1 - \sigma_1 v_{rv} g_0\right)$, $h_{3\beta} = \left(v_{rv} g_2 + g_1\right)$, $h_{4\beta} = \sigma_0\left(g_0 + v_{rv} g_1\right)$, and $h_{5\beta} = h_0\left(g_2 + v_{rv}\, g_3\right)$. Note that Eqs. (23) and (24) have been already divided by ϵ throughout, to get the above perturbed differential equations. However, since all the nonlinear terms appears at higher order of ϵ, the unperturbed equations obtained by setting $\epsilon = 0$ in Eqs. (23) and (24) are system of linear ODEs, and hence, there are no complications in the linear and nonlinear analysis to be presented in subsequent sections.

3. Linear stability analysis

In this section, the linear stability analysis of System-α and System-β is presented to identify different stable and unstable regimes in the space of control parameters. We emphasize here that this linear analysis not only provides information about the stability but also provides the solution to an unperturbed linear equation, which will be further used in the nonlinear analysis of our system. Therefore, the linear analysis of both systems is essential and has to be performed carefully. For the sake of brevity, we present a detailed linear stability analysis of System-α only and use the same approach to get information about the stability of System-β. The linearized coupled system of the equations for System-α can be obtained by setting $\epsilon = 0$ in Eq. (23) to obtain

$$\dot{y}_{1\alpha} = y_{2\alpha} , \tag{25a}$$
$$\dot{y}_{2\alpha} = -2\zeta y_{2\alpha} - y_{1\alpha} - k_i y_{3\alpha} - k_r\left(y_{1\alpha} - y_{4\alpha}\right) - 2\kappa\left(y_{2\alpha} - y_{5\alpha}\right) , \tag{25b}$$
$$\dot{y}_{3\alpha} = y_{1\alpha} , \tag{25c}$$

$$\dot{y}_{4\alpha} = y_{5\alpha}\,, \tag{25d}$$

$$\dot{y}_{5\alpha} = 2\kappa m_r y_{2\alpha} - k_r m_r \left(y_{4\alpha} - y_{1\alpha}\right) - m_r h_{1\alpha} y_{5\alpha} - m_r h_{2\alpha} y_{6\alpha}\,, \tag{25e}$$

$$\dot{y}_{6\alpha} = -v_{rv} g_1 h_0 y_{5\alpha} - v_{rv}\sigma_0 g_0 y_{6\alpha}\,. \tag{25f}$$

The corresponding characteristic equation is obtained by assuming synchronous solution for $y_{i\alpha}$ (for $i = 1..6$) and accordingly, setting

$$\begin{pmatrix} y_{1\alpha}(\tau) \\ y_{2\alpha}(\tau) \\ y_{3\alpha}(\tau) \\ y_{4\alpha}(\tau) \\ y_{5\alpha}(\tau) \\ y_{6\alpha}(\tau) \end{pmatrix} = \begin{pmatrix} y_{1\alpha 0} \\ y_{2\alpha 0} \\ y_{3\alpha 0} \\ y_{4\alpha 0} \\ y_{5\alpha 0} \\ y_{6\alpha 0} \end{pmatrix} e^{\lambda\tau}\,, \tag{26}$$

into Eq. (25) to get

$$y_{1\alpha 0}\lambda - y_{2\alpha 0} = 0\,, \tag{27a}$$

$$(1 + k_r) y_{1\alpha 0} + (\lambda + 2\zeta + 2\kappa)\, y_{2\alpha 0} + k_i y_{3\alpha 0} - k_r y_{4\alpha 0} - 2\kappa y_{5\alpha 0} = 0\,, \tag{27b}$$

$$y_{1\alpha 0} - \lambda y_{3\alpha 0} = 0\,, \tag{27c}$$

$$y_{5\alpha 0} - y_{4\alpha 0} = 0\,, \tag{27d}$$

$$k_r m_r y_{1\alpha 0} + 2\kappa m_r y_{2\alpha} - k_r m_r y_{4\alpha 0} - \left(\lambda + m_r h_{1\alpha}\right) y_{5\alpha 0} - m_r h_{2\alpha} y_{6\alpha 0} = 0\,, \tag{27e}$$

$$v_{rv} g_1 h_0 y_{5\alpha 0} + \left(\lambda + v_{rv}\sigma_0 g_0\right) y_{6\alpha 0} = 0\,. \tag{27f}$$

To get the non-trivial solutions for $y_{i\alpha 0}$ (for $i = 1..6$), we set the determinant of the coefficient matrix of Eqs. (27) to zero which further leads to the characteristic equation as

$$\lambda^6 + f_1\lambda^5 + f_2\lambda^4 + f_3\lambda^3 + f_4\lambda^2 + f_5\lambda + f_6 = 0\,. \tag{28}$$

with f_i (for $i = 1..6$) are the involved functions of system and control parameters, and are reported in Appendix A. The roots of this characteristic equation determine the stability of the system in the space of control parameters. If all roots lie in the left half-plane, i.e., if all roots have negative real part ($\Re(\lambda) < 0$) then the system is stable. However, if any root lies in the right half-plane, i.e., existence of a root with positive real part ($\Re(\lambda) > 0$) in the system leads to instability. Therefore, if the system gains or loses its stability, a pair of complex conjugate roots crosses the imaginary axis, i.e, $\Re(\lambda = 0)$ and Hopf bifurcation occurs. In the case of Hopf bifurcation, we let $\lambda = i\omega$ for $\omega > 0$ in the above equation (Eq. (28)) and separate real and imaginary parts to get

$$-\omega^6 + f_2\,\omega^4 - f_4\,\omega^2 + f_6 = 0\,, \tag{29a}$$

$$f_1\,\omega^5 - f_3\,\omega^3 + f_5\,\omega = 0\,. \tag{29b}$$

It can be noted that separating real and imaginary parts gives us two simultaneous equations, which can be utilized to solve for any of two control parameters at critical/Hopf point in terms of other parameters and frequency ω. In the current analysis, we use nondimensional integral gain, k_i, and nondimensional reference/setpoint velocity signal, v_{rv}, as our control parameters. However, the appearance of exponential functions of v_{rv}, i.e., g_0 and g_1 (recall Eq. (17)) in the above equations makes them as transcendental equations and difficult to get the analytical closed-form for $k_{i,cr}$ and $v_{rv,cr}$. Therefore, we use numerical methods to solve Eqs. (29a) and (29b) to get the critical values of nondimensional integral gain and reference velocity signal, i.e., $k_{i,cr}$ and $v_{rv,cr}$ corresponding to Hopf point.

Furthermore, the stability of the steady states in the space of operating parameters is determined by calculating the real part of the rate of change of eigenvalue with respect to one of the parameters at the Hopf point. If the real part of the rate of change of eigenvalue at the Hopf point is positive, then the steady states lose stability at the Hopf point. If it is negative, then the steady states gain stability at the Hopf-point.

We emphasize that the solution of the linearized equations of the system (given by Eq. (25)) will be a periodic solution at the Hopf point, therefore, it can be represented in terms of the eigenvectors as

$$\mathbf{y}_\alpha(\tau) = A_{1\alpha}\mathbf{r}_{1\alpha}e^{i\omega\tau} + A_{2\alpha}\mathbf{r}_{2\alpha}e^{-i\omega\tau}\,, \tag{30}$$

where $\mathbf{y}_\alpha(\tau) = [y_{1\alpha}(\tau), y_{2\alpha}(\tau), y_{3\alpha}(\tau), y_{4\alpha}(\tau), y_{5\alpha}(\tau), y_{6\alpha}(\tau)]^T$, $A_{1\alpha}$ and $A_{2\alpha}$ are the arbitrary complex conjugate constants (for the real values of $\mathbf{y}_\alpha(\tau)$), and $\mathbf{r}_{1\alpha}$ and $\mathbf{r}_{2\alpha}$ are the right eigenvectors of the characteristic matrix for System-α corresponding to eigenvalues $\lambda = i\omega$ and $\lambda = -i\omega$, respectively. The right eigenvector $\mathbf{r}_{1\alpha}$ for System-α is

$$\mathbf{r}_{1\alpha} = \begin{bmatrix} 1 \\ i\omega \\ -i/\omega \\ Re_{1\alpha} + iIm_{1\alpha} \\ Re_{2\alpha} + iIm_{2\alpha} \\ Re_{3\alpha} + iIm_{3\alpha} \end{bmatrix}, \tag{31}$$

where $Re_{n\alpha}$ and $Im_{n\alpha}$ for $n = 1, 2, 3$ are defined in Appendix A. Note that the right eigenvector $\mathbf{r}_{2\alpha}$ (corresponding to the eigenvalue $\lambda = -i\omega$) is the complex conjugate of $\mathbf{r}_{1\alpha}$ and hence, not reported here for the sake of brevity. For the nonlinear analysis of our coupled system of equations, we also require the generalized left eigenvectors for the removal of secular terms [31]. Therefore, we also determine the left eigenvectors of the characteristic matrix for System-α corresponding to the eigenvalues $\lambda = i\omega$ and $\lambda = -i\omega$, and these are

$$\mathbf{l}_{1\alpha} = \begin{bmatrix} 1 & Lre_{1\alpha} + iLim_{1\alpha} & Lre_{2\alpha} + iLim_{2\alpha} & Lre_{3\alpha} + iLim_{3\alpha} & Lre_{4\alpha} + iLim_{4\alpha} & Lre_{5\alpha} + iLim_{5\alpha} \end{bmatrix}, \tag{32}$$

corresponding to the eigenvalue $\lambda = i\omega$ and its complex conjugate as $\mathbf{l}_{2\alpha}$ for the eigenvalue $\lambda = -i\omega$. $Lre_{n\alpha}$ and $Lim_{n\alpha}$, for $n = 1, 2, 3, 4, 5$ are functions of the system and control parameters and they are defined in Appendix A.

The transcendental equations governing the critical values of k_i and v_{rv} (at the Hopf point) for System-β can be obtained by following the steps mentioned above for System-α and are given by

$$\omega^4 - \left((h_{1\beta} + 2\zeta)v_{rv}\,\sigma_0 g_0 - v_{rv} g_1 h_0 h_{2\beta} + 1\right)\omega^2 + k_i v_{rv}\sigma_0 g_0 = 0\,, \tag{33a}$$

and

$$-\left(h_{1\beta} + 2\zeta + v_{rv}\sigma_0\, g_0\right)\omega^3 + \left(k_i + v_{rv}\sigma_0 g_0\right)\omega = 0\,. \tag{33b}$$

Accordingly, the solution for the linearized System-β at the Hopf point can be represented in terms of right eigenvectors as

$$\mathbf{y}_\beta(\tau) = A_{1\beta}\mathbf{r}_{1\beta}e^{i\omega\tau} + A_{2\beta}\mathbf{r}_{2\beta}e^{-i\omega\tau}\,, \tag{34}$$

where $\mathbf{y}_\beta(\tau) = [y_{1\beta}(\tau), y_{2\beta}(\tau), y_{3\beta}(\tau), y_{4\beta}(\tau)]^T$, $A_{1\beta}$ and $A_{2\beta}$ are the arbitrary complex conjugate constants, and $\mathbf{r}_{1\beta}$ and $\mathbf{r}_{2\beta}$ are the right eigenvectors of the characteristic matrix for System-β corresponding to eigenvalues $\lambda = i\omega$ and $\lambda = -i\omega$, respectively, and are defined in Appendix A. Having established the solution for the linearized System-α and System-β at the Hopf point, next we present the nonlinear analysis of our system using the method of multiple scales.

4. Nonlinear analysis using the method of multiple scales

The linear analysis in Section 3 gives us information about the stability of the steady states in different regimes of control parameter space, i.e., small perturbations around the steady states die out with time in linear stable regime, and increase in the linear unstable regime. However, the time-evolution of these perturbations in stable and unstable regimes truly depends on the existing nonlinearities in the system and, accordingly, decides the global stability of the steady states. If all perturbations, irrespective of the value of amplitude, decay with time and settle down to the steady states in the linearly stable regime, then the steady states are considered to be globally stable. However, if the time-evolution of perturbations is sensitive towards initial conditions in linear stable regime, i.e., if small perturbations decay and large perturbations lead to limit cycles, then the steady states will no longer be considered to be globally stable in the linearly stable regime. We emphasize that these dynamical characteristics of the system depend on the nature of nonlinearity present in the system

and cannot be assessed by linear stability analysis only. Therefore, it is required to carry out a detailed nonlinear analysis of System-α and System-β, specifically around the stability boundaries, to establish the global stability of steady states. Again, for the sake of brevity, we present a detailed analysis of System-α only.

We use the method of multiple scales (MMS) for the nonlinear analysis of our systems with pure slipping motion, and obtain the amplitude of limit cycles emerging from the Hopf point. We first start with defining multiple time scales as

$$T_0 = \tau\,, \quad T_1 = \epsilon\tau\,, \quad T_2 = \epsilon^2\tau\,, \ldots \tag{35}$$

with T_0 as the fast time scale, and T_i (for $i = 1, 2, \ldots$) are the slow time scales. Accordingly, the time-derivative operator gets perturbed to

$$\frac{\mathrm{d}}{\mathrm{d}\tau} = D_0 + \epsilon D_1 + \epsilon^2 D_2 + \mathcal{O}(\epsilon^3)\,, \tag{36}$$

$$\frac{\mathrm{d}^2}{\mathrm{d}\tau^2} = D_{0,0} + 2\epsilon D_{0,1} + \epsilon^2\left(2D_{0,2} + D_{1,1}\right) + \mathcal{O}(\epsilon^3)\,, \tag{37}$$

where $D_n = \dfrac{\partial}{\partial T_n}$ and $D_{m,n} = \dfrac{\partial^2}{\partial T_m \partial T_n}$. Due to the introduction of multiple time scales in the system, the solution of the perturbed nonlinear equation (Eq. (23)) can be assumed to be a series in powers of ϵ till $\mathcal{O}(\epsilon^2)$ and written as

$$\begin{aligned}\mathbf{y}_\alpha(\tau) &= \mathbf{y}_{0\alpha}\left(T_0, T_1, T_2\right) + \epsilon\mathbf{y}_{1\alpha}\left(T_0, T_1, T_2\right) + \epsilon^2\mathbf{y}_{2\alpha}\left(T_0, T_1, T_2\right)\\ &= \mathbf{y}_{0\alpha} + \epsilon\mathbf{y}_{1\alpha} + \epsilon^2\mathbf{y}_{2\alpha}\,.\end{aligned} \tag{38}$$

where $\mathbf{y}_\alpha(\tau) = [y_{1,\alpha}(\tau), y_{2,\alpha}(\tau), y_{3,\alpha}(\tau), y_{4,\alpha}(\tau), y_{5,\alpha}(\tau), y_{6,\alpha}(\tau)]^T$, $\mathbf{y}_{m\alpha}(\tau)(T_0, T_1, T_2) = [y_{1,m\alpha}(T_0, T_1, T_2), y_{2,m\alpha}(T_0, T_1, T_2), y_{3,m\alpha}(T_0, T_1, T_2), y_{4,m\alpha}(T_0, T_1, T_2), y_{5,m\alpha}(T_0, T_1, T_2), y_{6,m\alpha}(T_0, T_1, T_2)]^T$ for $m = 0, 1, 2$. Now, to understand the nature of Hopf bifurcation on the stability boundaries we perturb one of the control parameters close to the Hopf point. For the sake of simplicity of the analysis, we choose non-dimensional integral gain k_i as the bifurcation parameter and accordingly, perturb k_i from its critical value as

$$k_i = k_{i,cr} + \epsilon^2 k_1\,, \tag{39}$$

where $k_{i,cr}$ is the value of k_i at the Hopf point with $v_{rv} = v_{rv,cr}$. We emphasize that the sign of k_1 is chosen such that k_i always lies in the unstable regime. Therefore, k_1 can be negative or positive, depending on the location of the unstable region with respect to the Hopf point.

Next, we substitute Eqs. (36)–(39) in Eq. (23), expand in Taylor series for smaller values of ϵ and equate the coefficients of different orders of ϵ to zero to get:

$\mathcal{O}(\epsilon^0)$

$$D_0 y_{1,0\alpha} - y_{2,0\alpha} = 0\,, \tag{40a}$$

$$D_0 y_{2,0\alpha} - 2\kappa\, y_{5,0\alpha} + y_{3,0\alpha}k_{ic} - k_r\, y_{4,0\alpha} + (2\zeta + 2\kappa)\, y_{2,0\alpha} + \left(k_r + 1\right) y_{1,0\alpha} = 0\,, \tag{40b}$$

$$D_0 y_{3,0\alpha} - y_{1,0\alpha} = 0\,, \tag{40c}$$

$$D_0 y_{4,0\alpha} - y_{5,0\alpha} = 0\,, \tag{40d}$$

$$D_0 y_{5,0\alpha} + m_r\, k_r\, y_{4,0\alpha} - m_r\, k_r\, y_{1,0\alpha} - 2\kappa\, m_r\, y_{2,0\alpha} + m_r\, h_{1\alpha}\, y_{5,0\alpha} + m_r h_{2\alpha}\, y_{6,0\alpha} = 0\,, \tag{40e}$$

$$D_0 y_{6,0\alpha} + v_{rv} g_1 h_0 y_{5,0\alpha} + v_{rv}\sigma_0 g_0 y_{6,0\alpha} = 0\,, \tag{40f}$$

$\mathcal{O}(\epsilon^1)$

$$D_0 y_{1,1\alpha} - y_{2,1\alpha} = -D_1 y_{1,0\alpha}\,, \tag{41a}$$

$$D_0 y_{2,1\alpha} - 2\kappa\, y_{5,1\alpha} + y_{3,1\alpha}k_{ic} - k_r\, y_{4,1\alpha} + (2\zeta + 2\kappa)\, y_{2,1\alpha} + \left(k_r + 1\right) y_{1,1\alpha} = -D_1 y_{2,0\alpha}\,, \tag{41b}$$

$$D_0 y_{3,1\alpha} - y_{1,1\alpha} = -D_1 y_{3,0\alpha}\,, \tag{41c}$$

$$D_0 y_{4,1\alpha} - y_{5,1\alpha} = -D_1 y_{4,0\alpha}\,, \tag{41d}$$

$$D_0 y_{5,1\alpha} + m_r\, k_r\, y_{4,1\alpha} - m_r\, k_r\, y_{1,1\alpha} - 2\kappa\, m_r\, y_{2,1\alpha} + m_r\, h_{1\alpha}\, y_{5,1\alpha} + m_r h_{2\alpha}\, y_{6,1\alpha} = m_r\,\sigma_1\, h_{4\alpha}\, y_{5,0\alpha} y_{6,0\alpha} - D_1 y_{5,0\alpha} + m_r\,\sigma_1\, h_0\, h_{3\alpha} y_{5,0\alpha}^2\,, \tag{41e}$$

$$D_0 y_{6,1\alpha} + v_{rv} g_1 h_0 y_{5,1\alpha} + v_{rv}\sigma_0 g_0 y_{6,1\alpha} = -D_1 y_{6,0\alpha} - h_0 h_{3\alpha} y_{5,0\alpha}^2 - h_{4\alpha}\, y_{5,0\alpha} y_{6,0\alpha}\,, \tag{41f}$$

$\mathcal{O}(\epsilon^2)$

$$D_0 y_{1,2\alpha} - y_{2,2\alpha} = D_2 y_{1,0\alpha} - D_1 y_{1,1\alpha}\,, \tag{42a}$$

$$D_0 y_{2,2\alpha} - 2\kappa\, y_{5,2\alpha} + y_{3,2\alpha}k_{ic} - k_r\, y_{4,2\alpha} + (2\zeta + 2\kappa)\, y_{2,2\alpha} + \left(k_r + 1\right) y_{1,2\alpha} = -D_1 y_{2,1\alpha} - D_2 y_{2,0\alpha} - y_{3,0\alpha}k_1\,, \tag{42b}$$

$$D_0 y_{3,2\alpha} - y_{1,2\alpha} = -D_2 y_{3,0\alpha} - D_1 y_{3,1\alpha}\,, \tag{42c}$$

$$D_0 y_{4,2\alpha} - y_{5,2\alpha} = -D_2 y_{4,0\alpha} - D_1 y_{4,1\alpha}\,, \tag{42d}$$

$$\begin{aligned}&D_0 y_{5,2\alpha} + m_r\, k_r\, y_{4,2\alpha} - m_r\, k_r\, y_{1,2\alpha} - 2\kappa\, m_r\, y_{2,2\alpha} + m_r\, h_{1\alpha}\, y_{5,2\alpha} + m_r h_{2\alpha}\, y_{6,2\alpha}\\ &= -\Big(-m_r\,\sigma_1\, h_{5\alpha}\, y_{5,0\alpha}^3 - m_r\,\sigma_1\, h_{4\alpha}\, y_{5,1\alpha} y_{6,0\alpha}\\ &\quad + D_2 y_{5,0\alpha} + D_1 y_{5,1\alpha} - m_r\,\sigma_1\, h_{4\alpha}\, y_{5,0\alpha} y_{6,1\alpha}\\ &\quad - m_r\,\sigma_1\,\sigma_0\, h_{3\alpha}\, y_{5,0\alpha}^2 y_{6,0\alpha} - 2\, m_r\,\sigma_1\, h_0\, h_{3\alpha}\, y_{5,0\alpha} y_{5,1\alpha}\Big)\,,\end{aligned} \tag{42e}$$

$$\begin{aligned}&D_0 y_{6,2\alpha} + v_{rv} g_1 h_0 y_{5,2\alpha} + v_{rv}\sigma_0 g_0 y_{6,2\alpha}\\ &= -\Big(h_{5\alpha}\, y_{5,0\alpha}^3 + D_2 y_{6,0\alpha} + h_{4\alpha}\, y_{5,1\alpha} y_{6,1\alpha} + h_{4\alpha}\, y_{5,1\alpha} y_{6,0}\\ &\quad + D_1 y_{6,1\alpha} + \sigma_0\, h_{3\alpha}\, y_{5,0\alpha}^2 y_{6,0\alpha} + 2\, h_0\, h_{3\alpha}\, y_{5,0\alpha} y_{5,1\alpha}\Big)\,,\end{aligned} \tag{42f}$$

It can be easily noted that equations for the order of ϵ^0 (Eq. (40)) are identical to the linearized unperturbed coupled equations (Eq. (25)) with critical control parameters (at the Hopf point). Using similar approach, the solution for the $\mathcal{O}(\epsilon^0)$ can be written as

$$\mathbf{y}_{0\alpha(T_0, T_1, T_2)} = A_{1\alpha}\left(T_1\,, T_2\right)\mathbf{r}_{1\alpha}\mathrm{e}^{i\omega T_0} + A_{2\alpha}\left(T_1\,, T_2\right)\mathbf{r}_{2\alpha}\mathrm{e}^{-i\omega T_0}\,. \tag{43}$$

We emphasize that unlike the solution for the unperturbed linear equations, i.e., Eq. (30), $A_{1\alpha}$ and $A_{2\alpha}$ instead of being complex conjugate constants are now complex conjugate functions of slow time scales T_1 and T_2. On the substitution of this assumed form of the solution for $\mathbf{y}_{0\alpha}$ (Eq. (43)) in $\mathcal{O}(\epsilon^1)$ equations (Eq. (41)), $e^{2i\omega T_0}$, $e^{-2i\omega T_0}$, $e^{i\omega T_0}$ and $e^{-i\omega T_0}$ appear on the right-side of the equations as forcing terms. However, note that terms $e^{i\omega T_0}$ and $e^{-i\omega T_0}$ act as resonant forcing terms, causing an unbounded growth in the solution for $\mathbf{y}_{1\alpha}$. These terms are known as secular terms. Therefore, to get the bounded solution for the $\mathbf{y}_{1\alpha}$, removal of these secular terms from the resulting equations is necessary. This step further requires that left eigenvectors corresponding to $e^{i\omega T_0}$ and $e^{-i\omega T_0}$ and the vectors consisting coefficient of $e^{i\omega T_0}$ and $e^{-i\omega T_0}$ to be perpendicular to each other [31]. The coefficient vectors $\mathbf{u}_{1\alpha}$ and $\mathbf{u}_{2\alpha}$ corresponding to $e^{i\omega T_0}$ and $e^{-i\omega T_0}$ are

$$\mathbf{u}_{1\alpha} = \frac{\partial A_{1\alpha}\left(T_1, T_2\right)}{\partial T_1}\begin{bmatrix}1\\ i\omega\\ -i/\omega\\ Re_{1\alpha} + iIm_{1\alpha}\\ Re_{2\alpha} + iIm_{2\alpha}\\ Re_{3\alpha} + iIm_{3\alpha}\end{bmatrix},\quad \mathbf{u}_{2\alpha} = \frac{\partial A_{2\alpha}\left(T_1, T_2\right)}{\partial T_1}\begin{bmatrix}1\\ -i\omega\\ i/\omega\\ Re_{1\alpha} - iIm_{1\alpha}\\ Re_{2\alpha} - iIm_{2\alpha}\\ Re_{3\alpha} - iIm_{3\alpha}\end{bmatrix}. \tag{44}$$

We can observe that $\mathbf{u}_{1\alpha}$ and $\mathbf{u}_{2\alpha}$ are complex conjugate of each other and have a structure similar to right eigenvectors corresponding to $e^{i\omega T_0}$ and $e^{-i\omega T_0}$. This observation can be further justified from the fact that in $\mathcal{O}(\epsilon^1)$ equations, only quadratic nonlinear terms appear along with linear ones on the right-side further giving rise to only $e^{2i\omega T_0}$ and $e^{i\omega T_0}$ (and their complex conjugate). As discussed above, removal of secular terms corresponding to $\mathrm{e}^{i\omega T_0}$ at $\mathcal{O}(\epsilon)$ leads to $\mathbf{l}_{1\alpha}\cdot\mathbf{u}_{1\alpha} = 0$. This solvability condition further leads to

$$\begin{aligned}&\frac{\partial A_{1\alpha}\left(T_1, T_2\right)}{\partial T_1}\Big[1 - \omega\, Lim_{1\alpha} + \frac{Lim_{2\alpha}}{\omega} + Lre_{3\alpha}Re_{1\alpha} - Lim_{3\alpha}Im_{1\alpha}\\ &+ Lre_{4\alpha}Re_{2\alpha} - Lim_{4\alpha}Im_{2\alpha} + Lre_{5\alpha}Re_{3\alpha} - Lim_{5\alpha}Im_{3\alpha}\\ &+ i\Big(Lre_{5\alpha}Im_{3\alpha} + Lim_{4\alpha}Re_{2\alpha} - \frac{Lre_{2\alpha}}{\omega} + Lre_{4\alpha}Im_{2\alpha} + Lim_{5\alpha}Re_{3\alpha}\end{aligned}$$

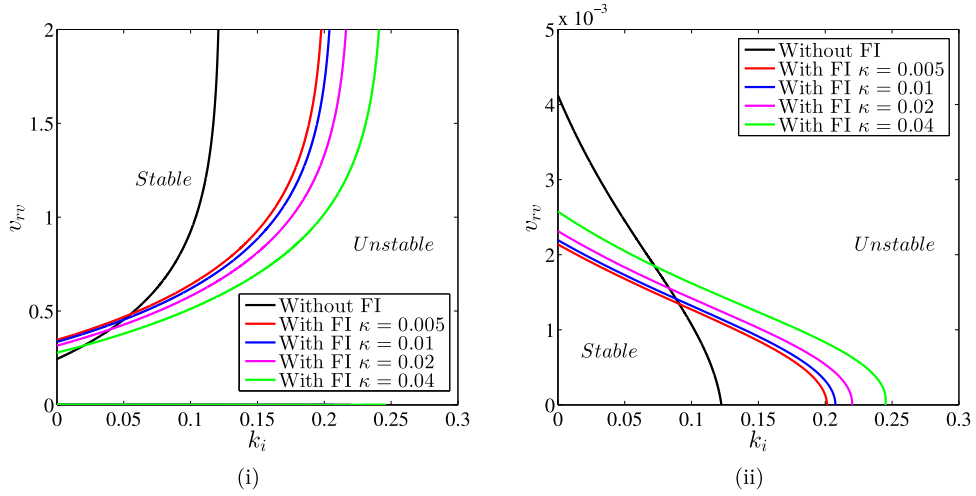

Fig. 3. Comparison of stability curves with and without FI for different values of κ for (i) larger values of v_{rv}, and (ii) for smaller values of v_{rv}. Other parameters are $\sigma_0 = 110$, $\sigma_1 = 1.37$, $\sigma_2 = 0.0823$, $f_s = 0.44$, $f_c = 0.35$, $\zeta = 0.02$, $a = 2.5$, $k_r = 0.5$, and $m_r = 2$. (For interpretation of color in this figure, the reader is referred to the web version of this article.)

$$+\omega\, Lre_{1\alpha} + Lim_{3\alpha} Re_{1\alpha} + Lre_{3\alpha} Im_{1\alpha}\Big)\Big] = 0\,. \tag{45}$$

For the general values of system and operating parameters, term inside the brackets will not be zero, which further implies

$$\frac{\partial A_{1\alpha}(T_1, T_2)}{\partial T_1} = 0\,. \tag{46}$$

Since the second solvability condition corresponding to removal of secular term for $e^{-i\omega T_0}$, i.e, $\mathbf{l}_{2\alpha}\cdot\mathbf{u}_{2\alpha} = 0$, gives rise to complex conjugate equation of Eq. (45), we get $\dfrac{\partial A_{2\alpha}(T_1, T_2)}{\partial T_1} = 0$. These results suggest that $A_{1\alpha}$ and $A_{2\alpha}$ does not depend on the slow time scale T_1 and are only the functions of slow time-scale T_2. Further, for the non-trivial solutions of $A_{1\alpha}$ and $A_{2\alpha}$, we need to proceed to the equations corresponding to the higher order of ϵ, i.e., $\mathcal{O}(\epsilon^2)$. Since in the equations corresponding to $\mathcal{O}(\epsilon^2)$ $\mathbf{y}_{1\alpha}$ appears on the right side along with $\mathbf{y}_{0\alpha}$ as forcing terms, we first solve Eqs. (41) for $\mathbf{y}_{1\alpha}$ using harmonic balance method.

After substituting the solution for $\mathbf{y}_{0\alpha}$ in Eq. (41) with the above drawn observation that A_1 and A_2 are independent of T_1, we substitute the following assumed form of the solution for $\mathbf{y}_{1\alpha}$ as a function of slow-time scale T_2

$$\begin{aligned}\mathbf{y}_{1\alpha}(T_0, T_1, T_2) = {} & A_{1\alpha}^2(T_2)\,\mathbf{B}_{11} e^{2i\omega T_0} + A_{2\alpha}^2(T_2)\,\mathbf{B}_{22} e^{-2i\omega T_0} \\ & + A_{1\alpha}(T_2)\,A_{2\alpha}(T_2)\,\mathbf{B}_{12}\,,\end{aligned} \tag{47}$$

where coefficient vector $\mathbf{B}_{11}$, $\mathbf{B}_{22}$ and $\mathbf{B}_{12}$ are defined as

$$\mathbf{B}_{11} = \begin{bmatrix} b_{11}\\ b_{12}\\ b_{13}\\ b_{14}\\ b_{15}\\ b_{16}\end{bmatrix},\quad \mathbf{B}_{22} = \begin{bmatrix} b_{21}\\ b_{22}\\ b_{23}\\ b_{24}\\ b_{25}\\ b_{26}\end{bmatrix}, \text{ and } \quad \mathbf{B}_{12} = \begin{bmatrix} b_{31}\\ b_{32}\\ b_{33}\\ b_{34}\\ b_{35}\\ b_{36}\end{bmatrix}. \tag{48}$$

On substituting this assumed form of the solution for $\mathbf{y}_{1\alpha}$ and performing harmonic balance, we get 18 algebraic simultaneous equations that can be solved for b_{mn} (for $m = 1, 2, 3$ and $n = 1..6$). These are reported in Appendix B. Since the elements of vectors $\mathbf{B}_{12}$ are the complex conjugate of $\mathbf{B}_{11}$, these are not reported here for the sake of brevity. Next, we substitute the solutions for $\mathbf{y}_{0\alpha}$ and $\mathbf{y}_{1\alpha}$ in terms of $A_{1\alpha}(T_2)$ and $A_{2\alpha}(T_2)$ in the equations corresponding to $\mathcal{O}(\epsilon^2)$. Again, the secular terms in the resulting equations can be removed using the solvability conditions of $\mathbf{l}_{1\alpha}\cdot\mathbf{V}_{1\alpha} = 0$ and $\mathbf{l}_{2\alpha}\cdot\mathbf{V}_{2\alpha} = 0$, where $\mathbf{V}_{1\alpha}$ and $\mathbf{V}_{2\alpha}$ are the coefficients vectors corresponding to $e^{i\omega T_0}$ and $e^{-i\omega T_0}$, respectively, and complex conjugate of each other. These vectors are

$$\mathbf{V}_{1\alpha} = \begin{bmatrix} \dfrac{\partial A_{1\alpha}(T_2)}{\partial T_2} \\ i\dfrac{\partial A_{1\alpha}(T_2)}{\partial T_2}\omega - \dfrac{i}{\omega}k_1 A_{1\alpha}(T[2]) \\ -\dfrac{i}{\omega}\dfrac{\partial A_{1\alpha}(T_2)}{\partial T_2} \\ \dfrac{\partial A_{1\alpha}(T_2)}{\partial T_2}\left(Re_{1\alpha} + iIm_{1\alpha}\right) \\ \dfrac{\partial A_{1\alpha}(T_2)}{\partial T_2} v_{11} + A_{1\alpha}(T_2)^2 A_{2\alpha}(T_2)\, v_{12} \\ \dfrac{\partial A_{1\alpha}(T_2)}{\partial T_2} v_{21} + A_{1\alpha}(T_2)^2 A_{2\alpha}(T_2)\, v_{22} \end{bmatrix}, \text{and}$$

$$\mathbf{V}_{2\alpha} = \begin{bmatrix} \dfrac{\partial A_{2\alpha}(T_2)}{\partial T_2} \\ -i\dfrac{\partial A_{2\alpha}(T_2)}{\partial T_2}\omega + \dfrac{i}{\omega}k_1 A_{2\alpha}(T[2]) \\ \dfrac{i}{\omega}\dfrac{\partial A_{2\alpha}(T_2)}{\partial T_2} \\ \dfrac{\partial A_{2\alpha}(T_2)}{\partial T_2}\left(Re_{1\alpha} - iIm_{1\alpha}\right) \\ \dfrac{\partial A_{2\alpha}(T_2)}{\partial T_2} \bar{v}_{11} + A_{2\alpha}(T_2)^2 A_{1\alpha}(T_2)\, \bar{v}_{12} \\ \dfrac{\partial A_{2\alpha}(T_2)}{\partial T_2} \bar{v}_{21} + A_{2\alpha}(T_2)^2 A_{1\alpha}(T_2)\, \bar{v}_{22} \end{bmatrix}. \tag{49}$$

Since $\bar{v}_{mn}$ are complex conjugate of v_{mn}, we have only defined v_{mn} in Appendix B for sake of brevity. Next, we switch to polar coordinates by substituting

$$A_{1\alpha}(T_2) = \frac{R(T_2)e^{i\phi(T_2)}}{2}\,, \quad \text{and} \quad A_{2\alpha}(T_2) = \frac{R(T_2)e^{-i\phi(T_2)}}{2}\,, \tag{50}$$

into the equation resulting from $\mathbf{l}_1\cdot\mathbf{V}_1 = 0$ and separate real and imaginary parts. On separating real and imaginary parts we get two equations and can be solved for $\partial R(T_2)/\partial T_2$ and $\partial\phi(T_2)/\partial T_2$ as

$$\frac{\partial R(T_2)}{\partial T_2} = p_{11}k_1 R + p_{12}R^3\,, \tag{51}$$

$$\frac{\partial \phi(T_2)}{\partial T_2} = p_{21}k_1 + p_{22}R^2\,, \tag{52}$$

where p_{11}, p_{12}, p_{21}, and p_{22} are functions of system parameters, control parameters at the Hopf-point, and frequency. Since the functional forms

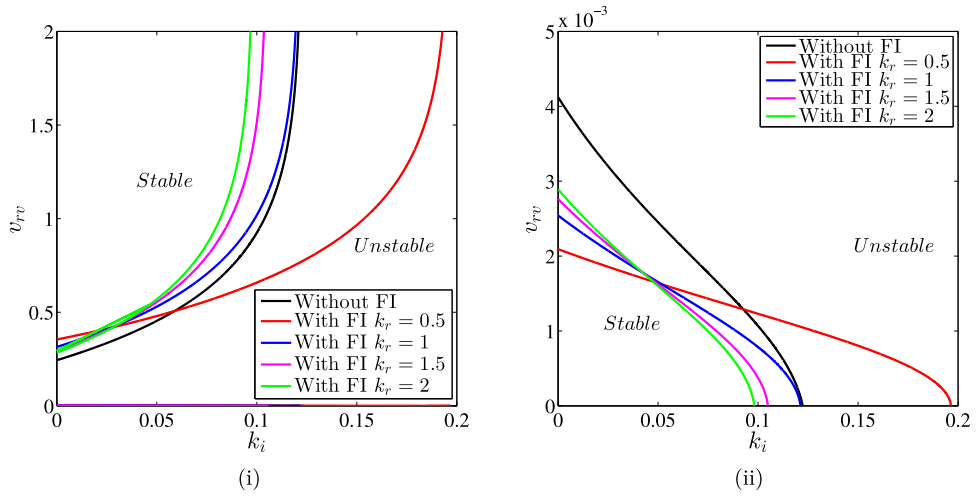

Fig. 4. Comparison of stability curves with and without FI for different values of k_r for (i) larger values of v_{rv}, and (ii) for smaller values of v_{rv}. Other parameters are $\sigma_0 = 110$, $\sigma_1 = 1.37$, $\sigma_2 = 0.0823$, $\mu_s = 0.44$, $\mu_k = 0.35$, $\zeta = 0.02$, $a = 2.5$, $\kappa = 0.001$, and $m_r = 2$.(For interpretation of color in this figure, the reader is referred to the web version of this article.)

of these terms are very lengthy, these are not reported in the paper for sake of brevity. Finally, the equation governing the evolution of amplitude R and phase ϕ in the original time scale τ can be written using Eq. (36) as

$$\frac{\mathrm{d}R}{\mathrm{d}\tau} = \epsilon\frac{\partial R}{\partial T_1} + \epsilon^2\frac{\partial R}{\partial T_2} = \epsilon^2\left(p_{11}k_1R + p_{12}R^3\right), \tag{53a}$$

$$\frac{\partial \phi}{\partial \tau} = \epsilon\frac{\partial \phi}{\partial T_1} + \epsilon^2\frac{\partial \phi}{\partial T_2} = \epsilon^2\left(p_{21}k_1 + p_{22}R^2\right). \tag{53b}$$

Accordingly, the solution in the original variables $x_{i\alpha}(\tau)$ can be obtained by utilizing Eqs. (22), (38), (43), (50) and (53). Note that Eq. (53) can also be used to determine the amplitude and stability of limit-cycles originating from Hopf point which further dictates the nature of Hopf-bifurcation. Using similar approach we can get the slow flow equations for System-β, however, for the sake of brevity this is not reported in the paper. A detailed discussion on these slow flow equations and verification of our analytical approach with numerical simulation is presented in the next section.

5. Results and discussions

As discussed in Section 3, linear stability analysis plays an important role in the subsequent nonlinear analysis since it provides information about the Hopf points on the stability boundary. Therefore, in this section, we first start with the parametric study on the linear stability of the steady states of System-α and System-β, i.e., the motion stage with and without FI, respectively. Later on, we present the validation of our analytical approach (using MMS) by comparing it against numerical simulations, which is followed by the criticality of bifurcation on the stability boundary and a detailed bifurcation analysis.

5.1. Linear stability curves

We have used the parameter values given in Table 1 for the linear and subsequent nonlinear analysis. Note that the values of k_i, v_{rv}, κ, k_r, and m_r vary throughout the analysis, and hence, the numerical values of these are not reported in Table 1. The linear stability curves produced on the control parameter space of $k_i - v_{rv}$ are shown in Figs. 3–5 for different parameter values. As discussed in Section 3, it is difficult to obtain the closed-form expressions for $k_{i,cr}$ and $v_{rv,cr}$ in terms of other system parameters and frequency, ω, these stability curves are produced by solving Eqs. (29a)–(29b) numerically using the arc-length continuation scheme discussed in [32] over a frequency range. To get a complete understanding of the effect of FI on the stability of steady-states, multiple stability curves are produced for different combinations

Table 1
Dimensional and non-dimensional parameters used in the simulation.

m_t [kg]	1.5	k_p	$2e^4$
k_d [N-s/m]	7	X_0 [m]	0.0007353
σ_0^* [N/m]	$2.2e^6$	σ_1^*, σ_2^* [N-s/m]	237, 14.25
f_c^* [N]	5.1	f_s^* [N]	6.5
ω_0 [rad/s]	115.5	ζ	0.02
σ_0	110	σ_1	1.37
σ_2	0.0823	f_s	0.44
f_c	0.35	a	2.5

of κ, k_r, and m_r. On these stability plots, the stable and unstable regions are marked by '*Stable*', and '*Unstable*', respectively.

As mentioned earlier, stability curves in the control parameter space of $k_i - v_{rv}$ are obtained by solving Eqs. (29a) and (29b) numerically for a given range of frequency $\omega \in [\omega_1, \omega_2]$, where $\omega_1 < \omega_2$, and are the functions of system parameters. On solving Eqs. (29a) and (29b), over the specified range, we get negative values of k_i and v_{rv} also. However, as we are only interested in the positive values of control parameters, these stability curves are shown in the upper right-half plane of control parameters. Furthermore, from Figs. 3–5, we can observe that two stable regimes exist on the positive space of control parameters for given values of system properties, viz., stable regime corresponding to higher values of v_{rv} and stable regime corresponding to very low values of v_{rv}. Therefore, in the subsequent analysis we present the dynamics of the motion stage for both stability regimes.

Figs. 3, 4, and 5 show the variation of stability regime for System-α, i.e., the motion stage with FI for different values of κ, k_r, and m_r, respectively. For the sake of completeness, we also compared these stability regimes with those corresponding to System-β, i.e., the motion stage without FI. From Fig. 3(i) we can observe that the increase in damping in the FI increases the overall stability of the steady-states as compared to the stability of the system without FI, and allows the use of higher values of k_i for a given value of v_{rv}. We emphasize that these non-dimensional values can be easily translated to dimensional values using nondimensional scales and parameters (Eq. (10)). As an example, in the dimensional space of parameters, the critical value of integral gain k_i^* (above which system becomes unstable) is $1.34\,e^5$ N/ms for $V_{rv} = 0.42$ m/s without FI. However, for the system with FI, the critical value of integral gain becomes $2.224\,e^5$ N/ms for $V_{rv} = 0.42$ m/s and $c_{fi} = 13.86$ Ns/m. A similar observation can be drawn from Fig. 3(ii), i.e., for very small values of v_{rv}, higher values of feedback gain can be used to suppress friction-induced vibrations. This observation can also be drawn from the fact that, in general, damping in the system increases

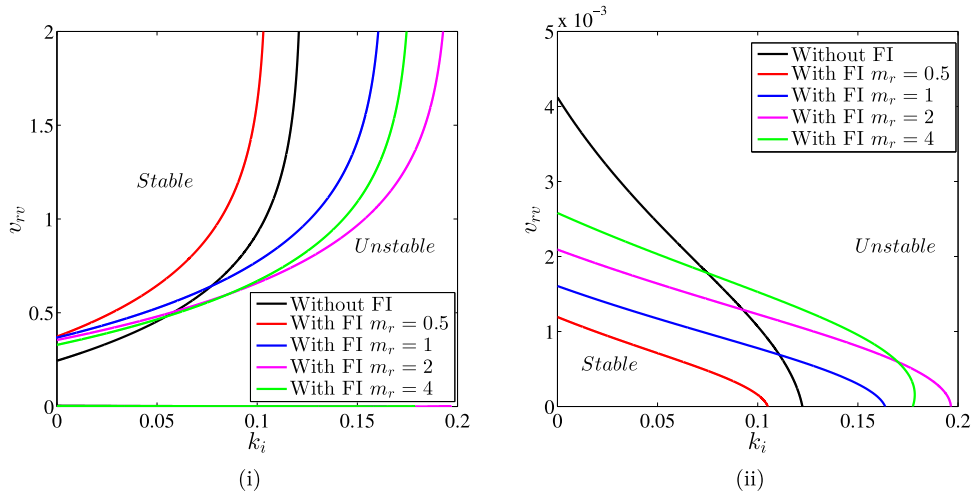

Fig. 5. Comparison of stability curves with and without FI for different values of m_r for (i) larger values of v_{rv}, and (ii) for smaller values of v_{rv}. Other parameters are $\sigma_0 = 110$, $\sigma_1 = 1.37$, $\sigma_2 = 0.0823$, $f_s = 0.44$, $f_c = 0.35$, $\zeta = 0.02$, $a = 2.5$, $\kappa = 0.001$, and $k_r = 0.5$. (For interpretation of color in figure, the reader is referred to the web version of this article.)

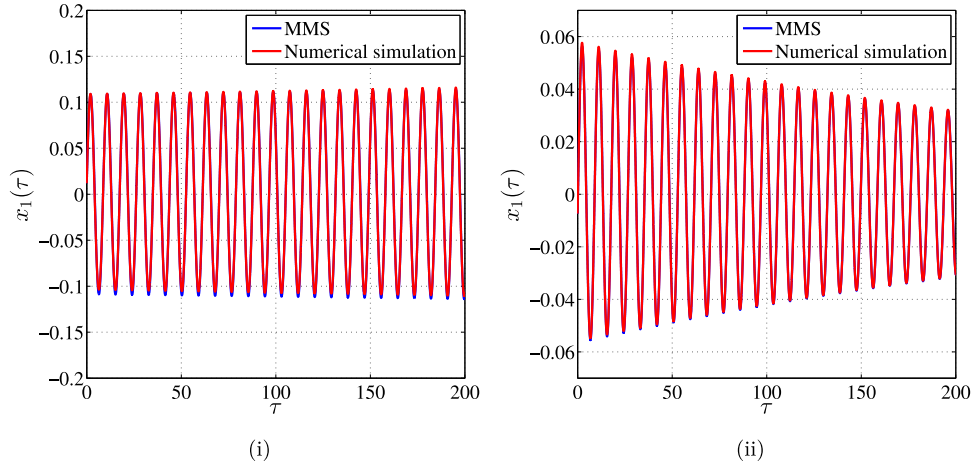

Fig. 6. Comparison of time-response of the System-α obtained from MMS and numerical simulation for two different values of k_i corresponding to (i) $k_i = 0.1636 > k_{i,cr} = 0.1536$, (ii) $k_i = 0.1436 < k_{i,cr} = 0.1536$. The other parameters for numerical simulation are $\sigma_0 = 110$, $\sigma_1 = 1.37$, $\sigma_2 = 0.0823$, $f_s = 0.44$, $f_k = 0.35$, $\zeta = 0.02$, $a = 2.5$, $\kappa = 0.001$, $k_r = 0.5$, $m_r = 2$, and $v_{rv} = 1$. (For interpretation of the references to color in this figure legend, the reader is referred to the web version of this article.)

the stability of the steady states. On a similar trend, Fig. 4 shows the variation of stability regime with the variation in stiffness ratio k_r. From this, it can be noticed that as the value of k_r increases from $k_r = 0.5$, the overall stability of the steady-state starts decreasing and even becomes smaller than the one corresponding to system-β, i.e., the motion stage without FI. This observation at first glance suggests the use of FI with stiffness lower than the stiffness of the motion stage to increase the overall stability and allow the use of higher values of feedback gain. However, on careful observation of Fig. 5, i.e., the variation of stability with variation in m_r, we notice that the overall stability of the system increases with increase in m_r, and becomes maximum at $m_r = 2$. With further increase in m_r from $m_r = 2$, the stability boundary start decreasing. We emphasize here that for Fig. 4, we have chosen $m_r = 2$, and for Fig. 5, we have used $k_r = 0.5$. In both of these scenarios product of k_r and m_r, which also presents the ratio of the natural frequencies of the motion stage to natural frequency of FI, becomes 1 for $k_r = 0.5$ in Fig. 4, and for $m_r = 2$ in Fig. 5. Therefore, from these observations, it can be concluded that the overall stability of the steady-states becomes maximum in the case of internal resonance between the motion stage and FI.

Before proceeding any further to ascertain the nature of bifurcation on the stability lobes and the amplitude of limit cycles from the slow flow equations close to the Hopf point, it is required to validate the analytical results with numerical simulation. This is presented in the next section.

5.2. Validation of analytical results from MMS

In this section, we present the validity of the analytical solutions for System-α obtained from the slow-flow equations (Eq. (53)) by comparing it with numerical simulations of Eq. (18). For this, we compare the time-response of the system (Eq. (18)) using Matlab routine 'ode45' with those obtained from the slow-flow equation and establish the accuracy of the MMS. To achieve this, we first start with System-α and choose two different sets of parameters close to Hopf point such that one point corresponds to the unstable regime ($v_{rv,cr} = 1, k_i = 0.1636 > k_{i,cr} = 0.1536$) while the other point lies in the stable regime ($v_{rv,cr} = 1, k_i = 0.1436 < k_{i,cr} = 0.1536$). Accordingly, we get a gradually increasing periodic response (till it settles down to stable limit cycle) and gradually decreasing periodic response (till it settles down to steady-state). From Fig. 6, we can easily observe that the time-response of the system obtained from MMS matches excellently with that obtained numerically using MATLAB routine 'ode45'. For the sake of completeness, we also present this comparison for System-β. The comparison between analytical and numerical simulations, corresponding to a different set of control parameters, for system-β is

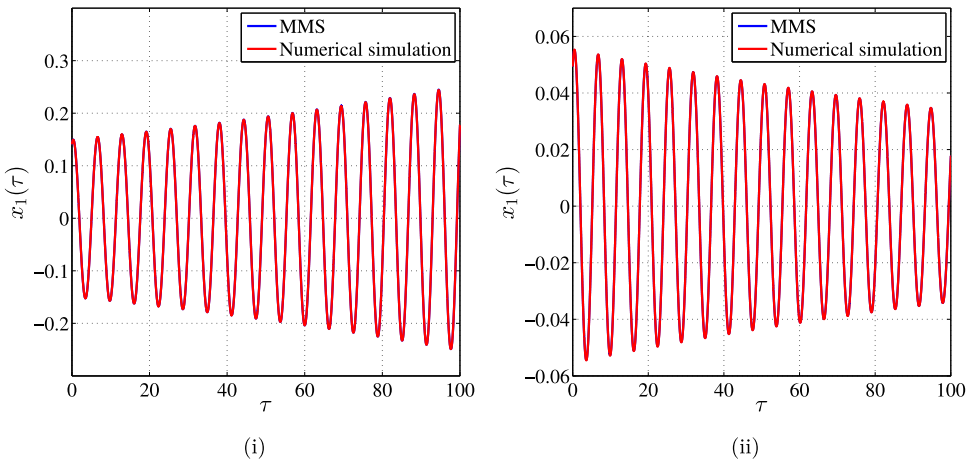

Fig. 7. Comparison of time-response of the System-β obtained from MMS and numerical simulation for two different values of k_i corresponding to (i) $k_i = 0.1139 > k_{i,cr} = 0.1039$, (ii) $k_i = 0.0939 < k_{i,cr} = 0.1039$. The other parameters for numerical simulation are $\sigma_0 = 110$, $\sigma_1 = 1.37$, $\sigma_2 = 0.0823$, $f_s = 0.44$, $f_c = 0.35$, $\zeta = 0.01$, $a = 2.5$, and $v_{rv} = 1$.

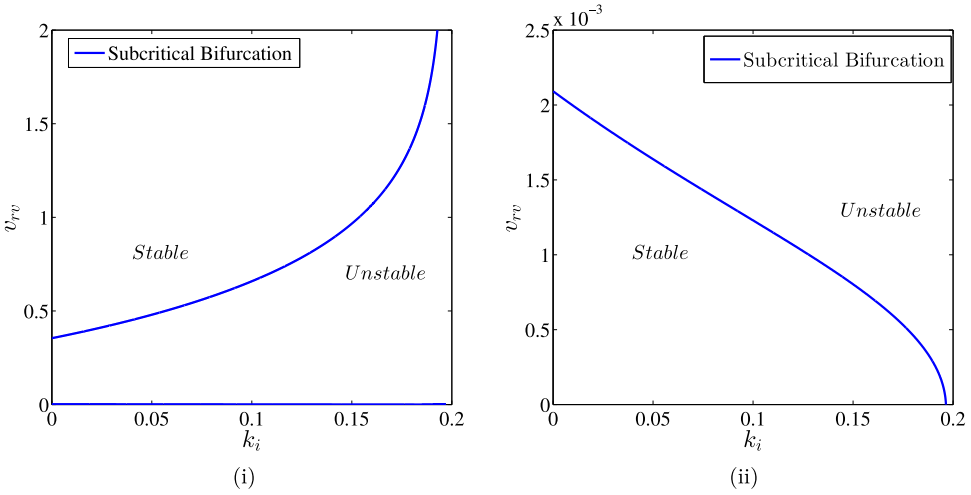

Fig. 8. Criticality of Hopf bifurcation in the System-α, i.e, motion stage with FI (i) for higher values of v_{rv}, and (ii) zoomed view of (i) for lower values of v_{rv}. The other parameters are $\sigma_0 = 110$, $\sigma_1 = 1.37$. $\sigma_2 = 0.0823$, $f_s = 0.44$, $f_c = 0.35$, $\zeta = 0.02$, $a = 2.5$, $\kappa = 0.001$, $k_r = 0.5$, and $m_r = 2$.

shown in Fig. 7. We again observe an excellent match between both approaches for System-β. Both of these observations for System-α and System-β further act as a validation of our analytical approach. Having established this agreement for both systems, next, we present the criticality of Hopf bifurcation on the stability curves.

5.3. Criticality of Hopf bifurcation

In this section, we show the nature of Hopf bifurcation associated with stability curves for System-α and System-β as obtained analytically using MMS. As discussed earlier, if either or both of the control parameters, i.e., k_i and v_{rv} changes their values such that the steady-states of the system move from the stable to the unstable regime, Hopf bifurcation occurs, and the system settles down to stable limit cycles close to stability boundaries. The amplitude of these stable limit cycles closed to stability boundaries can be determined with the help of slow flow equations (Eq. (53)) and, eventually, the nature of Hopf bifurcation. The appearance of stable limit cycles in the unstable regime closed to Hopf point implies the existence of supercritical Hopf bifurcation and global stability of the steady states in the linearly stable regime. Also, the existence of supercritical bifurcation implies that nonlinearity in the system is stabilizing in nature. However, if small-amplitude unstable limit cycles appear in the linearly stable regime, then subcritical bifurcation occurs, and steady-states lose global stability in the linearly stable regime. Therefore, in the linear stable regime small perturbation decays, while sufficiently large perturbation grows to large-amplitude solution and leading to loss of global stability.

To determine the global stability of the steady states close to the Hopf point and hence, the nature of Hopf bifurcation, we need to calculate the steady-state amplitude of limit cycles and its location relative to stability boundaries. The amplitude of limit cycles close to Hopf point can be obtained by nontrivial fixed points of the slow-flow equations, i.e., by setting $\dot{R} = 0$ in Eq. (53). Therefore, the nontrivial fixed point of Eq. (53) or the amplitude of limit cycles close to Hopf point is given by

$$R = \pm\sqrt{\frac{-p_{11}k_1}{p_{12}}}. \tag{54}$$

We emphasize here that the quantity $p_{11}k_1$ is always positive in the linear unstable regime and negative in the linear stable regime. Therefore, the nature of Hopf-bifurcation depends on the sign of p_{12} only. If p_{12} is negative, then limit cycles will exist in linearly unstable regimes only, and the Hopf bifurcation will be supercritical in nature. However, if p_{12} becomes positive, then the limit cycles will exist in the linear stable regimes, and the Hopf-bifurcation will be subcritical in nature. Therefore, the set of control parameters on the stability boundary corresponding to the transition point from subcritical to supercritical or vice-versa can be found by setting the denominator to

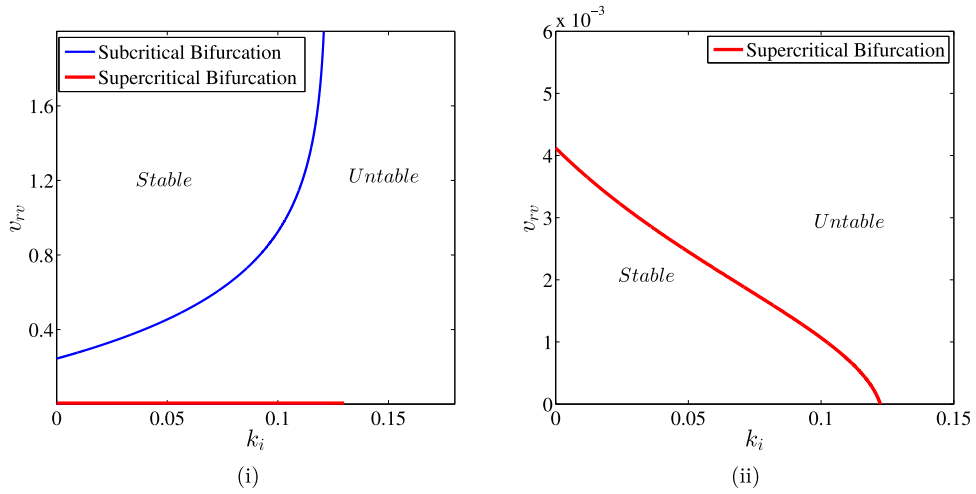

Fig. 9. Criticality of Hopf bifurcation in the System-β, i.e, motion stage without FI (i) for higher values of v_{rv}, and (ii) zoomed view of (i) for lower values of v_{rv}. Other parameters are $\sigma_0 = 110$, $\sigma_1 = 1.37$, $\sigma_2 = 0.0823$, $f_s = 0.44$, $f_c = 0.35$, $\zeta = 0.02$, and $a = 2.5$. (For interpretation of color in figure, the reader is referred to the web version of this article.)

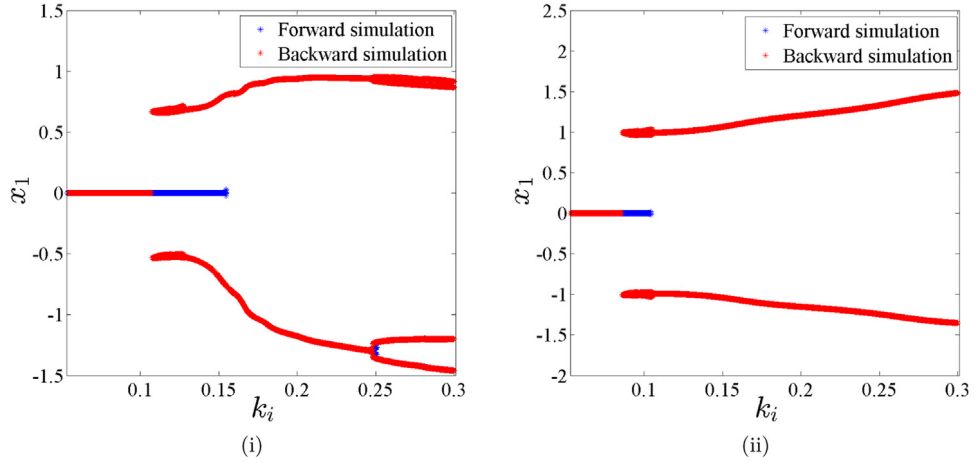

Fig. 10. Numerical bifurcation diagram with k_i as bifurcation parameter with $v_{rv} = 1$ for (i) System-α, and (ii) System-β. Other parameters are $\sigma_0 = 110$, $\sigma_1 = 1.37$, $\sigma_2 = 0.0823$, $f_s = 0.44$, $f_c = 0.35$, $\zeta = 0.02$, $a = 2.5$, $\kappa = 0.001$, $k_r = 0.5$, and $m_r = 2$. (For interpretation of color in this figure, the reader is referred to the web version of this article.)

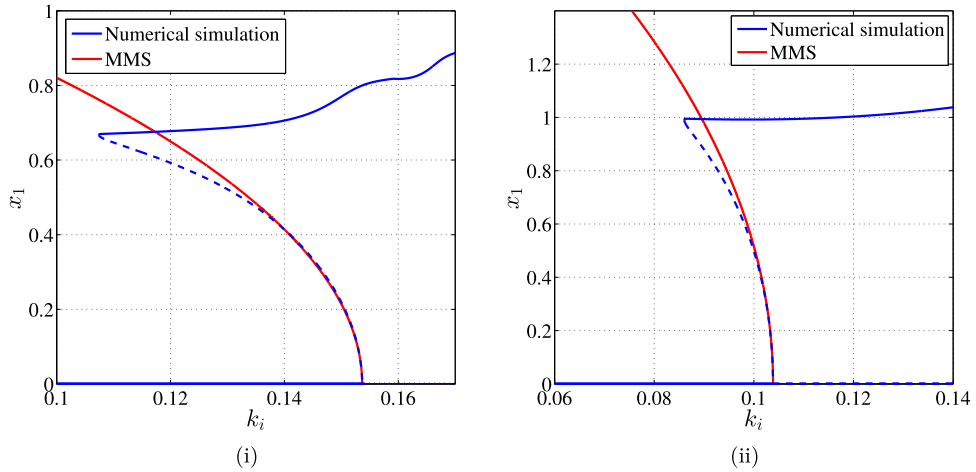

Fig. 11. Comparison of bifurcation diagram from numerical simulation and MMS with k_i as bifurcation parameter (i) System-α, and (ii) System-β. Other parameters are $\sigma_0 = 110$, $\sigma_1 = 1.37$, $\sigma_2 = 0.0823$, $f_s = 0.44$, $f_c = 0.35$, $\zeta = 0.02$, $a = 2.5$, $\kappa = 0.001$, $k_r = 0.5$, $m_r = 2$, and $v_{rv} = 1$. (For interpretation of color in this figure, the reader is referred to the web version of this article.)

0. Note that p_{12} is a function of system parameters and critical control parameters, i.e., control parameters at the Hopf point. Accordingly, we substitute $k_{i,cr}$, $v_{rv,cr}$, and associated frequency along with other system parameters and check for the sign of p_{12} to determine the nature of Hopf

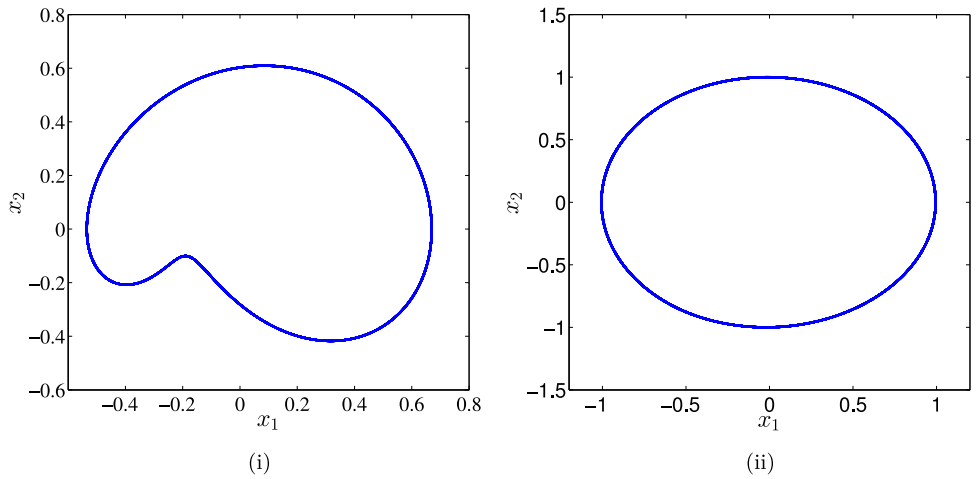

Fig. 12. Phase portraits for the stable limit cycles close to Hopf point with stick–slip motion (i) System-α, and (ii) System-β. The other parameters for numerical simulation are $\sigma_0 = 110$, $\sigma_1 = 1.37$, $\sigma_2 = 0.0823$, $f_s = 0.44$, $f_c = 0.35$, $v_{rv} = 1$ $\zeta = 0.02$, $a = 2.5$, $\kappa = 0.001$, $k_r = 0.5$, and $m_r = 2$.

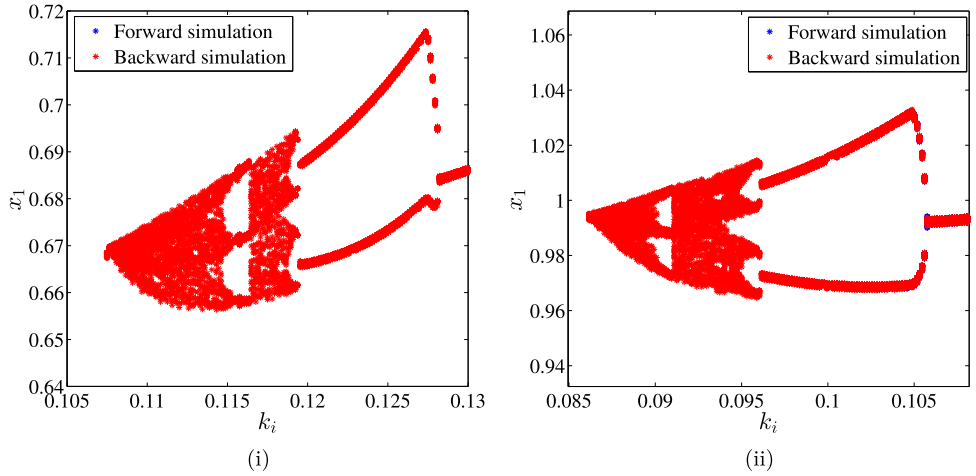

Fig. 13. Zoomed view of the numerical bifurcation near Hopf point (i) System-α, and (ii) System-β. The other parameters for the numerical simulation are $\sigma_0 = 110$, $\sigma_1 = 1.37$, $\sigma_2 = 0.0823$, $f_s = 0.44$, $f_c = 0.35$, $v_{rv} = 1$ $\zeta = 0.02$, $a = 2.5$, $\kappa = 0.001$, $k_r = 0.5$, and $m_r = 2$. (For interpretation of the references to color in this figure legend, the reader is referred to the web version of this article.)

bifurcation. The stability curves with associated Hopf bifurcations for System-α and System-β has been shown in Figs. 8 and 9, respectively. From Figs. 8i and 9i, we can easily observe that there is no transition point on the stability curves and hence, no change in the nature of Hopf bifurcation from supercritical to subcritical or vice versa. Also, we observe that there is no change in the nature of Hopf bifurcation on the inclusion of FI in the motion stage, and it remains subcritical in nature for higher values of v_{rv}. However, for lower values of v_{rv}, the nature of Hopf bifurcation changes from supercritical to subcritical due to the interaction between FI and integral control of the system (as shown in Figs. 8(ii) and 9(ii)). This observation further implies that for lower values of v_{rv}, the introduction of FI in the system increases the linear stability of steady states at the cost of losing global stability of steady states for the given system parameters.

It is to be noted here that the analytical results using MMS only give information about the amplitude of limit cycles close to Hopf-point and do not provide the overall nonlinear global behavior of our system. Therefore, we use numerical bifurcation analysis to get an understanding of the large-amplitude response of the precision motion stage, and this is presented in the next section. This step further acts as another verification of our analytical results.

5.4. Bifurcation analysis

In this section, we present numerical bifurcation analysis of System-α and System-β. For this, we have used built-in MATLAB routine 'ode45' with a high value of relative and absolute tolerance of '1e^{-13}' to solve our six first-order system of odes. The bifurcation diagrams, showing the extrema for x_1 (corresponding to $x_2 = 0$), for System-α and System-β are shown in Fig. 10(i) and (ii), respectively. These bifurcation diagrams can be plotted by fixing either of the control parameters, i.e., k_i or v_{rv} and varying other. Since in our analytical analysis, we have chosen k_i as our bifurcation parameter, we fix the value of v_{rv} and vary k_i in forward and backward direction. From both figures, we can observe the existence of subcritical Hopf bifurcation in System-α and System-β as predicted by the analytical results using MMS in the previous section. Also, the overall picture of these bifurcation diagrams is complex due to the existence of quasi-periodic and period-2 solutions and will be discussed later in this section.

After establishing a qualitative match from the analytical and numerical findings, we perform the quantitative match as well. For this step, we obtained the branch of limit cycles using fixed-arc-length continuation scheme [32]. These results are shown in Fig. 11(i) and (ii) for System-α and System-β, respectively. In these figures, solid lines represent the stable steady-state response, whereas dashed lines

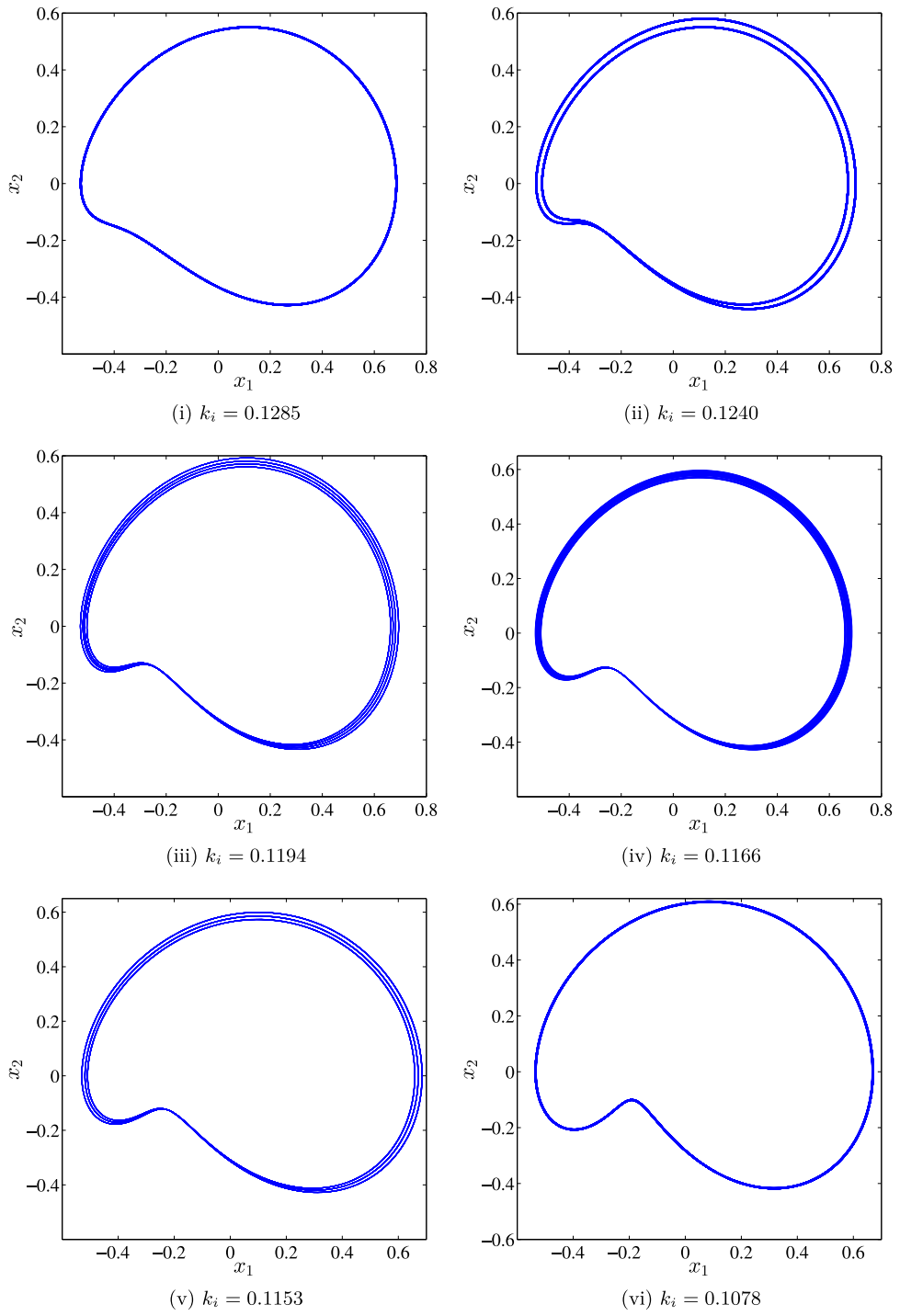

Fig. 14. Phase portraits showing the stability of limit cycles for System-α with different values of k_i close to Hopf point (i) period-1 solution, (ii) period-2 solution, (iii) period-4 solution, (iv) quasi-periodic solution, (v) period-3 solution, and (vi) period-1 solution. The other parameters for numerical simulation are $\sigma_0 = 110$, $\sigma_1 = 1.37$, $\sigma_2 = 0.0823$, $f_s = 0.44$, $f_c = 0.35$, $v_{rv} = 1$ $\zeta = 0.02$, $a = 2.5$, $\kappa = 0.001$, $k_r = 0.5$, and $m_r = 2$.

represent unstable steady-states. From both figures, we observe that there is a decent match between the numerical results from the continuation method and the MMS results for moderate amplitudes. The coexistence of unstable limit cycles with a stable equilibrium indicates that Hopf-bifurcation is subcritical in nature. Further, it can be noted from Fig. 11 the subcritical branch of limit cycles undergoes a smooth turning bifurcation resulting in limit cycles involving stick–slip motion. The illustrative phase portraits for stable limit cycles with stick–slip close to Hopf point are shown in Fig. 12.

To further explore the dynamics of a motion stage with and without FI, we examine the numerical bifurcation close to the Hopf point and away from the Hopf point. The dynamics of the motion stage with and without FI close to Hopf point is shown in Fig. 13. From Fig. 13, we can observe that for both cases, i.e., motion stage with and without FI, stable period-1 solutions lose stability and period-2, period-4, and subsequently quasi-periodic solutions start appearing as the value of k_i approaches towards $k_{i,cr}$. The occurrence of period-2 solutions signifies supercritical period-doubling bifurcation near the Hopf point for both cases of the motion stage. Period-doubling bifurcation preceded by

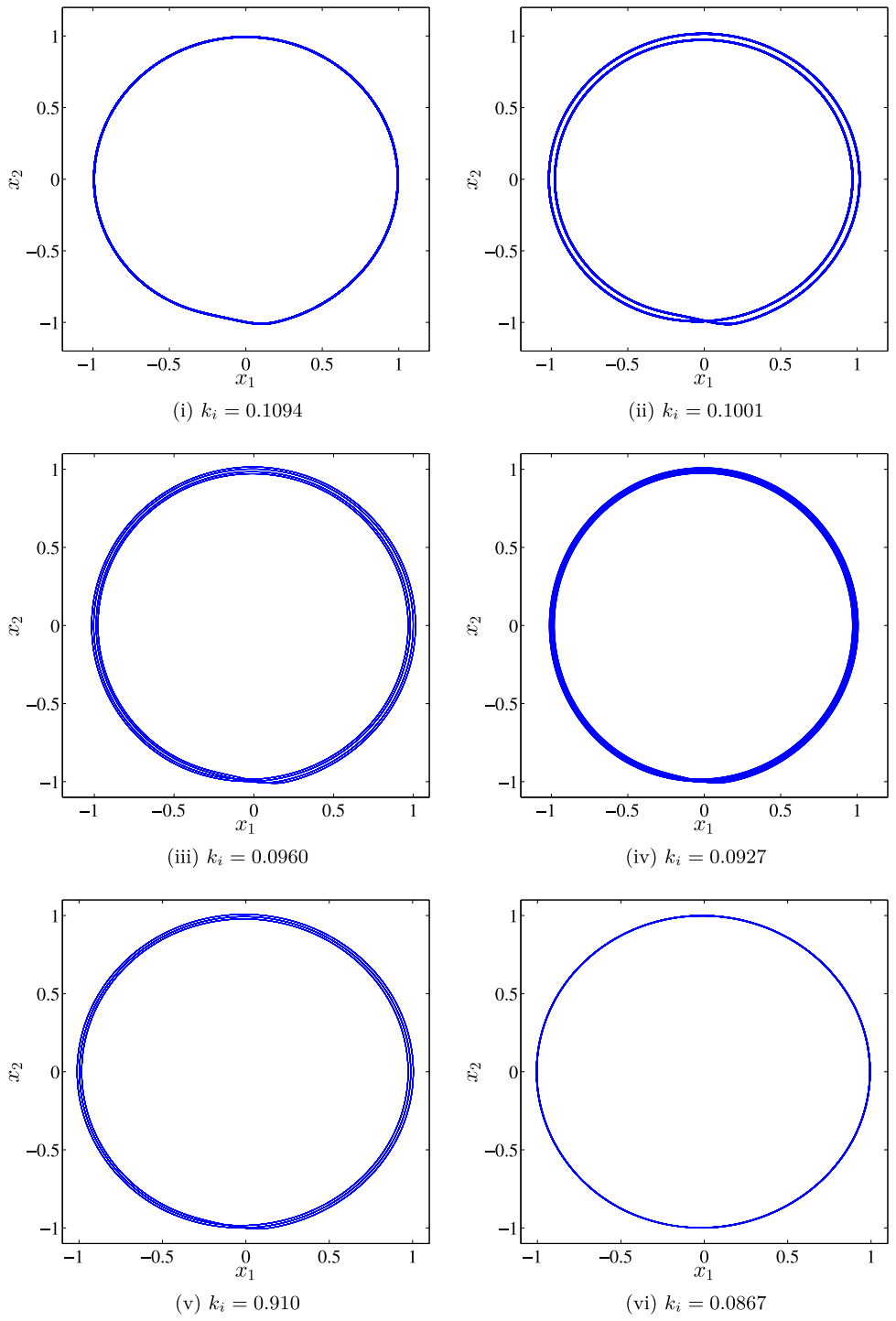

Fig. 15. Phase portraits showing the stability of limit cycles for System-β with different values of k_i close to Hopf point (i) period-1 solution, (ii) period-2 solution, (iii) period-4 solution, (iv) quasi-periodic solution, (v) period-3 solution, and (vi) period-1 solution. The other parameters for numerical simulation are $\sigma_0 = 110$, $\sigma_1 = 1.37$, $\sigma_2 = 0.0823$, $f_s = 0.44$, $f_c = 0.35$, $v_{rv} = 1$ $\zeta = 0.02$, $a = 2.5$.

symmetry-breaking bifurcation has been observed for a system with symmetrical solution (trivial fixed points) [33]. However, this dynamic phenomenon does not take place in the current system, i.e., here the periodic solutions do not hold inversion symmetry ($x(\tau) = -x(\tau + T/2)$ with T as time-period) before period-doubling bifurcation. This observation can be explained through the appearance of asymmetrical solutions, i.e., non-trivial fixed points of System-α and β (Eqs. (18)–(21)). For illustrative purpose we start with the stable periodic solution for System-α (Fig. 13(i)). As we start decreasing the value of k_i, stable stick–slip limit cycle loses stability through supercritical period-2 bifurcation, and period-2 solutions start appearing in the system. On further decreasing the value of k_i, we observe the existence of period-4 and quasi-periodic solutions, and close to Hopf point, stick–slip limit cycle again retains stability and undergoes smooth subcritical bifurcation. The representative phase-portraits for this dynamical phenomenon for both systems, i.e., for System-α and System-β are shown in Figs. 14 and 15, respectively.

The appearance of period-2 limit cycles and hence, occurrence of period-2 bifurcation can be better understood with the help of the

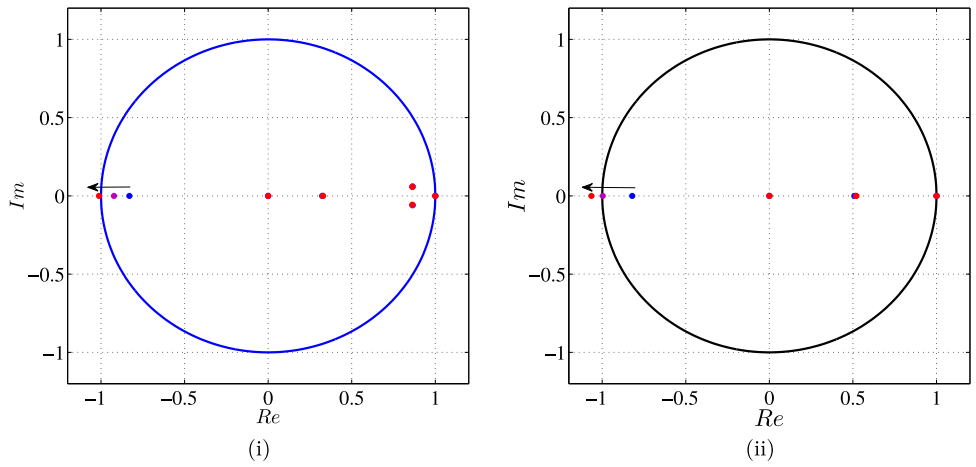

Fig. 16. Floquet multiplier crossing the unit circle through period-doubling bifurcation with blue, magenta and red colors for earlier, intermediate and final stage of Floquet multiplier with different values of k_i (i) for System-α ($k_i = 0.13$, $k_i = 0.1290$ and $k_i = 0.1281$), and (ii) for System-β ($k_i = 0.1088$, $k_i = 0.1057$ and $k_i = 0.1047$). (For interpretation of the references to color in this figure legend, the reader is referred to the web version of this article.)

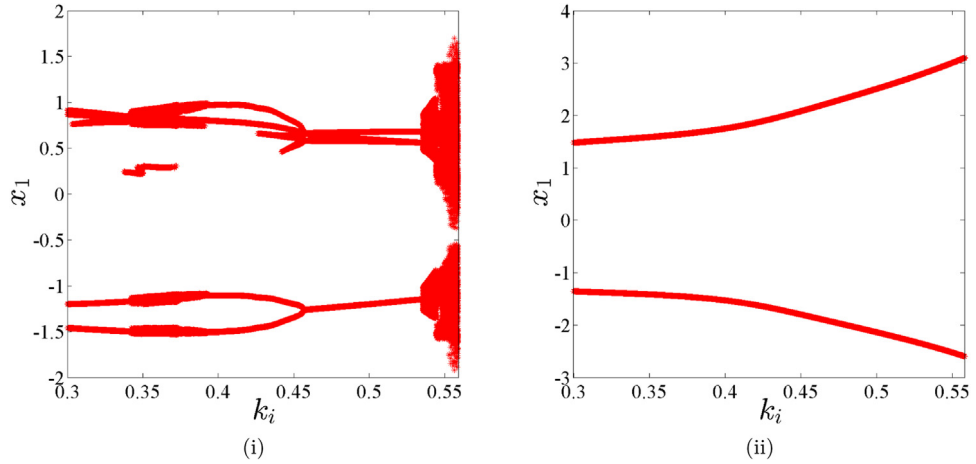

Fig. 17. Numerical bifurcation Hopf point (i) System-α, and (ii) System-β. The other parameters for numerical simulation are $\sigma_0 = 110$, $\sigma_1 = 1.37$, $\sigma_2 = 0.0823$, $f_s = 0.44$, $f_c = 0.35$, $v_{rv} = 1$ $\zeta = 0.02$, $a = 2.5$, $\kappa = 0.001$, $k_r = 0.5$, and $m_r = 2$.

stability of the period-1 solution, preceding the period-2 solutions, using Floquet theory. The movement of the various Floquet multipliers associated with the period-1 solution with decreasing k_i around the initiation of the period-2 solution for System-α and $-\beta$ are shown in Fig. 16i and ii, respectively. It can be easily observed that for both cases, the dominant Floquet multiplier crosses the unit circle at -1 on the real axis and hence, signifies the loss of stability of period-1 solution through a period-doubling bifurcation [34].

Having established the existence of supercritical period doubling bifurcation close to Hopf points, next we present the dynamics of the motion stage away from the Hopf point. For this we present the Poincare section of the system dynamics corresponding to $x_2 = 0$ for both cases, i.e., for System-α and System-β as shown in Fig. 17i and ii, respectively. From Fig. 17ii, we can observe that for System-β, period-1 solutions do not lose stability and remains stable as the value of k_i increases. However, for System-α, more complicated dynamics viz. period-2, period-4, quasi-periodic and finally chaotic solutions appear as k_i increases. The illustrative phase portraits corresponding to the lost of stability of period-1 limit cycles for System-α are shown in Fig. 18.

The appearance of chaotic solutions in System-α and eventually loss of stability of limit cycles can be further explained with the help of variation of Lyapunov exponents. Since the real part of a Floquet exponent represents Lyapunov exponent [35], we can use the following relation to determine the Lyapunov exponent

$$L.E. = \Re\left(\frac{\log(\Phi)}{T}\right), \tag{55}$$

where $L.E.$ represents the Lyapunov exponent, Φ represents the Floquet multiplier, and T represents the time-period. The variation of dominant, i.e., maximum Lyapunov exponent with k_i is shown in Fig. 19. It can be easily observed from Fig. 19 that for $k_i > \approx 0.539$, the dominant L.E. becomes positive, thus confirming the existence of chaotic attractor in the system. From this observation we can conclude that though the inclusion of FI in the system improves the stability of the system for a choice of design parameters and reduces the amplitude of motion, it also introduces complex dynamics in the system such as period-2, period-4, quasi-periodic, and chaotic solutions.

6. Conclusion

In this work, we studied the nonlinear dynamics of a servo -controlled motion stage with and without friction isolator. To include the dynamical effect of friction in the system, we have considered the LuGre model. Earlier studies with the LuGre model suggest that the nature of Hopf bifurcation always remains subcritical in nature. However, the current analysis revealed that for the given value of reference velocity, the nature of Hopf bifurcation can change due to the complex interplay between FI and integral control. A parametric

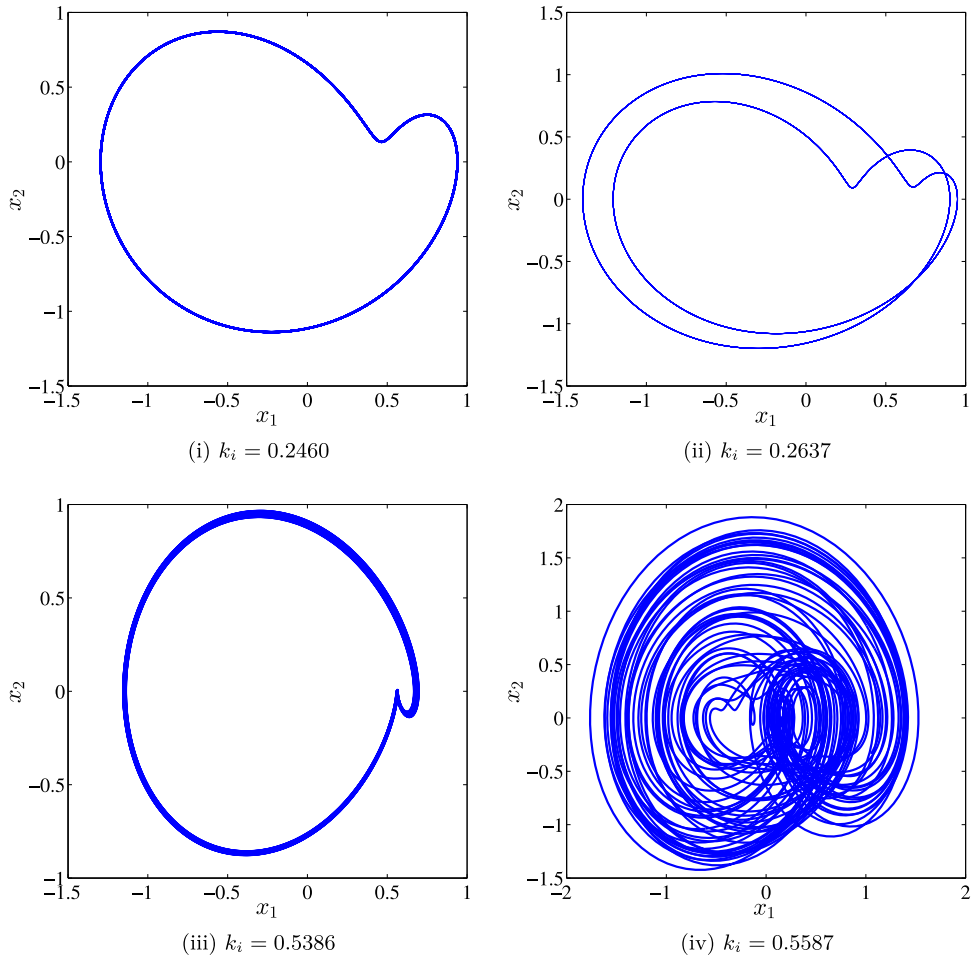

Fig. 18. Phase portraits showing the stability of limit cycles for System-α with different values of k_i away from Hopf point (i) period-1 solution, (ii) period-2 solution, (iii) quasi-periodic solution, and (iv) chaotic solution. The other parameters for numerical simulation are $\sigma_0 = 110$, $\sigma_1 = 1.37$, $\sigma_2 = 0.0823$, $f_s = 0.44$, $f_c = 0.35$, $v_{rv} = 1$ $\zeta = 0.02$, $a = 2.5$, $\kappa = 0.001$, $k_r = 0.5$, and $m_r = 2$.

study on the linear stability boundaries revealed that damping in the FI increases the overall stability of the steady states in the space of control parameters. Furthermore, we observed that the internal resonance between FI and the servo-controlled motion stage increases the stability significantly in the control parameter space.

The nonlinear dynamics of the motion stage with and without FI was analyzed analytically using the method of multiple scales and harmonic balance. We verified these analytical results by comparing them against numerical simulations. We observed an excellent match between the two approaches for both cases of motion stage with and without FI. A thorough nonlinear analysis was carried out to understand the nature of the bifurcation and limit cycle. We obtained the criticality of Hopf bifurcation on the different regions of the stability curves, and accordingly, different regions of supercritical and subcritical Hopf bifurcation were obtained. We observed that the inclusion of FI in the system did not change the nature of Hopf bifurcation and remains subcritical for higher values of control parameters. However, for lower values of control parameters, the inclusion of FI changes Hopf bifurcation from supercritical to subcritical. Therefore, it can be concluded that although FI increased the overall local stability of steady states, the global stability of steady states decreased. Furthermore, we explored the dynamics of the motion stage for both cases numerically to get a complete understanding of the effect of FI on the system and observed very rich dynamics in the system including period-doubling bifurcation, quasi-periodic, and chaotic solution. However, unlike systems with symmetrical solutions, we did not observe the occurrence of symmetry

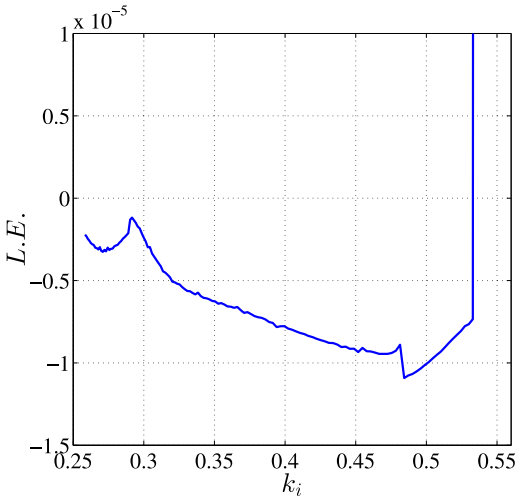

Fig. 19. Variation of dominant Lyapunov exponent with k_i. The other parameters for numerical simulation are $\sigma_0 = 110$, $\sigma_1 = 1.37$, $\sigma_2 = 0.0823$, $f_s = 0.44$, $f_c = 0.35$, $v_{rv} = 1$ $\zeta = 0.02$, $a = 2.5$, $\kappa = 0.001$, $k_r = 0.5$, and $m_r = 2$.

breaking bifurcation before period-doubling bifurcation due to the appearance of asymmetrical solutions, i.e., non-trivial fixed points.

Overall, our findings suggested that the inclusion of a FI in the system can increase the local stability and decrease the limit cycle amplitudes of a PID controlled motion stage, thus improving the performance of the manufacturing machine. However, this improvement comes at the cost of introducing more complex dynamics in the system.

CRediT authorship contribution statement

Sunit Kumar Gupta: Collection of the data, Analysis, Preparation of the manuscript. **Jiamin Wang:** Collection of the data, Analysis, Preparation of the manuscript. **Oumar R. Barry:** Collection of the data, Analysis, Preparation of the manuscript.

Declaration of competing interest

The authors declare that they have no known competing financial interests or personal relationships that could have appeared to influence the work reported in this paper.

Acknowledgment

This work is funded by National Science Foundation (NSF) Award CMMI #1855390: Toward a Fundamental Understanding of a Simple, Effective and Robust Approach for Mitigating Friction in Nanopositioning Stages.

Appendix A. Expressions used in Section 3

A.1. System-α

$$f_1 = \left(m_r\, h_{1\alpha} + 2\,\kappa\, m_r + g_0\, v_{rv}\, \sigma_0 + 2\,\zeta + 2\,\kappa\right) \tag{56}$$

$$\begin{aligned} f_2 = \big(&k_r\, m_r + k_r + 4\,\zeta\,\kappa\, m_r + m_r\, h_{1\alpha}\, g_0\, v_{rv}\, \sigma_0 + 2\,\kappa\, m_r\, g_0\, v_{rv}\, \sigma_0 \\ &- m_r\, h_{2\alpha}\, v_{rv}\, g_1\, h_0 + 2\,\zeta\, g_0\, v_{rv}\, \sigma_0 + 2\,\kappa\, g_0\, v_{rv}\, \sigma_0 + 2\,\zeta\, m_r\, h_{1\alpha} \\ &+2\,\kappa\, m_r\, h_{1\alpha} + 1\big) \end{aligned} \tag{57}$$

$$\begin{aligned} f_3 = \big(&2\,\kappa\, m_r + m_r\, h_{1\alpha} + k_i + g_0\, v_{rv}\, \sigma_0 + k_r\, m_r\, g_0\, v_{rv}\, \sigma_0 + 2\,\zeta\, k_r\, m_r \\ &+ k_r\, m_r\, h_{1\alpha} - 2\,\zeta\, m_r\, h_{2\alpha}\, v_{rv}\, g_1\, h_0 + 2\,\kappa\, m_r\, h_{1\alpha}\, g_0\, v_{rv}\, \sigma_0 \\ &+ k_r\, g_0\, v_{rv}\, \sigma_0 + 4\,\zeta\,\kappa\, m_r\, g_0\, v_{rv}\, \sigma_0 - 2\,\kappa\, m_r\, h_{2\alpha}\, v_{rv}\, g_1\, h_0 \\ &+2\,\zeta\, m_r\, h_{1\alpha}\, g_0\, v_{rv}\, \sigma_0\big) \end{aligned} \tag{58}$$

$$\begin{aligned} f_4 = \big(&2\,\kappa\, m_r\, g_0\, v_{rv}\, \sigma_0 + k_i\, g_0\, v_{rv}\, \sigma_0 - m_r\, h_{2\alpha}\, v_{rv}\, g_1\, h_0 + m_r\, h_{1\alpha}\, g_0\, v_{rv}\, \sigma_0 \\ &+ k_r\, m_r\, h_{1\alpha}\, g_0\, v_{rv}\, \sigma_0 + k_r\, m_r - k_r\, m_r\, h_{2\alpha}\, v_{rv}\, g_1\, h_0 + 2\,k_i\,\kappa\, m_r \\ &+k_i\, m_r\, h_{1\alpha} + 2\,\zeta\, k_r\, m_r\, g_0\, v_{rv}\, \sigma_0\big) \end{aligned} \tag{59}$$

$$\begin{aligned} f_5 = \big(&-k_i\, m_r\, h_{2\alpha}\, v_{rv}\, g_1\, h_0 + 2\,k_i\,\kappa\, m_r\, g_0\, v_{rv}\, \sigma_0 + k_i\, m_r\, h_{1\alpha}\, g_0\, v_{rv}\, \sigma_0 \\ &+k_r\, m_r\, g_0\, v_{rv}\, \sigma_0 + k_i\, k_r\, m_r\big) \end{aligned} \tag{60}$$

$$f_6 = k_i\, k_r\, m_r\, g_0\, v_{rv}\, \sigma_0 \tag{61}$$

$$\begin{aligned} Re_{1\alpha} &= \frac{\omega\, {k_r}^2 + k_r\,\omega - \omega^3 k_r + 4\,\omega^3\kappa\,\zeta + 4\,\omega^3\kappa^2 - 2\,\omega\,\kappa\, k_i}{\omega\, {k_r}^2 + 4\,\omega^3\kappa^2}, \\ Im_{1\alpha} &= \frac{-2\,\omega^2\kappa + 2\,\omega^4\kappa + 2\,k_r\,\omega^2\zeta - k_i\, k_r}{\omega\, {k_r}^2 + 4\,\omega^3\kappa^2} \end{aligned} \tag{62}$$

$$\begin{aligned} Re_{2\alpha} &= \frac{2\,\omega^2\kappa - 2\,\omega^4\kappa - 2\,k_r\,\omega^2\zeta + k_i\, k_r}{{k_r}^2 + 4\,\omega^2\kappa^2}, \\ Im_{2\alpha} &= \frac{\omega\, {k_r}^2 + k_r\,\omega - \omega^3 k\_r + 4\,\omega^3\kappa\,\zeta + 4\,\omega^3\kappa^2 - 2\,\omega\,\kappa\, k_i}{{k_r}^2 + 4\,\omega^2\kappa^2} \end{aligned} \tag{63}$$

$$\begin{aligned} Re_{3\alpha} = \big(&-2\,\omega^2 {v_{rv}}^2 g_1\, h_0\,\kappa\,\sigma_0\, g_0 + 2\,\omega^4 {v_{rv}}^2 g_1\, h_0\,\kappa\,\sigma_0\, g_0 - \omega^2 v_{rv}\, g_1\, h_0\, {k_r}^2 \\ &- \omega^2 v_{rv}\, g_1\, h_0\, k_r + \omega^4 v_{rv}\, g_1\, h_0\, k_r + 2\,{v_{rv}}^2 g_1\, h_0\,\omega^2\zeta\, k_r\,\sigma_0\, g_0 \\ &- {v_{rv}}^2 g_1\, h_0\, k_i\, k_r\,\sigma_0\, g_0 - 4\, v_{rv}\, g_1\, h_0\,\omega^4\kappa\,\zeta - 4\, v_{rv}\, g_1\, h_0\,\omega^4\kappa^2 \\ &+2\, v_{rv}\, g_1\, h_0\,\omega^2\kappa\, k_i\big) / \left({k_r}^2 {v_{rv}}^2\sigma_0^2 {g_0}^2 + \omega^2 {k_r}^2\right. \\ &\left.+4\,\omega^2\kappa^2 {v_{rv}}^2\sigma_0^2 {g_0}^2 + 4\,\omega^4\kappa^2\right) \end{aligned} \tag{64}$$

$$\begin{aligned} Im_{3\alpha} = \big(&-{v_{rv}}^2 g_1\, h_0\,\omega\, {k_r}^2\sigma_0\, g_0 - {v_{rv}}^2 g_1\, h_0\,\omega\, k_r\,\sigma_0\, g_0 \\ &+ {v_{rv}}^2 g_1\, h_0\,\omega^3 k_r\,\sigma_0\, g\_0 + 2\, v_{rv}\, g_1\, h_0\,\omega^3\kappa - 2\, v_{rv}\, g_1\, h_0\,\omega^5\kappa \\ &- 4\,{v_{rv}}^2 g_1\, h_0\,\omega^3\kappa\,\sigma_0\, g_0\,\zeta - 4\,{v_{rv}}^2 g_1\, h_0\,\omega^3\kappa^2\sigma_0\, g_0 \\ &+2\,{v_{rv}}^2 g_1\, h_0\,\omega\,\kappa\,\sigma_0\, g_0\, k_i - 2\, v_{rv}\, g_1\, h_0\,\omega^3 k_r\,\zeta + v_{rv}\, g_1\, h_0\,\omega\, k_i\, k_r\big) / \\ &\times \left({k_r}^2 {v_{rv}}^2\sigma_0^2 {g_0}^2 + \omega^2 {k_r}^2 + 4\,\omega^2\kappa^2 {v_{rv}}^2\sigma_0^2 {g_0}^2 + 4\,\omega^4\kappa^2\right) \end{aligned} \tag{65}$$

$$Lre_{1\alpha} = \frac{\left(2\omega^2\kappa k_r + 2\kappa^2 k\_i + {k_r}^2\zeta - k_r\kappa\right)\omega^2}{\omega^4 {k_r}^2 + 4\omega^2 k_r\kappa k_i + 4\kappa^2 {k_i}^2 + 4{k_r}^2\omega^2\zeta^2 - 8k_r\omega^2\zeta\kappa + 4\omega^2\kappa^2} \tag{66}$$

$$Lim_{1\alpha} = -\frac{\omega\left(\omega^2 {k_r}^2 + 2k_i\kappa k_r - 4k_r\omega^2\zeta\kappa + 4\omega^2\kappa^2\right)}{\omega^4 {k_r}^2 + 4\omega^2 k_r\kappa k_i + 4\kappa^2 {k_i}^2 + 4{k_r}^2\omega^2\zeta^2 - 8k_r\omega^2\zeta\kappa + 4\omega^2\kappa^2} \tag{67}$$

$$Lre_{2\alpha} = \frac{\left(\omega^2 {k_r}^2 + 2k_i\kappa k_r - 4k_r\omega^2\zeta\kappa + 4\omega^2\kappa^2\right)k_i}{\omega^4 {k_r}^2 + 4\omega^2 k_r\kappa k_i + 4\kappa^2 {k_i}^2 + 4{k_r}^2\omega^2\zeta^2 - 8k_r\omega^2\zeta\kappa + 4\omega^2\kappa^2} \tag{68}$$

$$Lim_{2\alpha}\frac{2\left(\omega^2\kappa k_r + 2\kappa^2 k_i + {k_r}^2\zeta - k_r\kappa\right)k_i\omega}{\omega^4 {k_r}^2 + 4\omega^2 k_r\kappa k_i + 4\kappa^2 {k_i}^2 + 4{k_r}^2\omega^2\zeta^2 - 8k_r\omega^2\zeta\kappa + 4\omega^2\kappa^2} \tag{69}$$

$$Lre_{3\alpha} = \frac{k_r\left(4\kappa\omega^2\zeta - 2\omega^2\kappa k_i - \omega^4 k_r - 4\zeta^2\omega^2 k_r + 2k_i k_r\zeta + \omega^2 k_r\right)}{\omega^4 {k_r}^2 + 4\omega^2 k_r\kappa k_i + 4\kappa^2 {k_i}^2 + 4{k_r}^2\omega^2\zeta^2 - 8k_r\omega^2\zeta\kappa + 4\omega^2\kappa^2} \tag{70}$$

$$Lim_{3\alpha} = \frac{\left(4k_i\zeta\kappa\omega^2 + 2\omega^4\kappa - 2\kappa {k_i}^2 - 2\omega^2\kappa - \omega^2 k_r k_i + 2k_r\omega^2\zeta\right)k_r}{\left(\omega^4 {k_r}^2 + 4\omega^2 k_r\kappa k_i + 4\kappa^2 {k_i}^2 + 4{k_r}^2\omega^2\zeta^2 - 8k_r\omega^2\zeta\kappa + 4\omega^2\kappa^2\right)\omega} \tag{71}$$

Eqs. (72) and (73) are given in Box I.

$$\begin{aligned} Lre_{5\alpha} = h_{2\alpha}\big(&\omega^2 k_r v_{rv}\sigma_0 g_0 k_i - 2\omega^4 k_r v_{rv}\sigma_0 g_0\kappa - 4\kappa v_{rv}\sigma_0 g_0 k_i\omega^2\zeta \\ &- 4\kappa^2 v_{rv}\sigma_0 g_0 k_i\omega^2 + 2\kappa v_{rv}\sigma_0 g_0 {k_i}^2 - 4\omega^4\zeta^2 k_r - 4\omega^4\zeta\kappa k_r \\ &+ 2k_i\omega^2 k_r\zeta + 4\omega^4\kappa\zeta + 4\omega^4\kappa^2 + \omega^4 {k_r}^2 + \omega^4 k_r - \omega^6 k_r \\ &+ 2\omega^2 k_r\kappa k_i - 2\omega^4\kappa k_i - 2\omega^2 v_{rv}\sigma_0 g_0 {k_r}^2\zeta - 2\omega^2\zeta k_r v_{rv}\sigma_0 g_0 \\ &+ 2\omega^2\kappa k_r v_{rv}\sigma_0 g_0 \\ &+2\kappa v_{rv}\sigma_0 g_0\omega^2 - 2\omega^4\kappa v_{rv}\sigma_0 g_0\big) / \left(\left({v_{rv}}^2\sigma_0^2 {g_0}^2 + \omega^2\right)\right. \\ &\left.\times\ \left(\omega^4 {k_r}^2 + 4\omega^2 k_r\kappa k_i + 4\kappa^2 {k_i}^2 + 4{k_r}^2\omega^2\zeta^2 - 8k_r\omega^2\zeta\kappa + 4\omega^2\kappa^2\right)\right) \end{aligned} \tag{74}$$

$$\begin{aligned} Lim_{5\alpha} = \big(&\omega h_{2\alpha}\left(2\omega^4 k_r\kappa - \omega^2 k_r k_i + 4k_i\zeta\kappa\omega^2 + 4\kappa^2 k_i\omega^2 - 2\kappa {k_i}^2\right. \\ &- 4v_{rv}\sigma_0 g_0 k_r\zeta^2\omega^2 - 4v_{rv}\sigma_0 g_0 k_r\zeta\omega^2\kappa + 2v_{rv}\sigma_0 g_0 k_r\zeta k_i \\ &+ 4\kappa v_{rv}\sigma_0 g_0\omega^2\zeta + 4\omega^2\kappa^2 v_{rv}\sigma_0 g_0 + \omega^2 v_{rv}\sigma_0 g_0 {k_r}^2 \\ &+ \omega^2 k_r v_{rv}\sigma_0 g_0 - \omega^4 k_r v_{rv}\sigma_0 g_0 + 2\kappa v_{rv}\sigma_0 g_0 k_i k_r - 2\kappa v_{rv}\sigma_0 g_0 k_i\omega^2 \\ &\left.+2\omega^2 {k_r}^2\zeta + 2k_r\omega^2\zeta - 2\omega^2\kappa k_r - 2\omega^2\kappa + 2\omega^4\kappa\right)\big) / \\ &\times \left(\left({v_{rv}}^2\sigma_0^2 {g_0}^2 + \omega^2\right)\left(\omega^4 {k_r}^2 + 4\omega^2 k_r\kappa k_i + 4\kappa^2 {k_i}^2 + 4{k_r}^2\omega^2\zeta^2\right.\right. \\ &\left.\left.-8k_r\omega^2\zeta\kappa + 4\omega^2\kappa^2\right)\right) \end{aligned} \tag{75}$$

$$Lre_{4\alpha} = \frac{2\omega^4 k_r\kappa - \omega^2 k_r k_i + 4k_i\zeta\kappa\omega^2 + 4\kappa^2 k_i\omega^2 - 2\kappa {k_i}^2 + 2\omega^2 {k_r}^2\zeta + 2k_r\omega^2\zeta - 2\omega^2\kappa k_r - 2\omega^2\kappa + 2\omega^4\kappa}{m_r\left(\omega^4 {k_r}^2 + 4\omega^2 k_r\kappa k_i + 4\kappa^2 {k_i}^2 + 4{k_r}^2\omega^2\zeta^2 - 8k_r\omega^2\zeta\kappa + 4\omega^2\kappa^2\right)} \tag{72}$$

$$Lim_{4\alpha} = \frac{\omega\left(4\zeta^2\omega^2 k_r + 4k_r\omega^2\zeta\kappa - 2k_i k_r\zeta - 4\kappa\omega^2\zeta - 4\omega^2\kappa^2 - \omega^2 {k_r}^2 - \omega^2 k_r + \omega^4 k_r - 2k_i\kappa k_r + 2\omega^2\kappa k_i\right)}{m_r\left(\omega^4 {k_r}^2 + 4\omega^2 k_r\kappa k_i + 4\kappa^2 {k_i}^2 + 4{k_r}^2\omega^2\zeta^2 - 8k_r\omega^2\zeta\kappa + 4\omega^2\kappa^2\right)} \tag{73}$$

Box I.

A.2. System-β

$$\mathbf{r_{1\beta}} = \begin{bmatrix} 1 \\ i\omega \\ -i/\omega \\ Re_{1\beta} + iIm_{1\beta} \end{bmatrix}, \tag{76}$$

$$\mathbf{l_{1\beta}} = \begin{bmatrix} 1 & Lre_{1\beta} + iLim_{1\beta} & Lre_{2\beta} + iLim_{2\beta} & Lre_{3\beta} + iLim_{3\beta} \end{bmatrix}$$

$$Re_{1\beta} = -\frac{v_{rv} g_1 h_0 \omega^2}{{v_{rv}}^2{\sigma_0}^2{g_0}^2 + \omega^2} \qquad Im_{1\beta} = \frac{-{v_{rv}}^2\sigma_0 g_0 g_1 h_0\omega}{{v_{rv}}^2{\sigma_0}^2{g_0}^2 + \omega^2}$$

$$Lre_{1\beta} = \frac{k_i\omega^2}{{k_i}^2 + \omega^2}, \quad Lim_{1\beta} = \frac{-\omega^3}{{k_i}^2 + \omega^2}, \quad Lre_{2\beta} = \frac{k_i\omega^2}{{k_i}^2 + \omega^2},$$

$$Lim_{2\beta} = \frac{{k_i}^2\omega}{{k_i}^2 + \omega^2}$$

$$Lre_{3\beta} = \frac{\omega^2 h_{2\beta}\left(k_i v_{rv}\sigma_0 g_0 - \omega^2\right)}{\left({v_{rv}}^2{\sigma_0}^2{g_0}^2 + \omega^2\right)\left(-{k_i}^2 - \omega^2\right)},$$

$$Lim_{3\beta} = \frac{\omega^3 h_{2\beta}\left(v_{rv}\sigma_0 g_0 + k_i\right)}{\left({v_{rv}}^2{\sigma_0}^2{g_0}^2 + \omega^2\right)\left(-{k_i}^2 - \omega^2\right)}$$

Appendix B. Expressions used in Section 4

$$\begin{aligned}
b_{11} = {} & \left(-2\,i\left(iRe_{3\alpha}h_{4\alpha} + iRe_{2\alpha}h_0\,h_{3\alpha} - Im_{2\alpha}h_0\,h_{3\alpha} - Im_{3\alpha}h_{4\alpha}\right)\right. \\
& \times \left(-Im_{2\alpha} + iRe_{2\alpha}\right) m_r\,\left(-h_{3\alpha}\,{v_{rv,cr}}^2\sigma_0\,\sigma_1 + 2\,i\omega\,\sigma_1 + h_{2\alpha}\right. \\
& \left.\left. + v_{rv,cr}\,h_{4\alpha}\,\sigma_1 + \sigma_0\,{v_{rv,cr}}^3 g_2\,\sigma_1\right)\omega\,\left(k_r + 4\,i\kappa\,\omega\right)\right) \\
& / \left(-8\,ik_r\,\sigma_0\,{v_{rv,cr}}^3 g_2\,\omega^3 + 8\,ik_r\,{v_{rv,cr}}^2\sigma_0\,h_{3\alpha}\,\omega^3\right. \\
& - 16\,i{v_{rv,cr}}^2\omega^3 h_{5\alpha}\,\kappa\,m_r\,h_{2\alpha} - 16\,iv_{rv,cr}\,h_{4\alpha}\,\kappa\,\omega^3 m_r\,h_{1\alpha} \\
& - 64\,\omega^6 - 8\,ik_r\,v_{rv,cr}\,h_{4\alpha}\,\omega^3 - 8\,i\omega^3 k_r\,m_r\,h_{1\alpha} \\
& + 16\,i\omega^3 m_r\,h_{2\alpha}\,v_{rv,cr}\,h_0\,h_{3\alpha}\,\kappa + 16\,i\omega^3 m_r\,h_{2\alpha}\,g_3\,{v_{rv,cr}}^3 h_0\,\kappa \\
& + 16\,iv_{rv,cr}{}^2\sigma_0\,h_{3\alpha}\,\kappa\,\omega^3 m_r\,h_{1\alpha} - 16\,i\sigma_0\,{v_{rv,cr}}^3 g_2\,\kappa\,\omega^3 m_r\,h_{1\alpha} \\
& + 32\,\omega^4\zeta\,\sigma_0\,{v_{rv,cr}}^3 g_2 - 32\,\omega^4\zeta\,{v_{rv,cr}}^2\sigma_0\,h_{3\alpha} + 16\,\omega^4 m_r\,h_{1\alpha}\,v_{rv,cr}\,h_{4\alpha} \\
& + 16\,\omega^4 m_r\,h_{2\alpha}\,{v_{rv,cr}}^2 h_{5\alpha} + 32\,\omega^4\kappa\,\sigma_0\,{v_{rv,cr}}^3 g_2 - 32\,\omega^4\kappa\,{v_{rv,cr}}^2\sigma_0\,h_{3\alpha} \\
& - 4\,\omega^2 k_r\,m_r\,h_{1\alpha}\,v_{rv,cr}\,h_{4\alpha} - 4\,\omega^2 k_r\,m_r\,h_{2\alpha}\,{v_{rv,cr}}^2 h_{5\alpha} \\
& - 4\,\omega^2 m_r\,h_{1\alpha}\,\sigma_0\,{v_{rv,cr}}^3 g_2 + 4\,\omega^2 m_r\,h_{1\alpha}\,{v_{rv,cr}}^2\sigma_0\,h_{3\alpha} + 4\,\omega^2 m_r\,h_{2\alpha}\,v_{rv,cr} \\
& \times h_0\,h_{3\alpha} + 4\,\omega^2 m_r\,h_{2\alpha}\,g_3\,{v_{rv,cr}}^3 h_0 - 8\,\omega^2\zeta\,k_r\,m_r\,v_{rv,cr}\,h_{4\alpha} \\
& + 8\,\omega^2\kappa\,k_r\,m_r\,v_{rv,cr}\,h_{4\alpha} - 4\,\omega^2 m_r\,h_{1\alpha}\,v_{rv,cr}\,h_{4\alpha} - 4\,\omega^2 m_r\,h_{2\alpha}\,v_{rv,cr}{}^2 h_{5\alpha} \\
& + 32\,\omega^4\zeta\,m_r\,h_{1\alpha} + 32\,\omega^4\zeta\,v_{rv,cr}\,h_{4\alpha} + 32\,\omega^4\kappa\,m_r\,h_{1\alpha} + 32\,\omega^4\kappa\,v_{rv,cr}\,h_{4\alpha} \\
& + 16\,\omega^4 + 16\,\omega^4 k_r\,m_r - 64\,\omega^4\kappa^2 m_r - 8\,ik_{ic}\,\omega^3 + 64\,i\omega^5\zeta + 16\,\omega^4 k_r \\
& - 4\,\omega^2 k_r\,m_r + 16\,i\omega^3\kappa\,m_r\,k_r + 64\,i\omega^5\kappa - 8\,\omega^2\zeta\,k_r\,m_r\,\sigma_0\,{v_{rv,cr}}^3 g_2 \\
& + 8\,\omega^2\zeta\,k_r\,m_r\,{v_{rv,cr}}^2\sigma_0\,h_{3\alpha} + 8\,\omega^2\kappa\,k_r\,m_r\,\sigma_0 \\
& \times {v_{rv,cr}}^3 g_2 - 8\,\omega^2\kappa\,k_r\,m_r\,{v_{rv,cr}}^2\sigma_0\,h_{3\alpha} - 4\,\omega^2 k_r\,m_r\,h_{1\alpha}\,\sigma_0\,{v_{rv,cr}}^3 g_2 \\
& + 4\,\omega^2 k_r\,m_r\,h_{1\alpha}\,{v_{rv,cr}}^2\sigma_0\,h_{3\alpha} + 4\,\omega^2 k_r\,m_r\,h_{2\alpha}\,v_{rv,cr}\,h_0\,h_{3\alpha} \\
& + 4\,\omega^2 k_r\,m_r\,h_{2\alpha}\,g_3\,{v_{rv,cr}}^3 h_0 + 16\,\omega^4 m_r\,h_{1\alpha}\,\sigma_0\,{v_{rv,cr}}^3 g_2 - 16\,\omega^4 m_r\,h_{1\alpha} \\
& \times {v_{rv,cr}}^2\sigma_0\,h_{3\alpha} - 16\,\omega^4 m_r\,h_{2\alpha}\,v_{rv,cr}\,h_0\,h_{3\alpha} - 16\,\omega^4 m_r\,h_{2\alpha}\,g_3\,{v_{rv,cr}}^3 h_0 \\
& + 32\,im_r\,h_{1\alpha}\,\omega^5 - 8\,im_r\,h_{1\alpha}\,\omega^3 - 8\,i\omega^3 v_{rv,cr}\,h_{4\alpha} + 32\,i\omega^5 v_{rv,cr}\,h_{4\alpha} \\
& + 8\,i\omega^3 {v_{rv,cr}}^2\sigma_0\,h_{3\alpha} - 8\,i\omega^3\sigma_0\,{v_{rv,cr}}^3 g_2 - 32\,i\omega^5 {v_{rv,cr}}^2\sigma_0\,h_{3\alpha} \\
& + 32\,i\omega^5\sigma_0\,{v_{rv,cr}}^3 g_2 + 2\,im_r\,\omega\,k_r\,k_{ic} - 16\,im_r\,\omega^3 k_r\,\zeta + 16\,im_r\,h_0 \\
& \times h_{2\alpha}\,h_{3\alpha}\,\omega^3 v_{rv,cr}\,\zeta - 2\,im_r\,h_{1\alpha}\,h_{3\alpha}\,k_{ic}\,\omega\,\sigma_0\,{v_{rv,cr}}^2 - 2\,im_r\,h_0\,h_{2\alpha} \\
& \times h_{3\alpha}\,k_{ic}\,\omega\,v_{rv,cr} - 16\,im_r\,g_2\,h_{1\alpha}\,\omega^3\sigma_0\,{v_{rv,cr}}^3\zeta + 16\,im_r\,g_3\,h_0\,h_{2\alpha} \\
& \times \omega^3 {v_{rv,cr}}^3\zeta + 16\,im_r\,h_{1\alpha}\,h_{3\alpha}\,\omega^3\sigma_0\,{v_{rv,cr}}^2\zeta + 2\,im_r\,g_2\,h_{1\alpha}\,k_{ic}\,\omega\,\sigma_0\,{v_{rv,cr}}^3 \\
& - 2\,im_r\,g_3\,h_0\,h_{2\alpha}\,k_{ic}\,\omega\,{v_{rv,cr}}^3 - 4\,h_{4\alpha}\,k_{ic}\,\omega^2 v_{rv,cr} - 4\,m_r\,h_{1\alpha}\,k_{ic}\,\omega^2 \\
& - 4\,g_2\,k_{ic}\,\omega^2\sigma_0\,{v_{rv,cr}}^3 + 4\,h_{3\alpha}\,k_{ic}\,\omega^2\sigma_0\,{v_{rv,cr}}^2 + m_r\,k_r\,v_{rv,cr}\,h_{4\alpha}\,k_{ic} \\
& - 8\,im_r\,k_r\,\sigma_0\,{v_{rv,cr}}^3 g_2\,\omega^3 + 8\,im_r\,k_r\,v_{rv,cr}{}^2\sigma_0\,h_{3\alpha}\,\omega^3 \\
& + 2\,im_r\,\omega\,k_r\,\sigma_0\,{v_{rv,cr}}^3 g_2 - 2\,im_r\,\omega\,k_r\,v_{rv,cr}{}^2\sigma_0\,h_{3\alpha} - 16\,im_r\,h_{2\alpha}\,h_{5\alpha} \\
& \times \omega^3 {v_{rv,cr}}^2\zeta - 16\,im_r\,h_{1\alpha}\,h_{4\alpha}\,\omega^3 v_{rv,cr}\,\zeta + 2\,im_r\,h_{2\alpha}\,h_{5\alpha}\,k_{ic}\,\omega\,{v_{rv,cr}}^2 \\
& + 2\,im_r\,h_{1\alpha}\,h_{4\alpha}\,k_{ic}\,\omega\,v_{rv,cr} - 32\,im_r\,\omega^3 {v_{rv,cr}}^2\sigma_0\,h_{3\alpha}\,\kappa^2 + 32\,im_r \\
& \times \omega^3\sigma_0\,{v_{rv,cr}}^3 g_2\,\kappa^2 + m_r\,k_r\,\sigma_0\,{v_{rv,cr}}^3 g_2\,k_{ic} - m_r\,k_r\,{v_{rv,cr}}^2\sigma_0\,h_{3\alpha}\,k_{ic} \\
& \left. -8\,im_r\,k_r\,v_{rv,cr}\,h_{4\alpha}\,\omega^3 + 2\,im_r\,\omega\,k_r\,v_{rv,cr}\,h_{4\alpha} + 32\,im_r\,\omega^3 v_{rv,cr}\,h_{4\alpha}\,\kappa^2\right)
\end{aligned} \tag{77}$$

$$\begin{aligned}
b_{12} = {} & 4\left(\left(iRe_{3\alpha}h_{4\alpha} + iRe_{2\alpha}h_0\,h_{3\alpha} - Im_{2\alpha}h_0\,h_{3\alpha} - imr_3 h_{4\alpha}\right)\right. \\
& \times \left(-Im_{2\alpha} + iRe_{2\alpha}\right) m_r\,\left(-h_{3\alpha}\,{v_{rv,cr}}^2\sigma_0\,\sigma_1 + 2\,i\omega\,\sigma_1 + h_{2\alpha}\right. \\
& \left.\left. + v_{rv,cr}\,h_{4\alpha}\,\sigma_1 + \sigma_0\,{v_{rv,cr}}^3 g_2\,\sigma_1\right)\left(k_r + 4\,i\kappa\,\omega\right)\omega^2\right) \\
& / \left(-8\,ik_r\,\sigma_0\,{v_{rv,cr}}^3 g_2\,\omega^3 + 8\,ik_r\,{v_{rv,cr}}^2\sigma_0\,h_{3\alpha}\,\omega^3\right. \\
& - 16\,i{v_{rv,cr}}^2\omega^3 h_{5\alpha}\,\kappa\,m_r\,h_{2\alpha} - 16\,iv_{rv,cr}\,h_{4\alpha}\,\kappa\,\omega^3 m_r\,h_{1\alpha} - 64\,\omega^6 \\
& - 8\,ik_r\,v_{rv,cr}\,h_{4\alpha}\,\omega^3 - 8\,i\omega^3 k_r\,m_r\,h_{1\alpha} + 16\,i\omega^3 m_r\,h_{2\alpha}\,v_{rv,cr}\,h_0\,h_{3\alpha}\,\kappa \\
& + 16\,i\omega^3 m_r\,h_{2\alpha}\,g_3\,{v_{rv,cr}}^3 h_0\,\kappa + 16\,iv_{rv,cr}{}^2\sigma_0\,h_{3\alpha}\,\kappa\,\omega^3 m_r\,h_{1\alpha} \\
& - 16\,i\sigma_0\,{v_{rv,cr}}^3 g_2\,\kappa\,\omega^3 m_r\,h_{1\alpha} + 32\,\omega^4\zeta\,\sigma_0\,{v_{rv,cr}}^3 g_2 - 32\,\omega^4\zeta\,{v_{rv,cr}}^2\sigma_0 \\
& \times h_{3\alpha} + 16\,\omega^4 m_r\,h_{1\alpha}\,v_{rv,cr}\,h_{4\alpha} + 16\,\omega^4 m_r\,h_{2\alpha}\,{v_{rv,cr}}^2 h_{5\alpha} \\
& + 32\,\omega^4\kappa\,\sigma_0\,{v_{rv,cr}}^3 g_2 - 32\,\omega^4\kappa\,{v_{rv,cr}}^2\sigma_0\,h_{3\alpha} - 4\,\omega^2 k_r\,m_r\,h_{1\alpha}\,v_{rv,cr}\,h_{4\alpha} \\
& - 4\,\omega^2 k_r\,m_r\,h_{2\alpha}\,{v_{rv,cr}}^2 h_{5\alpha} - 4\,\omega^2 m_r\,h_{1\alpha}\,\sigma_0\,{v_{rv,cr}}^3 g_2 \\
& + 4\,\omega^2 m_r\,h_{1\alpha}\,{v_{rv,cr}}^2\sigma_0\,h_{3\alpha} + 4\,\omega^2 m_r\,h_{2\alpha}\,v_{rv,cr}\,h_0\,h_{3\alpha} + 4\,\omega^2 m_r\,h_{2\alpha} \\
& \times g_3\,{v_{rv,cr}}^3 h_0 - 8\,\omega^2\zeta\,k_r\,m_r\,v_{rv,cr}\,h_{4\alpha} + 8\,\omega^2\kappa\,k_r\,m_r\,v_{rv,cr}\,h_{4\alpha} \\
& - 4\,\omega^2 m_r\,h_{1\alpha}\,v_{rv,cr}\,h_{4\alpha} - 4\,\omega^2 m_r\,h_{2\alpha}\,{v_{rv,cr}}^2 h_{5\alpha} + 32\,\omega^4\zeta\,m_r\,h_{1\alpha} \\
& + 32\,\omega^4\zeta\,v_{rv,cr}\,h_{4\alpha} + 32\,\omega^4\kappa\,m_r\,h_{1\alpha} + 32\,\omega^4\kappa\,v_{rv,cr}\,h_{4\alpha} + 16\,\omega^4 \\
& + 16\,\omega^4 k_r\,m_r - 64\,\omega^4\kappa^2 m_r - 8\,ik_{ic}\,\omega^3 + 64\,i\omega^5\zeta + 16\,\omega^4 k_r \\
& - 4\,\omega^2 k_r\,m_r + 16\,i\omega^3\kappa\,m_r\,k_r + 64\,i\omega^5\kappa - 8\,\omega^2\zeta\,k_r\,m_r\,\sigma_0\,{v_{rv,cr}}^3 g_2 \\
& + 8\,\omega^2\zeta\,k_r\,m_r\,{v_{rv,cr}}^2\sigma_0\,h_{3\alpha} + 8\,\omega^2\kappa\,k_r\,m_r\,\sigma_0 \\
& \times {v_{rv,cr}}^3 g_2 - 8\,\omega^2\kappa\,k_r\,m_r\,{v_{rv,cr}}^2\sigma_0\,h_{3\alpha} - 4\,\omega^2 k_r\,m_r\,h_{1\alpha}\,\sigma_0\,{v_{rv,cr}}^3 g_2 \\
& + 4\,\omega^2 k_r\,m_r\,h_{1\alpha}\,{v_{rv,cr}}^2\sigma_0\,h_{3\alpha} + 4\,\omega^2 k_r\,m_r\,h_{2\alpha}\,v_{rv,cr}\,h_0\,h_{3\alpha} \\
& + 4\,\omega^2 k_r\,m_r\,h_{2\alpha}\,g_3\,{v_{rv,cr}}^3 h_0 + 16\,\omega^4 m_r\,h_{1\alpha}\,\sigma_0\,{v_{rv,cr}}^3 g_2 \\
& - 16\,\omega^4 m_r\,h_{1\alpha}\,v_{rv,cr}{}^2\sigma_0\,h_{3\alpha} - 16\,\omega^4 m_r\,h_{2\alpha}\,v_{rv,cr}\,h_0\,h_{3\alpha} \\
& - 16\,\omega^4 m_r\,h_{2\alpha}\,g_3\,{v_{rv,cr}}^3 h_0 + 32\,im_r\,h_{1\alpha}\,\omega^5 - 8\,im_r\,h_{1\alpha}\,\omega^3 \\
& - 8\,i\omega^3 v_{rv,cr}\,h_{4\alpha} + 32\,i\omega^5 v_{rv,cr}\,h_{4\alpha} + 8\,i\omega^3 {v_{rv,cr}}^2\sigma_0\,h_{3\alpha} \\
& - 8\,i\omega^3\sigma_0\,{v_{rv,cr}}^3 g_2 - 32\,i\omega^5 {v_{rv,cr}}^2\sigma_0\,h_{3\alpha} + 32\,i\omega^5\sigma_0\,{v_{rv,cr}}^3 g_2 \\
& + 2\,im_r\,\omega\,k_r\,k_{ic} - 16\,im_r\,\omega^3 k_r\,\zeta + 16\,im_r\,h_0\,h_{2\alpha}\,h_{3\alpha}\,\omega^3 v_{rv,cr}\,\zeta
\end{aligned}$$

$$
\begin{aligned}
&- 2\,im_r\,h_{1\alpha}\,h_{3\alpha}\,k_{ic}\,\omega\,\sigma_0\,v_{rv,cr}{}^2 - 2\,im_r\,h_0\,h_{2\alpha}\,h_{3\alpha}\,k_{ic}\,\omega\,v_{rv,cr}\\
&- 16\,im_r\,g_2\,h_{1\alpha}\,\omega^3\sigma_0\,v_{rv,cr}{}^3\zeta + 16\,im_r\,g_3\,h_0\,h_{2\alpha}\,\omega^3 v_{rv,cr}{}^3\zeta\\
&+ 16\,im_r\,h_{1\alpha}\,h_{3\alpha}\,\omega^3\sigma_0\,v_{rv,cr}{}^2\zeta + 2\,im_r\,g_2\,h_{1\alpha}\,k_{ic}\,\omega\,\sigma_0\,v_{rv,cr}{}^3\\
&- 2\,im_r\,g_3\,h_0\,h_{2\alpha}\,k_{ic}\,\omega\,v_{rv,cr}{}^3 - 4\,h_{4\alpha}\,k_{ic}\,\omega^2 v_{rv,cr} - 4\,m_r\,h_{1\alpha}\,k_{ic}\,\omega^2\\
&- 4\,g_2\,k_{ic}\,\omega^2\sigma_0\,v_{rv,cr}{}^3 + 4\,h_{3\alpha}\,k_{ic}\,\omega^2\sigma_0\,v_{rv,cr}{}^2 + m_r\,k_r\,v_{rv,cr}\,h_{4\alpha}\,k_{ic}\\
&- 8\,im_r\,k_r\,\sigma_0\,v_{rv,cr}{}^3 g_2\,\omega^3 + 8\,im_r\,k_r\,v_{rv,cr}{}^2\sigma_0\,h_{3\alpha}\,\omega^3 + 2\,im_r\,\omega\,k_r\\
&\times\ \sigma_0\,v_{rv,cr}{}^3 g_2 - 2\,im_r\,\omega\,k_r\,v_{rv,cr}{}^2\sigma_0\,h_{3\alpha} - 16\,im_r\,h_{2\alpha}\,h_{5\alpha}\,\omega^3 v_{rv,cr}{}^2\zeta\\
&- 16\,im_r\,h_{1\alpha}\,h_{4\alpha}\,\omega^3 v_{rv,cr}\,\zeta + 2\,im_r\,h_{2\alpha}\,h_{5\alpha}\,k_{ic}\,\omega\,v_{rv,cr}{}^2 + 2\,im_r\,h_{1\alpha}\\
&\times\ h_{4\alpha}\,k_{ic}\,\omega\,v_{rv,cr} - 32\,im_r\,\omega^3 v_{rv,cr}{}^2\sigma_0\,h_{3\alpha}\,\kappa^2 + 32\,im_r\,\omega^3\sigma_0\,v_{rv,cr}{}^3 g_2\,\kappa^2\\
&+ m_r\,k_r\,\sigma_0\,v_{rv,cr}{}^3 g_2\,k_{ic} - m_r\,k_r\,v_{rv,cr}{}^2\sigma_0\,h_{3\alpha}\,k_{ic} - 8\,im_r\,k_r\,v_{rv,cr}\,h_{4\alpha}\,\omega^3\\
&+2\,im_r\,\omega\,k_r\,v_{rv,cr}\,h_{4\alpha} + 32\,im_r\,\omega^3 v_{rv,cr}\,h_{4\alpha}\,\kappa^2\big) \qquad (78)
\end{aligned}
$$

$$
\begin{aligned}
b_{13} = &\left(-i\left(iIm_{3\alpha}h_{4\alpha} + Re_{2\alpha}h_0\,h_{3\alpha} + iIm_{2\alpha}h_0\,h_{3\alpha} + h_{4\alpha}\,rer_3\right)\right.\\
&\times\left(-Im_{2\alpha} + iRe_{2\alpha}\right)m_r\left(-h_{3\alpha}\,v_{rv,cr}{}^2\sigma_0\,\sigma_1 + 2\,i\omega\,\sigma_1 + h_{2\alpha}\right.\\
&\left.\left.+v_{rv,cr}\,h_{4\alpha}\,\sigma_1 + \sigma_0\,v_{rv,cr}{}^3 g_2\,\sigma_1\right)\left(k_r + 4\,i\kappa\,\omega\right)\right)/\\
&\times\left(-8\,ik_r\,\sigma_0\,v_{rv,cr}{}^3 g_2\,\omega^3 + 8\,ik_r\,v_{rv,cr}{}^2\sigma_0\,h_{3\alpha}\,\omega^3 - 16\,iv_{rv,cr}{}^2\omega^3 h_{5\alpha}\right.\\
&\times\ \kappa\,m_r\,h_{2\alpha} - 16\,iv_{rv,cr}\,h_{4\alpha}\,\kappa\,\omega^3 m_r\,h_{1\alpha} - 64\,\omega^6 - 8\,ik_r\,v_{rv,cr}\,h_{4\alpha}\,\omega^3\\
&- 8\,i\omega^3 k_r\,m_r\,h_{1\alpha} + 16\,i\omega^3 m_r\,h_{2\alpha}\,v_{rv,cr}\,h_0\,h_{3\alpha}\,\kappa + 16\,i\omega^3 m_r\,h_{2\alpha}\\
&\times\ g_3\,v_{rv,cr}{}^3 h_0\,\kappa + 16\,iv_{rv,cr}{}^2\sigma_0\,h_{3\alpha}\,\kappa\,\omega^3 m_r\,h_{1\alpha} - 16\,i\sigma_0\,v_{rv,cr}{}^3 g_2\\
&\times\ \kappa\,\omega^3 m_r\,h_{1\alpha} + 32\,\omega^4\zeta\,\sigma_0\,v_{rv,cr}{}^3 g_2 - 32\,\omega^4\zeta\,v_{rv,cr}{}^2\sigma_0\,h_{3\alpha}\\
&+ 16\,\omega^4 m_r\,h_{1\alpha}\,v_{rv,cr}\,h_{4\alpha} + 16\,\omega^4 m_r\,h_{2\alpha}\,v_{rv,cr}{}^2 h_{5\alpha} + 32\,\omega^4\kappa\,\sigma_0\\
&\times\ v_{rv,cr}{}^3 g_2 - 32\,\omega^4\kappa\,v_{rv,cr}{}^2\sigma_0\,h_{3\alpha} - 4\,\omega^2 k_r\,m_r\,h_{1\alpha}\,v_{rv,cr}\,h_{4\alpha}\\
&- 4\,\omega^2 k_r\,m_r\,h_{2\alpha}\,v_{rv,cr}{}^2 h_{5\alpha} - 4\,\omega^2 m_r\,h_{1\alpha}\,\sigma_0\,v_{rv,cr}{}^3 g_2 + 4\,\omega^2 m_r\,h_{1\alpha}\\
&\times\ v_{rv,cr}{}^2\sigma_0\,h_{3\alpha} + 4\,\omega^2 m_r\,h_{2\alpha}\,v_{rv,cr}\,h_0\,h_{3\alpha} + 4\,\omega^2 m_r\,h_{2\alpha}\,g_3\,v_{rv,cr}{}^3 h_0\\
&- 8\,\omega^2\zeta\,k_r\,m_r\,v_{rv,cr}\,h_{4\alpha} + 8\,\omega^2\kappa\,k_r\,m_r\,v_{rv,cr}\,h_{4\alpha} - 4\,\omega^2 m_r\,h_{1\alpha}\,v_{rv,cr}\,h_{4\alpha}\\
&- 4\,\omega^2 m_r\,h_{2\alpha}\,v_{rv,cr}{}^2 h_{5\alpha} + 32\,\omega^4\zeta\,m_r\,h_{1\alpha} + 32\,\omega^4\zeta\,v_{rv,cr}\,h_{4\alpha}\\
&+ 32\,\omega^4\kappa\,m_r\,h_{1\alpha} + 32\,\omega^4\kappa\,v_{rv,cr}\,h_{4\alpha} + 16\,\omega^4 + 16\,\omega^4 k_r\,m_r - 64\,\omega^4\kappa^2 m_r\\
&- 8\,ik_{ic}\,\omega^3 + 64\,i\omega^5\zeta + 16\,\omega^4 k_r - 4\,\omega^2 k_r\,m_r + 16\,i\omega^3\kappa\,m_r\,k_r + 64\,i\omega^5\kappa\\
&- 8\,\omega^2\zeta\,k_r\,m_r\,\sigma_0\,v_{rv,cr}{}^3 g_2 + 8\,\omega^2\zeta\,k_r\,m_r\,v_{rv,cr}{}^2\sigma_0\,h_{3\alpha} + 8\,\omega^2\kappa\,k_r\,m_r\\
&\times\ \sigma_0\,v_{rv,cr}{}^3 g_2 - 8\,\omega^2\kappa\,k_r\,m_r\,v_{rv,cr}{}^2\sigma_0\,h_{3\alpha} - 4\,\omega^2 k_r\,m_r\,h_{1\alpha}\,\sigma_0\,v_{rv,cr}{}^3 g_2\\
&+ 4\,\omega^2 k_r\,m_r\,h_{1\alpha}\,v_{rv,cr}{}^2\sigma_0\,h_{3\alpha} + 4\,\omega^2 k_r\,m_r\,h_{2\alpha}\,v_{rv,cr}\,h_0\,h_{3\alpha}\\
&+ 4\,\omega^2 k_r\,m_r\,h_{2\alpha}\,g_3\,v_{rv,cr}{}^3 h_0 + 4\,\omega^2 m_r\,h_{1\alpha}\,\sigma_0\,v_{rv,cr}{}^3 g_2\\
&- 4\,\omega^2 m_r\,h_{2\alpha}\,g_3\,v_{rv,cr}{}^3 h_0 + 16\,\omega^4 m_r\,h_{1\alpha}\,\sigma_0\,v_{rv,cr}{}^3 g_2 - 16\,\omega^4 m_r\\
&\times\ h_{1\alpha}\,v_{rv,cr}{}^2\sigma_0\,h_{3\alpha} - 16\,\omega^4 m_r\,h_{2\alpha}\,v_{rv,cr}\,h_0\,h_{3\alpha} - 16\,\omega^4 m_r\,h_{2\alpha}\,g_3\\
&\times\ v_{rv,cr}{}^3 h_0 + 32\,im_r\,h_{1\alpha}\,\omega^5 - 8\,im_r\,h_{1\alpha}\,\omega^3 - 8\,i\omega^3 v_{rv,cr}\,h_{4\alpha}\\
&+ 32\,i\omega^5 v_{rv,cr}\,h_{4\alpha} + 8\,i\omega^3 v_{rv,cr}{}^2\sigma_0\,h_{3\alpha} - 8\,i\omega^3\sigma_0\,v_{rv,cr}{}^3 g_2\\
&- 32\,i\omega^5 v_{rv,cr}{}^2\sigma_0\,h_{3\alpha} + 32\,i\omega^5\sigma_0\,v_{rv,cr}{}^3 g_2 + 2\,im_r\,\omega\,k_r\,k_{ic}\\
&- 16\,im_r\,\omega^3 k_r\,\zeta + 16\,im_r\,h_0\,h_{2\alpha}\,h_{3\alpha}\,\omega^3 v_{rv,cr}\,\zeta - 2\,im_r\,h_{1\alpha}\,h_{3\alpha}\,k_{ic}\\
&\times\ \omega\,\sigma_0\,v_{rv,cr}{}^2 - 2\,im_r\,h_0\,h_{2\alpha}\,h_{3\alpha}\,k_{ic}\,\omega\,v_{rv,cr} - 16\,im_r\,g_2\,h_{1\alpha}\,\omega^3\sigma_0\\
&\times\ v_{rv,cr}{}^3\zeta + 16\,im_r\,g_3\,h_0\,h_{2\alpha}\,\omega^3 v_{rv,cr}{}^3\zeta + 16\,im_r\,h_{1\alpha}\,h_{3\alpha}\,\omega^3\sigma_0\,v_{rv,cr}{}^2\zeta\\
&+ 2\,im_r\,g_2\,h_{1\alpha}\,k_{ic}\,\omega\,\sigma_0\,v_{rv,cr}{}^3 - 2\,im_r\,g_3\,h_0\,h_{2\alpha}\,k_{ic}\,\omega\,v_{rv,cr}{}^3\\
&- 4\,h_{4\alpha}\,k_{ic}\,\omega^2 v_{rv,cr} - 4\,m_r\,h_{1\alpha}\,k_{ic}\,\omega^2 - 4\,g_2\,k_{ic}\,\omega^2\sigma_0\,v_{rv,cr}{}^3\\
&+ 4\,h_{3\alpha}\,k_{ic}\,\omega^2\sigma_0\,v_{rv,cr}{}^2 + m_r\,k_r\,v_{rv,cr}\,h_{4\alpha}\,k_{ic} - 8\,im_r\,k_r\,\sigma_0\,v_{rv,cr}{}^3 g_2\,\omega^3\\
&+ 8\,im_r\,k_r\,v_{rv,cr}{}^2\sigma_0\,h_{3\alpha}\,\omega^3 + 2\,im_r\,\omega\,k_r\,\sigma_0\,v_{rv,cr}{}^3 g_2 - 2\,im_r\,\omega\,k_r\\
&\times\ v_{rv,cr}{}^2\sigma_0\,h_{3\alpha} - 16\,im_r\,h_{2\alpha}\,h_{5\alpha}\,\omega^3 v_{rv,cr}{}^2\zeta - 16\,im_r\,h_{1\alpha}\,h_{4\alpha}\,\omega^3 v_{rv,cr}\,\zeta\\
&+ 2\,im_r\,h_{2\alpha}\,h_{5\alpha}\,k_{ic}\,\omega\,v_{rv,cr}{}^2 + 2\,im_r\,h_{1\alpha}\,h_{4\alpha}\,k_{ic}\,\omega\,v_{rv,cr}\\
&- 32\,im_r\,\omega^3 v_{rv,cr}{}^2\sigma_0\,h_{3\alpha}\,\kappa^2 + 32\,im_r\,\omega^3\sigma_0\,v_{rv,cr}{}^3 g_2\,\kappa^2 + m_r\,k_r\,\sigma_0\\
&\times\ v_{rv,cr}{}^3 g_2\,k_{ic} - m_r\,k_r\,v_{rv,cr}{}^2\sigma_0\,h_{3\alpha}\,k_{ic} - 8\,im_r\,k_r\,v_{rv,cr}\,h_{4\alpha}\,\omega^3\\
&\left.+2\,im_r\,\omega\,k_r\,v_{rv,cr}\,h_{4\alpha} + 32\,im_r\,\omega^3 v_{rv,cr}\,h_{4\alpha}\,\kappa^2\right) \qquad (79)
\end{aligned}
$$

$$
\begin{aligned}
b_{14} = &-\left(\left(iRe_{3\alpha}h_{4\alpha} + iRe_{2\alpha}h_0\,h_{3\alpha} - Im_{2\alpha}h_0\,h_{3\alpha} - Im_{3\alpha}h_{4\alpha}\right)\right.\\
&\times\left(-Im_{2\alpha} + iRe_{2\alpha}\right)m_r\left(-h_{3\alpha}\,v_{rv,cr}{}^2\sigma_0\,\sigma_1 + 2\,i\omega\,\sigma_1 + h_{2\alpha}\right.\\
&\left.+v_{rv,cr}\,h_{4\alpha}\,\sigma_1 + \sigma_0\,v_{rv,cr}{}^3 g_2\,\sigma_1\right)\left(k_{ic} + 2\,i\omega\,k_r - 8\,\omega^2\zeta + 2\,i\omega\right.\\
&\left.-8\,i\omega^3 - 8\,\omega^2\kappa\right)\omega\big)/\left(-8\,ik_r\,\sigma_0\,v_{rv,cr}{}^3 g_2\,\omega^3 + 8\,ik_r\,v_{rv,cr}{}^2\sigma_0\,h_{3\alpha}\,\omega^3\right.\\
&- 16\,iv_{rv,cr}{}^2\omega^3 h_{5\alpha}\,\kappa\,m_r\,h_{2\alpha} - 16\,iv_{rv,cr}\,h_{4\alpha}\,\kappa\,\omega^3 m_r\,h_{1\alpha} - 64\,\omega^6\\
&- 8\,ik_r\,v_{rv,cr}\,h_{4\alpha}\,\omega^3 - 8\,i\omega^3 k_r\,m_r\,h_{1\alpha} + 16\,i\omega^3 m_r\,h_{2\alpha}\,v_{rv,cr}\,h_0\,h_{3\alpha}\,\kappa\\
&+ 16\,i\omega^3 m_r\,h_{2\alpha}\,g_3\,v_{rv,cr}{}^3 h_0\,\kappa + 16\,iv_{rv,cr}{}^2\sigma_0\,h_{3\alpha}\,\kappa\,\omega^3 m_r\,h_{1\alpha}\\
&- 16\,i\sigma_0\,v_{rv,cr}{}^3 g_2\,\kappa\,\omega^3 m_r\,h_{1\alpha} + 32\,\omega^4\zeta\,\sigma_0\,v_{rv,cr}{}^3 g_2 - 32\,\omega^4\zeta\,v_{rv,cr}{}^2\sigma_0\\
&\times\ h_{3\alpha} + 16\,\omega^4 m_r\,h_{1\alpha}\,v_{rv,cr}\,h_{4\alpha} + 16\,\omega^4 m_r\,h_{2\alpha}\,v_{rv,cr}{}^2 h_{5\alpha} + 32\,\omega^4\kappa\\
&\times\ \sigma_0\,v_{rv,cr}{}^3 g_2 - 32\,\omega^4\kappa\,v_{rv,cr}{}^2\sigma_0\,h_{3\alpha} - 4\,\omega^2 k_r\,m_r\,h_{1\alpha}\,v_{rv,cr}\,h_{4\alpha}\\
&- 4\,\omega^2 k_r\,m_r\,h_{2\alpha}\,v_{rv,cr}{}^2 h_{5\alpha} - 4\,\omega^2 m_r\,h_{1\alpha}\,\sigma_0\,v_{rv,cr}{}^3 g_2\\
&+ 4\,\omega^2 m_r\,h_{1\alpha}\,v_{rv,cr}{}^2\sigma_0\,h_{3\alpha} + 4\,\omega^2 m_r\,h_{2\alpha}\,v_{rv,cr}\,h_0\,h_{3\alpha} + 4\,\omega^2 m_r\\
&\times\ h_{2\alpha}\,g_3\,v_{rv,cr}{}^3 h_0 - 8\,\omega^2\zeta\,k_r\,m_r\,v_{rv,cr}\,h_{4\alpha} + 8\,\omega^2\kappa\,k_r\,m_r\,v_{rv,cr}\,h_{4\alpha}\\
&- 4\,\omega^2 m_r\,h_{1\alpha}\,v_{rv,cr}\,h_{4\alpha} - 4\,\omega^2 m_r\,h_{2\alpha}\,v_{rv,cr}{}^2 h_{5\alpha} + 32\,\omega^4\zeta\,m_r\,h_{1\alpha}\\
&+ 32\,\omega^4\zeta\,v_{rv,cr}\,h_{4\alpha} + 32\,\omega^4\kappa\,m_r\,h_{1\alpha} + 32\,\omega^4\kappa\,v_{rv,cr}\,h_{4\alpha} + 16\,\omega^4\\
&+ 16\,\omega^4 k_r\,m_r - 64\,\omega^4\kappa^2 m_r - 8\,ik_{ic}\,\omega^3 + 64\,i\omega^5\zeta + 16\,\omega^4 k_r - 4\,\omega^2 k_r\,m_r\\
&+ 16\,i\omega^3\kappa\,m_r\,k_r + 64\,i\omega^5\kappa - 8\,\omega^2\zeta\,k_r\,m_r\,\sigma_0\,v_{rv,cr}{}^3 g_2 + 8\,\omega^2\zeta\,k_r
\end{aligned}
$$

$$
\begin{aligned}
&-8\,i\omega^3 - 8\,\omega^2\kappa\big)\big)/\left(-8\,ik_r\,\sigma_0\,v_{rv,cr}{}^3 g_2\,\omega^3 + 8\,ik_r\,v_{rv,cr}{}^2\sigma_0\,h_{3\alpha}\,\omega^3\right.\\
&- 16\,iv_{rv,cr}{}^2\omega^3 h_{5\alpha}\,\kappa\,m_r\,h_{2\alpha} - 16\,iv_{rv,cr}\,h_{4\alpha}\,\kappa\,\omega^3 m_r\,h_{1\alpha} - 64\,\omega^6\\
&- 8\,ik_r\,v_{rv,cr}\,h_{4\alpha}\,\omega^3 - 8\,i\omega^3 k_r\,m_r\,h_{1\alpha} + 16\,i\omega^3 m_r\,h_{2\alpha}\,v_{rv,cr}\,h_0\,h_{3\alpha}\,\kappa\\
&+ 16\,i\omega^3 m_r\,h_{2\alpha}\,g_3\,v_{rv,cr}{}^3 h_0\,\kappa + 16\,iv_{rv,cr}{}^2\sigma_0\,h_{3\alpha}\,\kappa\,\omega^3 m_r\,h_{1\alpha}\\
&- 16\,i\sigma_0\,v_{rv,cr}{}^3 g_2\,\kappa\,\omega^3 m_r\,h_{1\alpha} + 32\,\omega^4\zeta\,\sigma_0\,v_{rv,cr}{}^3 g_2 - 32\,\omega^4\zeta\,v_{rv,cr}{}^2\sigma_0\\
&\times\ h_{3\alpha} + 16\,\omega^4 m_r\,h_{1\alpha}\,v_{rv,cr}\,h_{4\alpha} + 16\,\omega^4 m_r\,h_{2\alpha}\,v_{rv,cr}{}^2 h_{5\alpha} + 32\,\omega^4\kappa\\
&\times\ \sigma_0\,v_{rv,cr}{}^3 g_2 - 32\,\omega^4\kappa\,v_{rv,cr}{}^2\sigma_0\,h_{3\alpha} - 4\,\omega^2 k_r\,m_r\,h_{1\alpha}\,v_{rv,cr}\,h_{4\alpha}\\
&- 4\,\omega^2 k_r\,m_r\,h_{2\alpha}\,v_{rv,cr}{}^2 h_{5\alpha} - 4\,\omega^2 m_r\,h_{1\alpha}\,\sigma_0\,v_{rv,cr}{}^3 g_2\\
&+ 4\,\omega^2 m_r\,h_{1\alpha}\,v_{rv,cr}{}^2\sigma_0\,h_{3\alpha} + 4\,\omega^2 m_r\,h_{2\alpha}\,v_{rv,cr}\,h_0\,h_{3\alpha} + 4\,\omega^2 m_r\\
&\times\ h_{2\alpha}\,g_3\,v_{rv,cr}{}^3 h_0 - 8\,\omega^2\zeta\,k_r\,m_r\,v_{rv,cr}\,h_{4\alpha} + 8\,\omega^2\kappa\,k_r\,m_r\,v_{rv,cr}\,h_{4\alpha}\\
&- 4\,\omega^2 m_r\,h_{1\alpha}\,v_{rv,cr}\,h_{4\alpha} - 4\,\omega^2 m_r\,h_{2\alpha}\,v_{rv,cr}{}^2 h_{5\alpha} + 32\,\omega^4\zeta\,m_r\,h_{1\alpha}\\
&+ 32\,\omega^4\zeta\,v_{rv,cr}\,h_{4\alpha} + 32\,\omega^4\kappa\,m_r\,h_{1\alpha} + 32\,\omega^4\kappa\,v_{rv,cr}\,h_{4\alpha} + 16\,\omega^4\\
&+ 16\,\omega^4 k_r\,m_r - 64\,\omega^4\kappa^2 m_r - 8\,ik_{ic}\,\omega^3 + 64\,i\omega^5\zeta + 16\,\omega^4 k_r - 4\,\omega^2 k_r\,m_r\\
&+ 16\,i\omega^3\kappa\,m_r\,k_r + 64\,i\omega^5\kappa - 8\,\omega^2\zeta\,k_r\,m_r\,\sigma_0\,v_{rv,cr}{}^3 g_2 + 8\,\omega^2\zeta\,k_r
\end{aligned}
$$

$$
\begin{aligned}
b_{15} = &\left(-2\,i\left(iRe_{3\alpha}h_{4\alpha} + iRe_{2\alpha}h_0\,h_{3\alpha} - Im_{2\alpha}h_0\,h_{3\alpha} - imr_3 h_{4\alpha}\right)\right.\\
&\times\left(-Im_{2\alpha} + iRe_{2\alpha}\right)m_r\left(-h_{3\alpha}\,v_{rv,cr}{}^2\sigma_0\,\sigma_1 + 2\,i\omega\,\sigma_1 + h_{2\alpha}\right.\\
&\left.+v_{rv,cr}\,h_{4\alpha}\,\sigma_1 + \sigma_0\,v_{rv,cr}{}^3 g_2\,\sigma_1\right)\left(k_{ic} + 2\,i\omega\,k_r - 8\,\omega^2\zeta + 2\,i\omega\right.\\
&\left.-8\,i\omega^3 - 8\,\omega^2\kappa\right)\omega\big)/\left(-8\,ik_r\,\sigma_0\,v_{rv,cr}{}^3 g_2\,\omega^3 + 8\,ik_r\,v_{rv,cr}{}^2\sigma_0\,h_{3\alpha}\,\omega^3\right.\\
&- 16\,iv_{rv,cr}{}^2\omega^3 h_{5\alpha}\,\kappa\,m_r\,h_{2\alpha} - 16\,iv_{rv,cr}\,h_{4\alpha}\,\kappa\,\omega^3 m_r\,h_{1\alpha} - 64\,\omega^6\\
&- 8\,ik_r\,v_{rv,cr}\,h_{4\alpha}\,\omega^3 - 8\,i\omega^3 k_r\,m_r\,h_{1\alpha} + 16\,i\omega^3 m_r\,h_{2\alpha}\,v_{rv,cr}\,h_0\,h_{3\alpha}\,\kappa\\
&+ 16\,i\omega^3 m_r\,h_{2\alpha}\,g_3\,v_{rv,cr}{}^3 h_0\,\kappa + 16\,iv_{rv,cr}{}^2\sigma_0\,h_{3\alpha}\,\kappa\,\omega^3 m_r\,h_{1\alpha}\\
&- 16\,i\sigma_0\,v_{rv,cr}{}^3 g_2\,\kappa\,\omega^3 m_r\,h_{1\alpha} + 32\,\omega^4\zeta\,\sigma_0\,v_{rv,cr}{}^3 g_2 - 32\,\omega^4\zeta\,v_{rv,cr}{}^2\sigma_0\\
&\times\ h_{3\alpha} + 16\,\omega^4 m_r\,h_{1\alpha}\,v_{rv,cr}\,h_{4\alpha} + 16\,\omega^4 m_r\,h_{2\alpha}\,v_{rv,cr}{}^2 h_{5\alpha} + 32\,\omega^4\kappa\\
&\times\ \sigma_0\,v_{rv,cr}{}^3 g_2 - 32\,\omega^4\kappa\,v_{rv,cr}{}^2\sigma_0\,h_{3\alpha} - 4\,\omega^2 k_r\,m_r\,h_{1\alpha}\,v_{rv,cr}\,h_{4\alpha}\\
&- 4\,\omega^2 k_r\,m_r\,h_{2\alpha}\,v_{rv,cr}{}^2 h_{5\alpha} - 4\,\omega^2 m_r\,h_{1\alpha}\,\sigma_0\,v_{rv,cr}{}^3 g_2\\
&+ 4\,\omega^2 m_r\,h_{1\alpha}\,v_{rv,cr}{}^2\sigma_0\,h_{3\alpha} + 4\,\omega^2 m_r\,h_{2\alpha}\,v_{rv,cr}\,h_0\,h_{3\alpha} + 4\,\omega^2 m_r\\
&\times\ h_{2\alpha}\,g_3\,v_{rv,cr}{}^3 h_0 - 8\,\omega^2\zeta\,k_r\,m_r\,v_{rv,cr}\,h_{4\alpha} + 8\,\omega^2\kappa\,k_r\,m_r\,v_{rv,cr}\,h_{4\alpha}\\
&- 4\,\omega^2 m_r\,h_{1\alpha}\,v_{rv,cr}\,h_{4\alpha} - 4\,\omega^2 m_r\,h_{2\alpha}\,v_{rv,cr}{}^2 h_{5\alpha} + 32\,\omega^4\zeta\,m_r\,h_{1\alpha}\\
&+ 32\,\omega^4\zeta\,v_{rv,cr}\,h_{4\alpha} + 32\,\omega^4\kappa\,m_r\,h_{1\alpha} + 32\,\omega^4\kappa\,v_{rv,cr}\,h_{4\alpha} + 16\,\omega^4\\
&+ 16\,\omega^4 k_r\,m_r - 64\,\omega^4\kappa^2 m_r - 8\,ik_{ic}\,\omega^3 + 64\,i\omega^5\zeta + 16\,\omega^4 k_r - 4\,\omega^2 k_r\,m_r\\
&+ 16\,i\omega^3\kappa\,m_r\,k_r + 64\,i\omega^5\kappa - 8\,\omega^2\zeta\,k_r\,m_r\,\sigma_0\,v_{rv,cr}{}^3 g_2 + 8\,\omega^2\zeta\,k_r
\end{aligned}
$$

$$\times m_r v_{rv,cr}{}^2\sigma_0 h_{3\alpha} + 8\omega^2\kappa k_r m_r \sigma_0 v_{rv,cr}{}^3 g_2 - 8\omega^2\kappa k_r m_r v_{rv,cr}{}^2\sigma_0 h_{3\alpha}$$
$$- 4\omega^2 k_r m_r h_{1\alpha}\sigma_0 v_{rv,cr}{}^3 g_2 + 4\omega^2 k_r m_r h_{1\alpha} v_{rv,cr}{}^2\sigma_0 h_{3\alpha}$$
$$+ 4\omega^2 k_r m_r h_{2\alpha} v_{rv,cr} h_0 h_{3\alpha} + 4\omega^2 k_r m_r h_{2\alpha} g_3 v_{rv,cr}{}^3 h_0$$
$$+ 16\omega^4 m_r h_{1\alpha}\sigma_0 v_{rv,cr}{}^3 g_2 - 16\omega^4 m_r h_{1\alpha} v_{rv,cr}{}^2\sigma_0 h_{3\alpha} - 16\omega^4 m_r$$
$$\times h_{2\alpha} v_{rv,cr} h_0 h_{3\alpha} - 16\omega^4 m_r h_{2\alpha} g_3 v_{rv,cr}{}^3 h_0 + 32 i m_r h_{1\alpha}\omega^5$$
$$- 8 i m_r h_{1\alpha}\omega^3 - 8 i\omega^3 v_{rv,cr} h_{4\alpha} + 32 i\omega^5 v_{rv,cr} h_{4\alpha} + 8 i\omega^3 v_{rv,cr}{}^2\sigma_0 h_{3\alpha}$$
$$- 8 i\omega^3\sigma_0 v_{rv,cr}{}^3 g_2 - 32 i\omega^5 v_{rv,cr}{}^2\sigma_0 h_{3\alpha} + 32 i\omega^5\sigma_0 v_{rv,cr}{}^3 g_2$$
$$+ 2 i m_r\omega k_r k_{ic} - 16 i m_r\omega^3 k_r\zeta + 16 i m_r h_0 h_{2\alpha} h_{3\alpha}\omega^3 v_{rv,cr}\zeta$$
$$- 2 i m_r h_{1\alpha} h_{3\alpha} k_{ic}\omega\sigma_0 v_{rv,cr}{}^2 - 2 i m_r h_0 h_{2\alpha} h_{3\alpha} k_{ic}\omega v_{rv,cr}$$
$$- 16 i m_r g_2 h_{1\alpha}\omega^3\sigma_0 v_{rv,cr}{}^3\zeta + 16 i m_r g_3 h_0 h_{2\alpha}\omega^3 v_{rv,cr}{}^3\zeta$$
$$+ 16 i m_r h_{1\alpha} h_{3\alpha}\omega^3\sigma_0 v_{rv,cr}{}^2\zeta + 2 i m_r g_2 h_{1\alpha} k_{ic}\omega\sigma_0 v_{rv,cr}{}^3$$
$$- 2 i m_r g_3 h_0 h_{2\alpha} k_{ic}\omega v_{rv,cr}{}^3 - 4 h_{4\alpha} k_{ic}\omega^2 v_{rv,cr} - 4 m_r h_{1\alpha} k_{ic}\omega^2$$
$$- 4 g_2 k_{ic}\omega^2\sigma_0 v_{rv,cr}{}^3 + 4 h_{3\alpha} k_{ic}\omega^2\sigma_0 v_{rv,cr}{}^2 + m_r k_r v_{rv,cr} h_{4\alpha} k_{ic}$$
$$- 8 i m_r k_r\sigma_0 v_{rv,cr}{}^3 g_2\omega^3 + 8 i m_r k_r v_{rv,cr}{}^2\sigma_0 h_{3\alpha}\omega^3 + 2 i m_r\omega k_r$$
$$\times \sigma_0 v_{rv,cr}{}^3 g_2 - 2 i m_r\omega k_r v_{rv,cr}{}^2\sigma_0 h_{3\alpha} - 16 i m_r h_{2\alpha} h_{5\alpha}\omega^3 v_{rv,cr}{}^2\zeta$$
$$- 16 i m_r h_{1\alpha} h_{4\alpha}\omega^3 v_{rv,cr}\zeta + 2 i m_r h_{2\alpha} h_{5\alpha} k_{ic}\omega v_{rv,cr}{}^2 + 2 i m_r h_{1\alpha}$$
$$h_{4\alpha} k_{ic}\omega v_{rv,cr} - 32 i m_r\omega^3 v_{rv,cr}{}^2\sigma_0 h_{3\alpha}\kappa^2 + 32 i m_r\omega^3\sigma_0 v_{rv,cr}{}^3 g_2\kappa^2$$
$$+ m_r k_r\sigma_0 v_{rv,cr}{}^3 g_2 k_{ic} - m_r k_r v_{rv,cr}{}^2\sigma_0 h_{3\alpha} k_{ic} - 8 i m_r k_r v_{rv,cr} h_{4\alpha}\omega^3$$
$$+2 i m_r\omega k_r v_{rv,cr} h_{4\alpha} + 32 i m_r\omega^3 v_{rv,cr} h_{4\alpha}\kappa^2) \quad (81)$$

$$b_{16} = \left(i\left(iRe_{3\alpha}h_{4\alpha} + iRe_{2\alpha}h_0 h_{3\alpha} - Im_{2\alpha}h_0 h_{3\alpha} - Im_{3\alpha}h_{4\alpha}\right)\right.$$
$$\times \left(-Im_{2\alpha} + iRe_{2\alpha}\right)\left(32\omega^5 - 8\omega^3 - 8\omega^3 k_r + 32 m_r\omega^3\kappa^2\right.$$
$$+ 2 m_r\omega k_r - 8 m_r\omega^3 k_r + 4 i k_{ic}\omega^2 - 32 i\omega^4\zeta - 32 i\omega^4\kappa$$
$$- 16 i m_r h_{1\alpha}\omega^4 - i m_r k_r k_{ic} + 4 i m_r h_{1\alpha}\omega^2 - 16 i m_r h_0 h_{3\alpha}\omega^4\sigma_1 v_{rv,cr}$$
$$- 4 i m_r h_{5\alpha} k_r\omega^2\sigma_1 v_{rv,cr}{}^2 - 16 i m_r g_3 h_0\omega^4\sigma_1 v_{rv,cr}{}^3 + 4 i h_{3\alpha} h_0$$
$$\times m_r\sigma_1\omega^2 v_{rv,cr} + 4 i h_0 m_r\sigma_1 g_3\omega^2 v_{rv,cr}{}^3 + 16 i m_r h_{5\alpha}\omega^4\sigma_1 v_{rv,cr}{}^2$$
$$\times -4 i m_r\sigma_1 h_{5\alpha}\omega^2 v_{rv,cr}{}^2 + 4 i m_r g_3 h_0 k_r\omega^2\sigma_1 v_{rv,cr}{}^3 + 4 i m_r h_0$$
$$\times h_{3\alpha} k_r\omega^2\sigma_1 v_{rv,cr} + 8 i m_r\omega^2\zeta k_r + 4 i m_r h_{1\alpha} k_r\omega^2 - 8 i m_r\omega^2\kappa k_r$$
$$\times -16 m_r g_3 h_0\kappa\omega^3\sigma_1 v_{rv,cr}{}^3 - 16 m_r g_3 h_0\omega^3\sigma_1 v_{rv,cr}{}^3\zeta$$
$$+ 2 m_r g_3 h_0 k_{ic}\omega\sigma_1 v_{rv,cr}{}^3 - 16 m_r h_0 h_{3\alpha}\kappa\omega^3\sigma_1 v_{rv,cr}$$
$$- 16 m_r h_0 h_{3\alpha}\omega^3\sigma_1 v_{rv,cr}\zeta + 2 m_r h_0 h_{3\alpha} k_{ic}\omega\sigma_1 v_{rv,cr}$$
$$+ 2 m_r h_{1\alpha} k_{ic}\omega - 16 m_r h_{1\alpha}\omega^3\zeta - 16 m_r h_{1\alpha}\kappa\omega^3 + 16 m_r h_{5\alpha}\kappa$$
$$\times \left.\omega^3\sigma_1 v_{rv,cr}{}^2 + 16 m_r h_{5\alpha}\omega^3\sigma_1 v_{rv,cr}{}^2\zeta - 2 m_r h_{5\alpha} k_{ic}\omega\sigma_1 v_{rv,cr}{}^2\right)) /$$
$$\times \left(-8 i k_r\sigma_0 v_{rv,cr}{}^3 g_2\omega^3 + 8 i k_r v_{rv,cr}{}^2\sigma_0 h_{3\alpha}\omega^3 - 16 i v_{rv,cr}{}^2\omega^3 h_{5\alpha}\right.$$
$$\times \kappa m_r h_{2\alpha} - 16 i v_{rv,cr} h_{4\alpha}\kappa\omega^3 m_r h_{1\alpha} - 64\omega^6 - 8 i k_r v_{rv,cr} h_{4\alpha}\omega^3$$
$$- 8 i\omega^3 k_r m_r h_{1\alpha} + 16 i\omega^3 m_r h_{2\alpha} v_{rv,cr} h_0 h_{3\alpha}\kappa + 16 i\omega^3 m_r h_{2\alpha} g_3$$
$$\times v_{rv,cr}{}^3 h_0\kappa + 16 i v_{rv,cr}{}^2\sigma_0 h_{3\alpha}\kappa\omega^3 m_r h_{1\alpha} - 16 i\sigma_0 v_{rv,cr}{}^3 g_2\kappa\omega^3 m_r h_{1\alpha}$$
$$+ 32\omega^4\zeta\sigma_0 v_{rv,cr}{}^3 g_2 - 32\omega^4\zeta v_{rv,cr}{}^2\sigma_0 h_{3\alpha} + 16\omega^4 m_r h_{1\alpha} v_{rv,cr} h_{4\alpha}$$
$$+ 16\omega^4 m_r h_{2\alpha} v_{rv,cr}{}^2 h_{5\alpha} + 32\omega^4\kappa\sigma_0 v_{rv,cr}{}^3 g_2 - 32\omega^4\kappa v_{rv,cr}{}^2\sigma_0 h_{3\alpha}$$
$$- 4\omega^2 k_r m_r h_{1\alpha} v_{rv,cr} h_{4\alpha} - 4\omega^2 k_r m_r h_{2\alpha} v_{rv,cr}{}^2 h_{5\alpha} - 4\omega^2 m_r h_{1\alpha}$$
$$\times \sigma_0 v_{rv,cr}{}^3 g_2 + 4\omega^2 m_r h_{1\alpha} v_{rv,cr}{}^2\sigma_0 h_{3\alpha} + 4\omega^2 m_r h_{2\alpha} v_{rv,cr} h_0 h_{3\alpha}$$
$$+ 4\omega^2 m_r h_{2\alpha} g_3 v_{rv,cr}{}^3 h_0 - 8\omega^2\zeta k_r m_r v_{rv,cr} h_{4\alpha} + 8\omega^2\kappa k_r m_r v_{rv,cr} h_{4\alpha}$$
$$- 4\omega^2 m_r h_{1\alpha} v_{rv,cr} h_{4\alpha} - 4\omega^2 m_r h_{2\alpha} v_{rv,cr}{}^2 h_{5\alpha} + 32\omega^4\zeta m_r h_{1\alpha}$$
$$+ 32\omega^4\zeta v_{rv,cr} h_{4\alpha} + 32\omega^4\kappa m_r h_{1\alpha} + 32\omega^4\kappa v_{rv,cr} h_{4\alpha} + 16\omega^4$$
$$+ 16\omega^4 k_r m_r - 64\omega^4\kappa^2 m_r - 8 i k_{ic}\omega^3 + 64 i\omega^5\zeta + 16\omega^4 k_r$$
$$- 4\omega^2 k_r m_r + 16 i\omega^3\kappa m_r k_r + 64 i\omega^5\kappa - 8\omega^2\zeta k_r m_r\sigma_0 v_{rv,cr}{}^3 g_2$$
$$+ 8\omega^2\zeta k_r m_r v_{rv,cr}{}^2\sigma_0 h_{3\alpha} + 8\omega^2\kappa k_r m_r\sigma_0 v_{rv,cr}{}^3 g_2 - 8\omega^2\kappa$$
$$\times k_r m_r v_{rv,cr}{}^2\sigma_0 h_{3\alpha} - 4\omega^2 k_r m_r h_{1\alpha}\sigma_0 v_{rv,cr}{}^3 g_2 + 4\omega^2 k_r m_r$$
$$\times h_{1\alpha} v_{rv,cr}{}^2\sigma_0 h_{3\alpha} + 4\omega^2 k_r m_r h_{2\alpha} v_{rv,cr} h_0 h_{3\alpha} + 4\omega^2 k_r m_r$$
$$\times h_{2\alpha} g_3 v_{rv,cr}{}^3 h_0 + 16\omega^4 m_r h_{1\alpha}\sigma_0 v_{rv,cr}{}^3 g_2 - 16\omega^4 m_r h_{1\alpha}$$
$$\times v_{rv,cr}{}^2\sigma_0 h_{3\alpha} - 16\omega^4 m_r h_{2\alpha} v_{rv,cr} h_0 h_{3\alpha} - 16\omega^4 m_r h_{2\alpha} g_3 v_{rv,cr}{}^3 h_0$$
$$+ 32 i m_r h_{1\alpha}\omega^5 - 8 i m_r h_{1\alpha}\omega^3 - 8 i\omega^3 v_{rv,cr} h_{4\alpha} + 32 i\omega^5 v_{rv,cr} h_{4\alpha}$$
$$+ 8 i\omega^3 v_{rv,cr}{}^2\sigma_0 h_{3\alpha} - 8 i\omega^3\sigma_0 v_{rv,cr}{}^3 g_2 - 32 i\omega^5 v_{rv,cr}{}^2\sigma_0 h_{3\alpha}$$
$$+ 32 i\omega^5\sigma_0 v_{rv,cr}{}^3 g_2 + 2 i m_r\omega k_r k_{ic} - 16 i m_r\omega^3 k_r\zeta + 16 i m_r h_0 h_{2\alpha}$$
$$\times h_{3\alpha}\omega^3 v_{rv,cr}\zeta - 2 i m_r h_{1\alpha} h_{3\alpha} k_{ic}\omega\sigma_0 v_{rv,cr}{}^2 - 2 i m_r h_0 h_{2\alpha} h_{3\alpha}$$
$$\times k_{ic}\omega v_{rv,cr} - 16 i m_r g_2 h_{1\alpha}\omega^3\sigma_0 v_{rv,cr}{}^3\zeta + 16 i m_r g_3 h_0 h_{2\alpha}\omega^3 v_{rv,cr}{}^3\zeta$$
$$+ 16 i m_r h_{1\alpha} h_{3\alpha}\omega^3\sigma_0 v_{rv,cr}{}^2\zeta + 2 i m_r g_2 h_{1\alpha} k_{ic}\omega\sigma_0 v_{rv,cr}{}^3$$
$$- 2 i m_r g_3 h_0 h_{2\alpha} k_{ic}\omega v_{rv,cr}{}^3 - 4 h_{4\alpha} k_{ic}\omega^2 v_{rv,cr} - 4 m_r h_{1\alpha} k_{ic}\omega^2$$
$$- 4 g_2 k_{ic}\omega^2\sigma_0 v_{rv,cr}{}^3 + 4 h_{3\alpha} k_{ic}\omega^2\sigma_0 v_{rv,cr}{}^2 + m_r k_r v_{rv,cr} h_{4\alpha} k_{ic}$$
$$- 8 i m_r k_r\sigma_0 v_{rv,cr}{}^3 g_2\omega^3 + 8 i m_r k_r v_{rv,cr}{}^2\sigma_0 h_{3\alpha}\omega^3 + 2 i m_r\omega k_r$$
$$\times \sigma_0 v_{rv,cr}{}^3 g_2 - 2 i m_r\omega k_r v_{rv,cr}{}^2\sigma_0 h_{3\alpha} - 16 i m_r h_{2\alpha} h_{5\alpha}\omega^3 v_{rv,cr}{}^2\zeta$$
$$- 16 i m_r h_{1\alpha} h_{4\alpha}\omega^3 v_{rv,cr}\zeta + 2 i m_r h_{2\alpha} h_{5\alpha} k_{ic}\omega v_{rv,cr}{}^2 + 2 i m_r h_{1\alpha}$$
$$\times h_{4\alpha} k_{ic}\omega v_{rv,cr} - 32 i m_r\omega^3 v_{rv,cr}{}^2\sigma_0 h_{3\alpha}\kappa^2 + 32 i m_r\omega^3\sigma_0 v_{rv,cr}{}^3 g_2\kappa^2$$
$$+ m_r k_r\sigma_0 v_{rv,cr}{}^3 g_2 k_{ic} - m_r k_r v_{rv,cr}{}^2\sigma_0 h_{3\alpha} k_{ic} - 8 i m_r k_r v_{rv,cr} h_{4\alpha}\omega^3$$
$$+2 i m_r\omega k_r v_{rv,cr} h_{4\alpha} + 32 i m_r\omega^3 v_{rv,cr} h_{4\alpha}\kappa^2) \quad (82)$$

$$b_{33} = 2\left(\left(h_{2\alpha} + v_{rv,cr} h_{4\alpha}\sigma_1 - h_{3\alpha} v_{rv,cr}{}^2\sigma_0\sigma_1 + \sigma_0 v_{rv,cr}{}^3 g_2\sigma_1\right)\right.$$
$$\times \left.\left(h_{4\alpha} Im_{2\alpha} Im_{3\alpha} + h_0 h_{3\alpha} Re_{2\alpha}{}^2 + h_{4\alpha} Re_{2\alpha} rer_3 + h_0 h_{3\alpha} Im_{2\alpha}{}^2\right)\right) /$$
$$\times \left(k_{ic} v_{rv,cr}\left(-v_{rv,cr}\sigma_0 h_{3\alpha} + \sigma_0 v_{rv,cr}{}^2 g_2 + h_{4\alpha}\right)\right) \quad (83)$$

$$b_{34} = 2\left(\left(h_{2\alpha} + v_{rv,cr} h_{4\alpha}\sigma_1 - h_{3\alpha} v_{rv,cr}{}^2\sigma_0\sigma_1 + \sigma_0 v_{rv,cr}{}^3 g_2\sigma_1\right)\right.$$
$$\times \left.\left(h_{4\alpha} Im_{2\alpha} Im_{3\alpha} + h_0 h_{3\alpha} Re_{2\alpha}{}^2 + h_{4\alpha} Re_{2\alpha} rer_3 + h_0 h_{3\alpha} Im_{2\alpha}{}^2\right)\right) /$$
$$\times \left(k_r v_{rv,cr}\left(-v_{rv,cr}\sigma_0 h_{3\alpha} + \sigma_0 v_{rv,cr}{}^2 g_2 + h_{4\alpha}\right)\right) \quad (84)$$

$$b_{36} = -2\,\frac{\left(h_{4\alpha} Im_{2\alpha} Im_{3\alpha} + h_0 h_{3\alpha} Re_{2\alpha}{}^2 + h_{4\alpha} Re_{2\alpha} rer_3 + h_0 h_{3\alpha} Im_{2\alpha}{}^2\right)}{v_{rv,cr}\left(-v_{rv,cr}\sigma_0 h_{3\alpha} + \sigma_0 v_{rv,cr}{}^2 g_2 + h_{4\alpha}\right)} \quad (85)$$

$$v_{11} = Re_{2\alpha} + i Im_{2\alpha} \quad (86)$$

$$v_{12} = -3 m_r\sigma_1\sigma_0 h_{3\alpha} Re_{2\alpha}{}^2 Re_{3\alpha} + i m_r\sigma_1 h_{4\alpha} b11_5 Im_{3\alpha} - 3 m_r\sigma_1 h_{5\alpha}$$
$$\times Re_{2\alpha} Im_{2\alpha}{}^2 - 3 i m_r\sigma_1 h_{5\alpha} Im_{2\alpha}{}^3 - m_r\sigma_1\sigma_0 h_{3\alpha} Im_{2\alpha}{}^2 Re_{3\alpha}$$
$$- 3 im_r\sigma_1 h_{5\alpha} Im_{2\alpha} Re_{2\alpha}{}^2 - 3 m_r\sigma_1 h_{5\alpha} Re_{2\alpha}{}^3 - 2 m_r\sigma_1\sigma_0 h_{3\alpha}$$
$$\times Re_{2\alpha} Im_{2\alpha} imr_3 - im_r\sigma_1 h_{4\alpha} Im_{2\alpha} b31_6 + im_r\sigma_1 h_{4\alpha} Im_{2\alpha} b11_6$$
$$- 3 im_r\sigma_1\sigma_0 h_{3\alpha} Im_{2\alpha}{}^2 Im_{3\alpha} - 2 im_r\sigma_1 h_0 h_{3\alpha} Im_{2\alpha} b31_5$$
$$+ 2 im_r\sigma_1 h_0 h_{3\alpha} Im_{2\alpha} b11_5 - m_r\sigma_1 h_{4\alpha} Re_{2\alpha} b31_6 - 2 m_r\sigma_1 h_0 h_{3\alpha}$$
$$\times Re_{2\alpha} b31_5 - 2 im_r\sigma_1\sigma_0 h_{3\alpha} Re_{2\alpha} imr_2 Re_{3\alpha} - im_r\sigma_1 h_{4\alpha} b31_5 Im_{3\alpha}$$
$$- m_r\sigma_1 h_{4\alpha} b31_5 Re_{3\alpha} - 2 m_r\sigma_1 h_0 h_{3\alpha} Re_{2\alpha} b11_5 - im_r\sigma_1\sigma_0 h_{3\alpha}$$
$$\times Re_{2\alpha}{}^2 Im_{3\alpha} - m_r\sigma_1 h_{4\alpha} b11_5 Re_{3\alpha} - m_r\sigma_1 h_{4\alpha} Re_{2\alpha} b11_6 \quad (87)$$

$$v_{21} = Re_{3\alpha} + i Im_{3\alpha} \quad (88)$$

$$v_{22} = 2 h_{3\alpha}\sigma_0 Re_{2\alpha} Im_{2\alpha} Im_{3\alpha} - i h_{4\alpha} b11_5 Im_{3\alpha} + 3 i h_{5\alpha} Im_{2\alpha}{}^3 - i h_{4\alpha}$$
$$\times Im_{2\alpha} b11_6 + 3 h_{5\alpha} Re_{2\alpha}{}^3 + 3 h_{5\alpha} Re_{2\alpha} Im_{2\alpha}{}^2 + 3 h_{3\alpha}\sigma_0 Re_{2\alpha}{}^2 Re_{3\alpha}$$
$$+ i h_{4\alpha} b13_5 Im_{3\alpha} + h_{3\alpha}\sigma_0 Im_{2\alpha}{}^2 Re_{3\alpha} + i h_{3\alpha}\sigma_0 Re_{2\alpha}{}^2 Im_{3\alpha}$$
$$+ 3 i h_{3\alpha}\sigma_0 Im_{2\alpha}{}^2 Im_{3\alpha} - 2 i h_0 h_{3\alpha} Im_{2\alpha} b11_5 + h_{4\alpha} b13_5 rer_3$$
$$+ h_{4\alpha} Re_{2\alpha} b13_6 + 2 h_0 h_{3\alpha} Re_{2\alpha} b13_5 + 2 i h_0 h_{3\alpha} Im_{2\alpha} b13_5$$
$$+ h_{4\alpha} b11_5 rer_3 + i h_{4\alpha} Im_{2\alpha} b13_6 + 2 h_0 h_{3\alpha} Re_{2\alpha} b11_5$$
$$+ 2 i h_{3\alpha}\sigma_0 Re_{2\alpha} Im_{2\alpha} Re_{3\alpha} + 3 i h_{5\alpha} Im_{2\alpha} Re_{2\alpha}{}^2 + h_{4\alpha} Re_{2\alpha} b11_6 \quad (89)$$

References

[1] Won-jong Kim, David L. Trumper, High-precision magnetic levitation stage for photolithography, Precis. Eng. 22 (2) (1998) 66–77.

[2] Won Jong Kim, Shobhit Verma, Huzefa Shakir, Design and precision construction of novel magnetic-levitation-based multi-axis nanoscale positioning systems, Precis. Eng. 31 (4) (2007) 337–350.
[3] Srinivasa M. Salapaka, Murti V. Salapaka, Scanning probe microscopy, IEEE Control Syst. Mag. 28 (2) (2008) 65–83.
[4] Abu Sebastian, Angeliki Pantazi, S.O. Reza Moheimani, Haris Pozidis, Evangelos Eleftheriou, Achieving subnanometer precision in a mems-based storage device during self-servo write process, IEEE Trans. Nanotechnol. 7 (5) (2008) 586–595.
[5] Andrew J. Fleming, Kam K. Leang, Design, Modeling and Control of Nanopositioning Systems, Springer, 2014.
[6] Hans Butler, Position control in lithographic equipment, IEEE Control Syst. Mag. 31 (5) (2011) 28–47.
[7] Yusuf Altintas, Alexander Verl, Christian Brecher, L. Uriarte, Günther Pritschow, Machine tool feed drives, CIRP Ann. 60 (2) (2011) 779–796.
[8] Shigeru Futami, Akihiro Furutani, Shoichiro Yoshida, Nanometer positioning and its micro-dynamics, Nanotechnology 1 (1) (1990) 31.
[9] Mun-Su Kim, Jung-Han Kim, Design of a gain scheduled pid controller for the precision stage in lithography, Int. J. Precis. Eng. Manuf. 12 (6) (2011) 993–1000.
[10] J.Y. Liu, W.S. Yin, Yu Zhu, Application of adaptive fuzzy pid controller to nano-scale precision motion stage system, Control. Eng. China 18 (2) (2011) 254–257.
[11] Farid Al-Bender, Jan Swevers, Characterization of friction force dynamics, IEEE Control Syst. Mag. 28 (6) (2008) 64–81.
[12] Filipe Marques, Paulo Flores, J.C. Pimenta Claro, Hamid M. Lankarani, A survey and comparison of several friction force models for dynamic analysis of multibody mechanical systems, Nonlinear Dynam. 86 (3) (2016) 1407–1443.
[13] Brian Armstrong-Hélouvry, Pierre Dupont, Carlos Canudas De Wit, A survey of models, analysis tools and compensation methods for the control of machines with friction, Automatica 30 (7) (1994) 1083–1138.
[14] Ron H.A. Hensen, M.J.G. Van de Molengraft, Maarten Steinbuch, Friction induced hunting limit cycles: A comparison between the lugre and switch friction model, Automatica 39 (12) (2003) 2131–2137.
[15] Yoshihiro Maeda, Makoto Iwasaki, Rolling friction model-based analyses and compensation for slow settling response in precise positioning, IEEE Trans. Ind. Electron. 60 (12) (2012) 5841–5853.
[16] Xin Dong, Deokkyun Yoon, Chinedum E. Okwudire, A novel approach for mitigating the effects of pre-rolling/pre-sliding friction on the settling time of rolling bearing nanopositioning stages using high frequency vibration, Precis. Eng. 47 (2017) 375–388.
[17] Xin Dong, Xingjian Liu, Deokkyun Yoon, Chinedum E. Okwudire, Simple and robust feedforward compensation of quadrant glitches using a compliant joint, CIRP Ann. 66 (1) (2017) 353–356.
[18] Xin Dong, Chinedum E. Okwudire, An experimental investigation of the effects of the compliant joint method on feedback compensation of pre-sliding/pre-rolling friction, Precis. Eng. 54 (2018) 81–90.
[19] Shuichi Dejima, Wei Gao, Kei Katakura, Satoshi Kiyono, Yoshiyuki Tomita, Dynamic modeling, controller design and experimental validation of a planar motion stage for precision positioning, Precis. Eng. 29 (3) (2005) 263–271.
[20] Jianyong Yao, Wenxiang Deng, Zongxia Jiao, Adaptive control of hydraulic actuators with lugre model-based friction compensation, IEEE Trans. Ind. Electron. 62 (10) (2015) 6469–6477.
[21] Xingjian Wang, Shaoping Wang, High performance adaptive control of mechanical servo system with lugre friction model: identification and compensation, J. Dyn. Syst. Meas. Control 134 (1) (2012) 011021.
[22] André Gustavo Scolari Conceição, Carlos E.T. Dórea, Luciana Martinez, Edson Roberto de Pieri, et al., Design and implementation of model-predictive control with friction compensation on an omnidirectional mobile robot, IEEE/ASME Trans. Mechatronics 19 (2) (2013) 467–476.
[23] Jay H. Lee, Model predictive control: Review of the three decades of development, Int. J. Control Autom. Syst. 9 (3) (2011) 415.
[24] Miroslav Krsti, Ioannis Kanellakopoulos, V. Petar, Nonlinear and Adaptive Control Design, Wiley, New York, 1995.
[25] C. Canudas De Wit, Hans Olsson, Karl Johan Astrom, Pablo Lischinsky, A new model for control of systems with friction, IEEE Trans. Automat. Control 40 (3) (1995) 419–425.
[26] Jiamin Wang, Xin Dong, Oumar R. Barry, Chinedum Okwudire, Dynamical analysis of friction induced vibration in a precision motion stage with a friction isolator, 2019, arXiv preprint arXiv:1910.03212.
[27] Xin Dong, Chinedum Okwudire, Jiamin Wang, Oumar Barry, On the friction isolator for precision motion control and its dynamics, in: ASME 2019 International Design Engineering Technical Conferences and Computers and Information in Engineering Conference, American Society of Mechanical Engineers Digital Collection, 2019.
[28] Karl Johanastrom, Carlos Canudas-De-Wit, Revisiting the lugre friction model, IEEE Control Syst. Mag. 28 (6) (2008) 101–114.
[29] Ashesh Saha, Analysis and Control of Friction-Induced Vibrations by Time-Delayed Feedback (Ph.D thesis), Indian Institute of Technology, Kanpur, India, 2013.
[30] Ashesh Saha, Pankaj Wahi, An analytical study of time-delayed control of friction-induced vibrations in a system with a dynamic friction model, Int. J. Non-Linear Mech. 63 (2014) 60–70.
[31] Balakumar Balachandran, Ali H. Nayfeh, Cyclic motions near a hopf bifurcation of a four-dimensional system, Nonlinear Dynam. 3 (1) (1992) 19–39.
[32] Pankaj Wahi, Anindya Chatterjee, Self-interrupted regenerative metal cutting in turning, Int. J. Non-Linear Mech. 43 (2) (2008) 111–123.
[33] Ali H. Nayfeh, Balakumar Balachandran, Motion near a hopf bifurcation of a three-dimensional system, Mech. Res. Commun. 17 (4) (1990) 191–198.
[34] Stephen K. Scott, Chemical Chaos, in: International Series of Monographs on Chemistry, Clarendon Press, 1993.
[35] Vadim S. Anishchenko, Tatyana E. Vadivasova, Galina I. Strelkova, Deterministic Nonlinear Systems: A Short Course, in: Springer Series in Synergetics, Springer International Publishing, 2014.